Brain Development in Syndromic Craniosynostosis: A Morphometric Analysis

Alexander T. Wilson

©2021, A.T. Wilson. All rights reserved. No part of this publication may be produced or transmitted in any forms or by any means, without permission of the author.

Brain Development in Syndromic Craniosynostosis:
A Morphometric Analysis

Hersenenontwikkeling bij syndromale craniosynostose:
een morfometrische analyse

Thesis

to obtain the degree of Doctor from the
Erasmus University Rotterdam
by command of the
rector magnificus

prof.dr. F.A. van der Duijn Schouten

and in accordance with the decision of the Doctorate Board.
The public defence shall be held on

Wednesday, the 29th of September 2021 at 15:30 hrs
by

Alexander Tate Wilson
born in Florence, South Carolina (USA)

Erasmus University Rotterdam

Doctoral Committee:

Promotor:	prof. dr. I.M.J. Mathijssen
Other members:	prof. dr. R.C. Tasker prof. dr. T.J.H. White prof. R.D. Hayward
Copromotor:	dr. ir. H.A. Vrooman

To my parents

TABLE OF CONTENTS

CHAPTER 1

Introduction and Background

Overview

The focus of this thesis is on neuromorphometry in syndromic craniosynostosis. First, typical skull and brain development are reviewed, followed by examination of how craniosynostosis differs in these processes resulting in structural abnormalities and functional deficits. Common syndromic variants of the disease are briefly discussed as well as the pathophysiology of intracranial hypertension in the developing brain. A review of the medical informatics literature is then presented with a particular focus on imaging analysis techniques used in this thesis. Finally, specific aims of this thesis are outlined.

Normal skull development

The human skull, or cranium, can be divided into two categories, the viscerocranium and the neurocranium. The viscerocranium consists of the facial skeleton which is attached to the base of the skull. The neurocranium houses and protects the brain and can be further subdivided into the cartilaginous chondrocranium which forms the skull base and the calvarium which is made up of flat bones – paired frontal bones, paired parietal bones, and the squamous portions of both temporal bones along with the interparietal portion of the occipital bone. The bones of the calvarium are formed via intermembranous ossification and joined together by fibrous joints called cranial sutures designed to permit flexibility of the skull during the birthing process and cranial growth as the developing brain expands during childhood[1].

Embryological development begins in the 3rd week of gestation when gastrulation occurs and 3 distinct germ layers are formed – the endoderm, mesoderm, and ectoderm (along with neural crest cells) from which all tissues arise. The endoderm is the inner-most layer which forms the inner epithelial lining of many structures including the pharynx and larynx. The mesoderm is the middle layer which gives rise to muscles, bone, mesenchyme, cartilage and blood vessels. The ectoderm is the outer-most layer which forms the epidermis, nervous system, hair, teeth, and nails. By the 4th week of gestation, the ectoderm-derived neural plate folds into a neural tube from which the nervous system is eventually formed. At the dorsal aspect of the neural tube, unique cell clusters are found called neural crest cells which undergo epithelial-mesenchymal transition (EMT) and follow a developmental pathway distinct from any of the other germ layers, giving rise to a variety of structures including melanocytes, craniofacial cartilage and bone, smooth muscle, enteric neurons and glia[2]. Therefore, calvarial

development has both mesodermal and neural crest cell origins. Anterior portions of the frontal bones are derived from neural crest cells and posterior portions of the calvarium are derived from the mesoderm[3,4]. At 6 weeks condensation of a dense mass of mesenchyme occurs and the desmocranium is formed which is the foundation for both the chondrocranium and osteocranium. Chondrification of the desmocranium initiates development of the cartilaginous skull base and ossification of the osteocranium occurs in the following weeks. Ossification occurs by one of two mechanisms. Endochondral ossification requires a cartilaginous scaffold that is replaced by mineralized bone and occurs in long bones and the cranial base. Intramembranous ossification is the process by which flat bones of the calvarium are formed and is characterized by differentiation from mesenchymal cells to osteoblasts to directly form bone[5].

Growth of the calvarium occurs at sutures comprised of osteogenic fronts where the boundaries between calvarial bones lie. Suture locations are derived from intracranial dural reflections corresponding to recesses in the developing brain[6]. These sutures permit proportional cranial growth throughout childhood, driven by the rapidly expanding brain in early development. Fusion first occurs in the metopic suture which runs medially through the forehead joining the paired frontal bones and typically ossifies before 9 months of age[7]. The remainder of sutures fuse during adulthood in the following sequence: sagittal at 20-22 years, coronal at 23-24 years, lambdoid at 26 years, and finally the squamosal at 60 years of age[8,9]. Other types of postnatal cranial growth include chondral growth which is accomplished by various synchondroses in the skull base throughout childhood and adolescence, and appositional growth whereby bone is resorbed at the intracranial surface and laid down on the external surface of the flat bones of the neurocranium[10-12].

Normal brain development

Just one week after formation of the neural tube, a cranial-caudal axis is established and the neural tube has organized itself into 5 distinct vesicles – the telencephalon, diencephalon, mesencephalon, metencephalon, and myelencephalon. These vesicles form the basis for all future brain development and can be further grouped into the hindbrain (myelencephalon and metencephalon), midbrain (mesencephalon), and forebrain (diencephalon and telecephalon). In the hindbrain, the myelencephalon goes on to form the medulla oblongata and inferior cerebellar peduncles, and the metencephalon forms the pons, cerebellum, and middle cerebellar peduncles. In the midbrain the

tegmentum, tectum, and aqueduct are formed from the mesencephalon. In the forebrain, the diencephalon derivatives include the thalamus, and caudal portions of the hypothalamus and third ventricle. Finally, the cerebral hemispheres, cortex, and corpus striatum are derived from the telencephalon[13].

The process of transitioning from primitive precursors to mature brain structures occurs through a series of folds, swellings, and divisions during the embryonic period which are coordinated with changes in neural patterning. Neuron production first begins on embryonic day 42 after significant expansion of the neural progenitor cell (NPC) population[14]. Initially, NPCs divide symmetrically yielding two identical daughter NPCs but at embryonic day 42 asymmetric division begins resulting in one NPC and one neuron. This occurs primarily in the ventricular zone (VZ) near the cavity of what was once the neural tube. Neurons produced here then migrate radially toward the developing neocortex. Early in development, when migratory distances are small, neurons move by somal translocation where the cell extends a long basal process to the pial surface and then moves its nucleus through the cytoplasm to the developing cortex[15]. As migratory distances increase a different mechanism is needed which relies upon radial glial cells (RGC). RGCs maintain their cell body in the VZ and have long extensions into the growing cortex, which act as a scaffolding system for nascent neurons to reach their target destination.

As the ordered migration of neurons continues, a six-layered cortex is formed. The deepest layer is formed by the neurons which migrate first and subsequent migrating neurons form successively superficial layers in an “inside-out” fashion. By convention, cortical layers are numbered from superficial to deep with layer 6 being the deepest and layer 1 being the most superficial. Migration is regulated by a special cell class called Cajal-Retzius cells which control cortical positioning and cause neurons to halt migration through Reelin molecular signaling[16-18]. Once a neuron reaches its target destination, integration into a neural network occurs through two types of neuronal processes necessary for communication inputs and outputs, dendritic arborization and axonal growth. Dendritic shape and pattern are determined from both intrinsic transcriptional factors and environmental cues which result in a stochastic distribution, reducing the chance of arbor clumping and promoting efficient sampling of the receptive field[19-21]. Axonal growth is led by a growth cone which samples the environment for positive and negative guidance cues until it reaches its target cell and a synapse is

formed[22]. Synapses continue to form throughout the prenatal period and neural circuitry is refined postnatally even into adulthood[23].

Refinement of neural pathways is achieved through a process called synaptic pruning whereby excess neurons and synaptic connections are eliminated to increase neuronal transmission efficiency[24]. This process is not random but is guided by sensory and cognitive input resulting in strengthening of useful pathways and removal of inefficient or superfluous ones[25]. Structurally, this manifests as thinning of the cerebral cortex. Cortical thickness is a general measure of neuronal density, dendritic arborization, and glial support[26]. Typical postnatal cortex development is marked by rapidly progressive thickening until the age of 14 months at which time it begins to plateau followed by a gradual decrease or stabilization in thickness[27]. This continues into adolescence when rapid and widespread cortical thinning occurs followed by stabilization into adulthood[28]. Maintaining adequate cortical thickness during stabilization periods is critical as reduced thickness is associated lower intelligence[29].

Structural changes to the cortex are not only marked by thinning but by increased gyrification resulting in surface area expansion. By the age of 2 years, cortical thickness is approximately 97% of adult values compared with surface area which is only 69%, suggesting that the majority of increase in cortical volume is attributable to surface area gains through folding of the cortex[30]. Cortical folding initially begins *in utero* and is essential for allowing the efficient packing of neurons in the intracranial space. The gross morphology of the human brain begins as a smooth lissencephalic structure to which primary, secondary, and tertiary folds or sulci are added. Primary sulci include the longitudinal fissure which separates cerebral hemispheres, sylvian, cingulate, parieto-occipital, calcarine, central and superior temporal, superior frontal, precentral, inferior frontal, postcentral, and intraparietal. Primary sulci are formed by gestational week 26 and followed by secondary sulci in weeks 30-35. Tertiary sulci begin in week 36 and continue postnatally[31]. Continued surface area expansion is important in the first years of life as it has been positively correlated with cognitive advantages[32]. As children age, cortical surface area continues to expand, peaking around 10 years of age following a distinct developmental trajectory from cortical thickness[33]. Overall, brain development is a complex process influenced by genetic and environmental forces which extend from the prenatal period into late adulthood.

Craniosynostosis

Craniosynostosis refers to the premature closure of cranial sutures which may occur prenatally (usually around gestational weeks 15-18) or postnatally and occurs 1 in 2000 to 1 in 2500 births[34,35]. Due to premature fusion, localized growth restriction of the skull occurs during a time when brain development is progressing rapidly. Brain size typically triples in the first year of life and quadruples by the age of two years[36]. Normally the expanding brain is the driving force behind cranial growth at suture sites. Synostosis then acts as a barrier to local expansion resulting in asymmetric cranial growth and malformation. This asymmetric growth is governed by Virchow's law which states compensatory growth is permitted parallel to a fused suture rather than perpendicular to it. Therefore, predictable skull growth patterns occur depending on which suture is involved. The most common type of craniosynostosis is scaphocephaly (boat shaped head with increased anterior-posterior diameter and decreased biparietal width) which occurs in up to 50% of cases and results from isolated fusion of the sagittal suture[36]. The second most common, occurring in 23-28% of cases, is trigonocephaly (keel shaped or triangular forehead) resulting from isolated fusion of the metopic suture[37,38]. In 13%-20% of cases, one or both of the coronal sutures may be involved[37]. In unicoronal synostosis, a harlequin deformity results which is characterized by lack of descent of the greater wing of the sphenoid. If both coronal sutures are involved simultaneously, brachycephaly occurs resulting in a broad flat forehead with recession of the supraorbital ridges, anterior-posterior shortening with elevation of skull height. The least common form of nonsyndromic craniosynostosis is lambdoid synostosis which occurs in less than 3% of patients[36]. This form is characterized by occipital plagiocephaly with ipsilateral flattening of the occiput and a mastoid bulge with a downward cant of the posterior skull base. This is not to be confused with deformational plagiocephaly which can occur in healthy children due to supine positioning and is characterized by a head shape resembling a parallelogram without a mastoid bulge.

In addition to non-syndromic craniosynostosis, syndromic forms with distinct phenotypes have been identified as well. Common forms of syndromic craniosynostosis include Apert, Crouzon, Pfeiffer, Muenke, and Saethre-Chotzen syndromes. Apert syndrome occurs in 1 in every 100,000 births and is due to either Ser252Trp or Pro253Arg autosomal dominant mutations in the fibroblast growth factor receptor 2 (*FGFR2*) gene[36,39]. A defining feature of Apert syndrome is the presence of complex syndactyly in the hands and/or feet. Bicoronal synostosis is most common and frequently contributes to severe turribrachycephaly with down-slanting palpebral fissures and a parrot beak deformity. The

most concerning feature of the syndrome clinically is the high incidence of raised intracranial pressure which can present in up to 83% of patients requiring timely operative intervention or ventriculoperitoneal shunting[40]. Severe midface hypoplasia also occurs in these patients resulting in a spoon-shaped deformity characterized by widening of the zygomas and maxillary shortening in the first years of life[41]. This can result in airway restriction and obstructive sleep apnea contributing to the already high rates of intracranial hypertension in these patients. Decreased intelligence quotient (IQ) is common (70%) however some go on to have normal intelligence[36].

Crouzon syndrome is also due to an autosomal dominant mutation in the *FGFR2* gene and is among the most common forms of syndromic craniosynostosis with an incidence of 1 in 25,000[36]. Morphologically these patients can suffer from a variety of synostosis combinations with the most common being pansynostosis or bicoronal synostosis[42]. Lu et al showed that cranial base shortening occurs across all subtypes of Crouzon syndrome but is least severe in isolated sagittal synostosis cases[42]. Additional features include midface hypoplasia, conductive hearing loss, exorbitism, and anterior open bite with class III malocclusion[36]. With treatment, many of these patients go on to develop normal levels of intelligence.

The majority of patients with Pfeiffer syndrome carry mutations in the *FGFR2* gene but around 5% have a less severe form of the disease and carry mutations in *FGFR1*[36]. The overall incidence of the disease is 1 in every 100,000 live births and the majority of patients have bicoronal synostoses with turribrachycephaly. Midface deformities are similar to Crouzon syndrome and include hypoplasia, exorbitism, hypertelorism, and down-slanting palpebral fissures. A defining characteristic is broad thumbs and halluces which may be accompanied by mild cutaneous syndactyly. Obstructive sleep apnea is common often requiring tracheostomy. Most develop normal intelligence despite undergoing an average of 2.5 cranial vault procedures and 1.6 neurosurgical procedures[43].

Muenke syndrome was only recently described in 1996 and is due to a pro250Arg mutation in *FGFR3* on chromosome 4p[44,45]. Interestingly, not all patients who have the mutation suffer from craniosynostosis. The syndrome occurs in 1 in 10,000 patients and most frequently results in unicoronal or bicoronal synostosis without midface hypoplasia. Bilateral sensorineural hearing loss occurs in up to 70%, as are neurobehavioral disorders such as attention deficit hyperactivity disorder

(ADHD). In a large multicenter natural history study of the syndrome, developmental delay occurred in two thirds of patients and persistent intellectual disability was present in 36% of patients[46].

Saethre-Chotzen occurs in 1 in 25,00 to 1 in 50,000 births and is due to an autosomal dominant mutation in the *TWIST1* gene on chromosome 7p21[36]. *TWIST1* is normally involved in mesodermal development and mutations cause dysregulation in cranial bone deposition. Morphologically, Saethre-Chotzen syndrome is characterized by asymmetrical brachycephaly due to either unicoronal or bicoronal synostosis. Distinguishing features of the syndrome include a low frontal hairline, ptosis, and a prominent crus helicis which extends into the conchal bowl[36]. Midface asymmetry without hypoplasia is common and the majority of patients develop normal intelligence.

Treatment for craniosynostosis involves early operative intervention but strategies and timing can vary significantly among craniofacial centers. Some centers perform a strip craniectomy in the first few months of life followed by helmeting to achieve a normal cranial shape while others perform whole vault cranioplasty without the need for postoperative helmet therapy. Still others perform spring-assisted expansion where coils are placed intraoperatively along osteotomies to actively maintain suture patency postoperatively. Advantages of strip craniectomy are earlier intervention (typically around 4 months) with less blood loss and drawbacks include the necessity of strict adherence to helmet therapy protocol and reossification or the potential need for additional operations at a later date[47]. Whole vault cranioplasty can be performed at 6 months of age and addresses the cranial deformity comprehensively in a single stage. Drawbacks for this technique are longer operative times and greater blood loss[48,49]. Lastly, spring-assisted expansion can be performed before the age of 6 months and has been shown to result in low blood loss with good aesthetic results[50]. A major drawback from this technique is the need for a second procedure for device removal and inability to change the expansion vector or rate after placement. Debate continues among craniofacial surgeons regarding optimal treatment algorithms and techniques.

Intracranial Hypertension

A common but dangerous sequela of syndromic craniosynostosis pathology is the development of intracranial hypertension (ICH). Although this may occur in non-syndromic cases, syndromic patients are at higher risk for its development both before and even after surgery[40,51-53]. ICH is dangerous

because, if left untreated, it may result in developmental or behavioral issues accompanied by the risk of visual loss and blindness[54,55].

The state of ICH may be best understood by the Monroe-Kellie doctrine which describes the pressure-volume relationship between the fixed intracranial space and its contents which include brain tissue, cerebrospinal fluid (CSF), and blood with accompanying vasculature[56,57]. These three components exist in equilibrium with one another such that when the volume of one rises the subsequent increase in pressure drives another outward from the intracranial space. Most commonly this results in changes to blood flow or CSF dynamics but may, on occasion, affect brain tissue resulting in cerebellar tonsillar herniation[58]. This occurs most frequently in syndromic variants where underdevelopment of the posterior fossa leads to overcrowding predisposing patients to this phenomenon[59,60].

Craniocerebral Disproportion

Raised intracranial pressure may occur in craniosynostosis patients due to a variety of factors, the first of which is craniocerebral disproportion. The primary insult of craniosynostosis is growth restriction of the calvarium which opposes outward expansion of the growing brain. As the brain continues to grow inside the fixed cranial vault, mechanical pressure increases and the cerebri are pressed against the inner table. In untreated cases or patients with longstanding ICH this may result in fingerlike impressions called *impressiones digitae* which may be detectable on radiologic imaging or intraoperatively[61]. Besides primary skull growth restriction from craniosynostosis pathology, postoperative reossification may also occur. In any case, growth restriction may be detected by trending occipito-frontal circumference (OFC) measurements at regular clinic visits. OFC measurements have been shown to correlate with intracranial volume in syndromic patients and downward deflections of its progression curve is indicative of growth restriction[62,63]. Clinical management of skull growth restriction typically involves cranial vault expansion.

Ventriculomegaly and Hydrocephalus

The purpose of CSF is to provide mechanical cushioning for the central nervous system structures and aid in nutrient transport and waste removal[64,65]. CSF is produced by the choroid plexus primarily in the lateral ventricles with additional contributions from the 3rd and 4th ventricles[65,66]. From the lateral ventricles it flows through the foramen of Monro to the 3rd ventricle and then through the Sylvian

aqueduct into the 4th ventricle. From there it flows out into the subarachnoid space through two lateral apertures and one median aperture. Absorption occurs at arachnoid granulations via a pressure dependent gradient and it is then collected in the sinuses[67,68].

Ventriculomegaly refers to the static enlargement of the lateral ventricles in proportion to overall brain size. Hydrocephalus refers to progressive enlargement of the lateral ventricles and may be due to overproduction, inadequate absorption, or obstruction of CSF flow. Hydrocephalus can be broadly categorized as communicating or non-communicating (e.g. shunt-independent or shunt-dependent). Ventricular dilation in syndromic craniosynostosis is quite common, whereas in non-syndromic patients its occurrence is similar to that of the general population[69]. It has been reported at a rate of 30-70% in Crouzon-Pfeiffer syndrome, and in 40-90% of Apert patients[69-74]. It is thought that hydrocephalus in these cases occurs primarily as a result of CSF outflow obstruction or malabsorption due to osseous pathology or venous sinus hypertension[75]. Nonprogressive ventriculomegaly is likely due to primary maldevelopment or parenchymal atrophy[76,77]. Clinically, the development of hydrocephalus with accompanying signs of raised intracranial pressure may be managed by ventriculo-peritoneal shunt placement. Static ventriculomegaly is less worrisome and may be managed more conservatively along with careful observation of intracranial pressure signs or symptoms[78].

Venous Outflow Obstruction

Intracranial blood drains to the jugular veins through a dural sinus network including the superior sagittal sinus, inferior sagittal sinus, transverse sinus, and cavernous sinus. Although the majority of intracranial blood is drained via this system, additional collateral veins contribute as well. Obstruction of venous outflow at any point in this system results in increased pressure and altered hemodynamics, particularly in the superior sagittal sinus[79]. A potential site for obstruction in craniosynostosis is at the jugular foramen[80]. Florisson et al showed that syndromic or complex craniosynostosis patients are at higher risk of venous hypertension due to bony narrowing of the jugular foramen[81]. In addition to this narrowing, anomalous venous collaterals have been shown to exist at a high rate in syndromic patients[82,83]. It was initially thought that venous outflow obstruction and the subsequent rise in intracranial pressure drove development of these collaterals but was later shown that their presence was not associated with papilledema, suggesting an inborn abnormality rather than a compensatory mechanism[81]. Clinically, venography is commonly used for patients in whom a posterior vault

expansion procedure is planned in order to avoid unnecessary bleeding due to aberrant vasculature[83,84].

Obstructive Sleep Apnea

Obstructive sleep apnea (OSA) is a disorder characterized by turbulent airflow upon inspiration while sleeping[85]. This results in inadequate ventilation and oxygenation, leading to symptoms of snoring, nocturnal awakening, headache, fatigue, and increased cardiovascular risk due to hypertension[86]. In craniosynostosis patients, OSA causes ICH through hypercapnia and hypoxia which results in cerebral vasodilation and increased cerebral blood flow[87]. Vasodilation contributes to elevated intracranial pressure resulting in reduced cerebral perfusion pressure and autoregulation results in the compensatory response of further vasodilation[88-90]. This downward spiral continues until arousal breaks the cycle.

OSA occurs in 28-68% of syndromic patients and is primarily attributable to midface hypoplasia although mandibular hypoplasia, pharyngeal collapse, and adenotonsillar hypertrophy have been implicated as well[87,91,92]. It was initially thought that central sleep apnea may play a role due to hindbrain herniation, but Driessen et. al showed that no pathological increase exists, despite a high prevalence of OSA[93]. Diagnosis of OSA is made by polysomnography following clinical suspicion due to predisposing factors and symptomatic history (e.g. snoring). An obstructive apnea hypopnea index (oAHI) greater than 5 is indicative of moderate disease and has been associated with ICH and elevated risk of optic neuropathy[87,94,95]. Definitive treatment includes midface advancement with craniofacial surgery. Although midface advancement procedures are typically performed at skeletal maturity, LeFort III and monobloc techniques have been used in the syndromic pediatric population with good results[96-99]. Less invasive treatment options include prone positioning, adenotonsillectomy, nasopharyngeal airways, and continuous positive airway pressure (CPAP)[92]. In rare but severe cases of airway compromise, tracheostomy may be required.

FreeSurfer MRI Analysis

In the last couple of decades, the emergence of medical informatics technology has drastically improved our ability to study the brain *in vivo*. In particular, the development of a software suite called FreeSurfer (FS) has provided us with the capability to quantify structural, functional, and

connective properties of the human brain through surface-based analysis (SBA). An alternative method called voxel-based morphometry (VBM) was previously used which employs volumetric and concentration-based techniques[100]. A voxel is the 3-dimensional analog of a pixel (picture element) which encodes volumetric information that varies in signal intensity based on tissue density in the setting of MRI. VBM works directly on the voxel grid with a high degree of efficiency and less processing time but is considered less accurate than SBA for several reasons[101,102].

One of the problems with VBM is called the partial volume effect. This refers to impaired spatial resolution and erroneous signal intensity due to the averaging of multiple tissue densities within the same voxel space. For example, a voxel on the border of gray and white matter structures in the brain will contain fractional amounts of each tissue type and the signal from the entire voxel will reflect the weighted average from both components thereby limiting resolution. A strategy to decrease this artifact is to improve resolution by reducing voxel size. This is achieved by taking thinner slices, using smaller fields of view or higher imaging matrix sizes as these components determine the three dimensions of each voxel. Lastly, VBM is also considered to be less robust to noise and mis-segmentation compared to SBA[103].

Alternatively, SBA morphometrics are derived from geometric models of the cortical surface. These models are constructed as triangulated mesh at both the gray matter/dural border, termed the pial surface, and at the gray matter/white matter boundary, termed the white matter (WM) surface. First, an estimate of the WM boundary is generated by fully automated segmentation of all WM using probabilistic atlases. All WM voxels are then classified into a single volume using a connected components algorithm[104]. The surface of interconnected voxels is then refined to achieve subvoxel accuracy of the WM boundary and is deformed outwardly until the pial surface is reached via a deformable surface algorithm which is guided by local MRI intensity values[105,106]. Subvoxel (i.e. submillimeter) accuracy of these surfaces is crucial for cortical analysis and is achieved through interpolation assuming the radius of the curvature of the surface as well as thickness of the tissue classes is greater than the size of the voxels and sufficient contrast to noise exists between tissue classes[105]. Some topological errors are initially present upon primary surface reconstruction but undergo automated correction in the FS pipeline as they occur[107]. The errors that arise are holes which either need to be filled or which require cutting of the handle/bridge between gyri. To

determine which correction is appropriate, intensity volume guidance is used. The deformational change (i.e., distance between WM and pial surfaces) represents the cortical ribbon from which many descriptive statistics may be calculated including volume, thickness, surface area, and curvature. A major drawback to using FS is the runtime required to process each MRI which can take up to 48 hours. With the aid of computing clusters this time can be reduced by processing multiple subjects in parallel simultaneously.

Aims of this thesis

The purpose of this thesis is to improve our understanding of structural brain development in the context of syndromic craniosynostosis. To this end, FreeSurfer MRI analysis will be used to model cortex and subcortical morphology as well as potential changes which may occur due to various pathologic variables or treatment protocols.

In **chapter 2** cortical thickness is evaluated as an *in vivo* biomarker for intracranial hypertension in syndromic craniosynostosis patients. 3D MRIs are evaluated by the FreeSurfer pipeline to generate cortical thickness estimates. The outcome is compared with other clinical and radiological data indicative of intracranial hypertension including papilledema, hydrocephalus, tonsillar position, skull circumference growth, and sleep apnea.

Because Crouzon-Pfeiffer patients often develop with normal levels of intelligence despite their syndromic status and high rates of intracranial hypertension, in **chapter 3** we evaluate cortical thickness in this syndromic subset in relation to type of primary cranial vault expansion[108,109]. It has previously been shown that posterior vault expansion yields greater intracranial volumes than fronto-orbital advancement, so we seek to determine if regional cortical thickness is similarly affected[110]. Additionally, synostosis pattern is evaluated for potential thinning of the cortex proximate to local skull growth restriction sites.

In **chapter 4**, both global and regional corpus callosum architecture in syndromic patients is evaluated in the context of intracranial hypertension and compared with typically developing controls. Studying how intracranial hypertension influences both gray and white matter in the syndromic brain will inform treatment protocols and improve our understanding of how cranial dysmorphology may increase risk to specific regions of the corpus callosum.

In **chapter 5**, Crouzon patients with sagittal synostosis undergoing either spring-assisted cranial vault expansion or fronto-biparietal remodeling are reviewed and postoperative results are evaluated including cranial index, papilledema, sleep apnea, skull growth arrest, ventriculomegaly, aesthetic outcome, and need for additional vault procedures. Advantages and drawbacks of each procedure are discussed, and recommendations made based on suture involvement in Crouzon syndrome.

Chapter 6 will explore the complexity of the cerebral cortex in syndromic craniosynostosis and controls by analyzing allometric scaling of cortical surface area relative to intracranial volume. Genetic mutations responsible for syndromic craniosynostosis occur in genes involved in mesodermal and ectodermal development, therefore, syndromes will be evaluated according to genetic mutations as well as specific syndrome to determine if cortical maldevelopment occurs in either class globally or regionally. Lastly these findings will be discussed in the context of educational outcomes to determine if reduced scaling is reflected in scholastic achievement level.

Chapter 7 will include the general discussion where the results from all the previous chapters will be integrated and analyzed together.

References:

1. Jin S-W, Sim K-B, Kim S-D. Development and Growth of the Normal Cranial Vault : An Embryologic Review. *J Korean Neurosurg Soc.* 2016;59(3):192-196.
2. Bronner ME, Simões-Costa M. The Neural Crest Migrating into the Twenty-First Century. *Curr Top Dev Biol.* 2016;116:115-134.
3. Kague E, Gallagher M, Burke S, Parsons M, Franz-Odendaal T, Fisher S. Skeletogenic fate of zebrafish cranial and trunk neural crest. *PloS one.* 2012;7(11):e47394.
4. Ishii M, Sun J, Ting M-C, Maxson RE. Chapter Six - The Development of the Calvarial Bones and Sutures and the Pathophysiology of Craniosynostosis. In: Chai Y, ed. *Current Topics in Developmental Biology.* Vol 115. Academic Press; 2015:131-156.
5. Berendsen AD, Olsen BR. Bone development. *Bone.* 2015;80:14-18.
6. Tubbs RS, Bosmia AN, Cohen-Gadol AA. The human calvaria: a review of embryology, anatomy, pathology, and molecular development. *Child's Nervous System.* 2012;28(1):23-31.
7. Weinzweig J, Kirschner RE, Farley A, et al. Metopic synostosis: Defining the temporal sequence of normal suture fusion and differentiating it from synostosis on the basis of computed tomography images. *Plastic and reconstructive surgery.* 2003;112(5):1211-1218.
8. Cohen MM, Jr. Sutural biology and the correlates of craniosynostosis. *Am J Med Genet.* 1993;47(5):581-616.
9. David L. Brown GHB, Benjamin Levi *Michigan Manual of Plastic Surgery* 2nd ed: Lippincott Williams & Wilkins; 2014.
10. Madeline LA, Elster AD. Suture closure in the human chondrocranium: CT assessment. *Radiology.* 1995;196(3):747-756.
11. Glorieux FH. *Pediatric bone: biology & diseases.* Elsevier; 2003.
12. Sadler TW. *Langman's medical embryology.* Vol 333: Lippincott Williams & Wilkins Philadelphia; 2006.
13. Standring S. *Gray's Anatomy The Anatomical Basis of Clinical Practice.* 41 ed2016.
14. Stiles J, Jernigan TL. The basics of brain development. *Neuropsychol Rev.* 2010;20(4):327-348.
15. Nadarajah B, Parnavelas JG. Modes of neuronal migration in the developing cerebral cortex. *Nat Rev Neurosci.* 2002;3(6):423-432.
16. Bielle F, Griveau A, Narboux-Nême N, et al. Multiple origins of Cajal-Retzius cells at the borders of the developing pallium. *Nat Neurosci.* 2005;8(8):1002-1012.
17. Huang Z. Molecular regulation of neuronal migration during neocortical development. *Mol Cell Neurosci.* 2009;42(1):11-22.
18. Valiente M, Marín O. Neuronal migration mechanisms in development and disease. *Curr Opin Neurobiol.* 2010;20(1):68-78.
19. Lefebvre JL, Sanes JR, Kay JN. Development of dendritic form and function. *Annu Rev Cell Dev Biol.* 2015;31:741-777.
20. Wen Q, Stepanyants A, Elston GN, Grosberg AY, Chklovskii DB. Maximization of the connectivity repertoire as a statistical principle governing the shapes of dendritic arbors. *Proceedings of the National Academy of Sciences.* 2009;106(30):12536-12541.
21. Snider J, Pillai A, Stevens CF. A Universal Property of Axonal and Dendritic Arbors. *Neuron.* 2010;66(1):45-56.
22. Brown M, Lumsden A, Keynes R. *The developing brain.* Oxford University Press; 2001.

23. Butz M, van Ooyen A. A simple rule for dendritic spine and axonal bouton formation can account for cortical reorganization after focal retinal lesions. *PLoS Comput Biol.* 2013;9(10):e1003259.
24. Santos E, Noggle CA. Synaptic Pruning. In: Goldstein S, Naglieri JA, eds. *Encyclopedia of Child Behavior and Development.* Boston, MA: Springer US; 2011:1464-1465.
25. Zillmer E, Spiers M, Culbertson W. *Principles of neuropsychology.* Nelson Education; 2007.
26. Duncan NW, Gravel P, Wiebking C, Reader AJ, Northoff G. Grey matter density and GABAA binding potential show a positive linear relationship across cortical regions. *Neuroscience.* 2013;235:226-231.
27. Wang F, Lian C, Wu Z, et al. Developmental topography of cortical thickness during infancy. *Proceedings of the National Academy of Sciences of the United States of America.* 2019;116(32):15855-15860.
28. Forde NJ, Ronan L, Zwiers MP, et al. Healthy cortical development through adolescence and early adulthood. *Brain Struct Funct.* 2017;222(8):3653-3663.
29. Bajaj S, Raikes A, Smith R, et al. The Relationship Between General Intelligence and Cortical Structure in Healthy Individuals. *Neuroscience.* 2018;388:36-44.
30. Lyall AE, Shi F, Geng X, et al. Dynamic Development of Regional Cortical Thickness and Surface Area in Early Childhood. *Cerebral cortex (New York, NY : 1991).* 2015;25(8):2204-2212.
31. Chi JG, Dooling EC, Gilles FH. Gyral development of the human brain. *Ann Neurol.* 1977;1(1):86-93.
32. Girault JB, Cornea E, Goldman BD, et al. Cortical Structure and Cognition in Infants and Toddlers. *Cerebral cortex (New York, NY : 1991).* 2020;30(2):786-800.
33. Wierenga LM, Langen M, Oranje B, Durston S. Unique developmental trajectories of cortical thickness and surface area. *NeuroImage.* 2014;87:120-126.
34. Kweldam CF, van der Vlugt JJ, van der Meulen JJ. The incidence of craniosynostosis in the Netherlands, 1997-2007. *J Plast Reconstr Aesthet Surg.* 2011;64(5):583-588.
35. Cornelissen M, Ottelander B, Rizopoulos D, et al. Increase of prevalence of craniosynostosis. *Journal of cranio-maxillo-facial surgery : official publication of the European Association for Cranio-Maxillo-Facial Surgery.* 2016;44(9):1273-1279.
36. Janis JE. *Essentials of Plastic Surgery.* 2nd ed2017.
37. Selber J, Reid RR, Chike-Obi CJ, et al. The changing epidemiologic spectrum of single-suture synostoses. *Plastic and reconstructive surgery.* 2008;122(2):527-533.
38. Beckett JS, Chadha P, Persing JA, Steinbacher DM. Classification of trigonocephaly in metopic synostosis. *Plastic and reconstructive surgery.* 2012;130(3):442e-447e.
39. Anderson J, Burns HD, Enriquez-Harris P, Wilkie AOM, Heath JK. Apert Syndrome Mutations in Fibroblast Growth Factor Receptor 2 Exhibit increased Affinity for FGF Ligand. *Human Molecular Genetics.* 1998;7(9):1475-1483.
40. Marucci DD, Dunaway DJ, Jones BM, Hayward RD. Raised intracranial pressure in Apert syndrome. *Plastic and reconstructive surgery.* 2008;122(4):1162-1168; discussion 1169-1170.
41. Lu X, Forte AJ, Sawh-Martinez R, et al. Spatial and temporal changes of midface in Apert's syndrome. *Journal of Plastic Surgery and Hand Surgery.* 2019;53(3):130-137.
42. Lu X, Sawh-Martinez R, Forte AJ, et al. Classification of Subtypes of Crouzon Syndrome Based on the Type of Vault Suture Synostosis. *The Journal of craniofacial surgery.* 2020;31(3):678-684.
43. Fearon JA, Rhodes J. Pfeiffer syndrome: a treatment evaluation. *Plastic and reconstructive surgery.* 2009;123(5):1560-1569.

44. Bellus GA, Gaudenz K, Zackai EH, et al. Identical mutations in three different fibroblast growth factor receptor genes in autosomal dominant craniosynostosis syndromes. *Nature genetics.* 1996;14(2):174-176.
45. Muenke M, Gripp KW, McDonald-McGinn DM, et al. A unique point mutation in the fibroblast growth factor receptor 3 gene (FGFR3) defines a new craniosynostosis syndrome. *Am J Hum Genet.* 1997;60(3):555-564.
46. Kruszka P, Addissie YA, Yarnell CM, et al. Muenke syndrome: An international multicenter natural history study. *American journal of medical genetics Part A.* 2016;170a(4):918-929.
47. O'Connell JE, Ellenbogen J, Parks C. Early Extended Midline Strip Craniectomy for Sagittal Synostosis. *The Journal of craniofacial surgery.* 2020;31(5):1223-1227.
48. van Veelen ML, Mathijssen IM. Spring-assisted correction of sagittal suture synostosis. *Child's nervous system : ChNS : official journal of the International Society for Pediatric Neurosurgery.* 2012;28(9):1347-1351.
49. Windh P, Davis C, Sanger C, Sahlin P, Lauritzen C. Spring-assisted cranioplasty vs pi-plasty for sagittal synostosis--a long term follow-up study. *The Journal of craniofacial surgery.* 2008;19(1):59-64.
50. van Veelen MC, Kamst N, Touw C, et al. Minimally Invasive, Spring-Assisted Correction of Sagittal Suture Synostosis: Technique, Outcome, and Complications in 83 Cases. *Plastic and reconstructive surgery.* 2018;141(2):423-433.
51. Christian EA, Imahiyerobo TA, Nallapa S, Urata M, McComb JG, Krieger MD. Intracranial hypertension after surgical correction for craniosynostosis: a systematic review. *Neurosurgical focus.* 2015;38(5):E6.
52. Thomas GP, Johnson D, Byren JC, et al. The incidence of raised intracranial pressure in nonsyndromic sagittal craniosynostosis following primary surgery. *Journal of neurosurgery Pediatrics.* 2015;15(4):350-360.
53. Abu-Sittah GS, Jeelani O, Dunaway D, Hayward R. Raised intracranial pressure in Crouzon syndrome: incidence, causes, and management. *Journal of neurosurgery Pediatrics.* 2016;17(4):469-475.
54. Tay T, Martin F, Rowe N, et al. Prevalence and causes of visual impairment in craniosynostotic syndromes. *Clin Exp Ophthalmol.* 2006;34(5):434-440.
55. Bartels MC, Vaandrager JM, de Jong TH, Simonsz HJ. Visual loss in syndromic craniosynostosis with papilledema but without other symptoms of intracranial hypertension. *The Journal of craniofacial surgery.* 2004;15(6):1019-1022; discussion 1023-1014.
56. Mokri B. The Monro-Kellie hypothesis: applications in CSF volume depletion. *Neurology.* 2001;56(12):1746-1748.
57. Neff S, Subramaniam RP. Monro-Kellie doctrine. *Journal of neurosurgery.* 1996;85(6):1195.
58. Munakomi S, J MD. Brain Herniation. In: *StatPearls.* Treasure Island (FL): StatPearls Publishing Copyright © 2020, StatPearls Publishing LLC.; 2020.
59. Lo WB, Thant KZ, Kaderbhai J, et al. Posterior calvarial distraction for complex craniosynostosis and cerebellar tonsillar herniation. *Journal of neurosurgery Pediatrics.* 2020:1-10.
60. Doerga PN, Rijken BFM, Bredero-Boelhouwer H, et al. Neurological deficits are present in syndromic craniosynostosis patients with and without tonsillar herniation. *Eur J Paediatr Neurol.* 2020;28:120-125.
61. Hoefkens MF, Vermeij-Keers C, Vaandrager JM. Crouzon syndrome: phenotypic signs and symptoms of the postnatally expressed subtype. *The Journal of craniofacial surgery.* 2004;15(2):233-240; discussion 241-232.

62. Breakey RWF, Knoops PGM, Borghi A, et al. Intracranial Volume and Head Circumference in Children with Unoperated Syndromic Craniosynostosis. *Plastic and reconstructive surgery.* 2018;142(5):708e-717e.
63. Rijken BF, den Ottelander BK, van Veelen ML, Lequin MH, Mathijssen IM. The occipitofrontal circumference: reliable prediction of the intracranial volume in children with syndromic and complex craniosynostosis. *Neurosurgical focus.* 2015;38(5):E9.
64. Spector R, Robert Snodgrass S, Johanson CE. A balanced view of the cerebrospinal fluid composition and functions: Focus on adult humans. *Exp Neurol.* 2015;273:57-68.
65. Khasawneh AH, Garling RJ, Harris CA. Cerebrospinal fluid circulation: What do we know and how do we know it? *Brain Circ.* 2018;4(1):14-18.
66. Cushing H. Studies on the Cerebro-Spinal Fluid : I. Introduction. *J Med Res.* 1914;31(1):1-19.
67. Brinker T, Stopa E, Morrison J, Klinge P. A new look at cerebrospinal fluid circulation. *Fluids and barriers of the CNS.* 2014;11:10.
68. Czosnyka Z, Czosnyka M, Lavinio A, Keong N, Pickard JD. Clinical testing of CSF circulation. *Eur J Anaesthesiol Suppl.* 2008;42:142-145.
69. Cinalli G, Sainte-Rose C, Kollar EM, et al. Hydrocephalus and craniosynostosis. *Journal of neurosurgery.* 1998;88(2):209-214.
70. Montaut J. Dysmorphies cranio-faciales. Les synostoses prématurées (craniosténoses et facioténoses). 1977.
71. Noetzel MJ, Marsh JL, Palkes H, Gado M. Hydrocephalus and mental retardation in craniosynostosis. *J Pediatr.* 1985;107(6):885-892.
72. Proudman TW, Clark BE, Moore MH, Abbott AH, David DJ. Central nervous system imaging in Crouzon's syndrome. *The Journal of craniofacial surgery.* 1995;6(5):401-405.
73. Cohen MM. Craniosynostosis. *Diagnosis, Evaluatuion, and Management.* 1986:60-62.
74. Renier D, Arnaud E, Cinalli G, Sebag G, Zerah M, Marchac D. Prognosis for mental function in Apert's syndrome. *Journal of neurosurgery.* 1996;85(1):66-72.
75. Collmann H, Sorensen N, Krauss J. Hydrocephalus in craniosynostosis: a review. *Child's nervous system : ChNS : official journal of the International Society for Pediatric Neurosurgery.* 2005;21(10):902-912.
76. Cohen Jr MM, Kreiborg S. The central nervous system in the Apert syndrome. *American journal of medical genetics.* 1990;35(1):36-45.
77. Tokumaru AM, Barkovich AJ, Ciricillo SF, Edwards M. Skull base and calvarial deformities: association with intracranial changes in craniofacial syndromes. *American Journal of Neuroradiology.* 1996;17(4):619-630.
78. Spruijt B, Joosten KF, Driessen C, et al. Algorithm for the Management of Intracranial Hypertension in Children with Syndromic Craniosynostosis. *Plastic and reconstructive surgery.* 2015;136(2):331-340.
79. Mursch K, Brockmann K, Lang JK, Markakis E, Behnke-Mursch J. Visually evoked potentials in 52 children requiring operative repair of craniosynostosis. *Pediatric neurosurgery.* 1998;29(6):320-323.
80. Rich PM, Cox TC, Hayward RD. The jugular foramen in complex and syndromic craniosynostosis and its relationship to raised intracranial pressure. *AJNR American journal of neuroradiology.* 2003;24(1):45-51.
81. Florisson JM, Barmpalios G, Lequin M, et al. Venous hypertension in syndromic and complex craniosynostosis: the abnormal anatomy of the jugular foramen and collaterals. *Journal of*

cranio-maxillo-facial surgery : official publication of the European Association for Cranio-Maxillo-Facial Surgery. 2015;43(3):312-318.
82. Taylor WJ, Hayward RD, Lasjaunias P, et al. Enigma of raised intracranial pressure in patients with complex craniosynostosis: the role of abnormal intracranial venous drainage. *Journal of neurosurgery.* 2001;94(3):377-385.
83. Jeevan DS, Anlsow P, Jayamohan J. Abnormal venous drainage in syndromic craniosynostosis and the role of CT venography. *Child's nervous system : ChNS : official journal of the International Society for Pediatric Neurosurgery.* 2008;24(12):1413-1420.
84. Rollins N, Booth T, Shapiro K. MR venography in children with complex craniosynostosis. *Pediatr Neurosurg.* 2000;32(6):308-315.
85. Maspero C, Giannini L, Galbiati G, Rosso G, Farronato G. Obstructive sleep apnea syndrome: a literature review. *Minerva Stomatol.* 2015;64(2):97-109.
86. Patel SR. Obstructive Sleep Apnea. *Ann Intern Med.* 2019;171(11):Itc81-itc96.
87. Spruijt B, Mathijssen IM, Bredero-Boelhouwer HH, et al. Sleep Architecture Linked to Airway Obstruction and Intracranial Hypertension in Children with Syndromic Craniosynostosis. *Plastic and reconstructive surgery.* 2016;138(6):1019e-1029e.
88. Hayward R. Venous hypertension and craniosynostosis. *Child's nervous system : ChNS : official journal of the International Society for Pediatric Neurosurgery.* 2005;21(10):880-888.
89. Rosner MJ. Pathophysiology and management of increased intracranial pressure. *Neurosurgical intensive care.* 1993.
90. Rosner MJ, Becker D. Cerebral perfusion pressure: link between intracranial pressure and systemic circulation. *Cerebral blood flow.* 1987:425-448.
91. Bannink N, Maliepaard M, Raat H, Joosten KF, Mathijssen IM. Reliability and validity of the obstructive sleep apnea-18 survey in healthy children and children with syndromic craniosynostosis. *J Dev Behav Pediatr.* 2011;32(1):27-33.
92. Nash R, Possamai V, Manjaly J, Wyatt M. The Management of Obstructive Sleep Apnea in Syndromic Craniosynostosis. *The Journal of craniofacial surgery.* 2015;26(6):1914-1916.
93. Driessen C, Mathijssen IM, De Groot MR, Joosten KF. Does central sleep apnea occur in children with syndromic craniosynostosis? *Respir Physiol Neurobiol.* 2012;181(3):321-325.
94. Nguyen JQN, Resnick CM, Chang YH, et al. Impact of Obstructive Sleep Apnea on Optic Nerve Function in Patients With Craniosynostosis and Recurrent Intracranial Hypertension. *Am J Ophthalmol.* 2019;207:356-362.
95. Malhotra RK, Kirsch DB, Kristo DA, et al. Polysomnography for Obstructive Sleep Apnea Should Include Arousal-Based Scoring: An American Academy of Sleep Medicine Position Statement. *J Clin Sleep Med.* 2018;14(7):1245-1247.
96. Mitsukawa N, Kaneko T, Saiga A, Akita S, Satoh K. Early midfacial distraction for syndromic craniosynostotic patients with obstructive sleep apnoea. *J Plast Reconstr Aesthet Surg.* 2013;66(9):1206-1211.
97. Nout E, Bannink N, Koudstaal MJ, et al. Upper airway changes in syndromic craniosynostosis patients following midface or monobloc advancement: correlation between volume changes and respiratory outcome. *Journal of cranio-maxillo-facial surgery : official publication of the European Association for Cranio-Maxillo-Facial Surgery.* 2012;40(3):209-214.
98. Flores RL, Shetye PR, Zeitler D, et al. Airway changes following Le Fort III distraction osteogenesis for syndromic craniosynostosis: a clinical and cephalometric study. *Plastic and reconstructive surgery.* 2009;124(2):590-601.

99. Mathijssen I, Arnaud E, Marchac D, et al. Respiratory outcome of mid-face advancement with distraction: a comparison between Le Fort III and frontofacial monobloc. *The Journal of craniofacial surgery.* 2006;17(5):880-882.
100. Ashburner J, Friston KJ. Voxel-based morphometry--the methods. *NeuroImage.* 2000;11(6 Pt 1):805-821.
101. Lai KL, Niddam DM, Fuh JL, Chen WT, Wu JC, Wang SJ. Cortical morphological changes in chronic migraine in a Taiwanese cohort: Surface- and voxel-based analyses. *Cephalalgia.* 2020;40(6):575-585.
102. Clarkson MJ, Cardoso MJ, Ridgway GR, et al. A comparison of voxel and surface based cortical thickness estimation methods. *NeuroImage.* 2011;57(3):856-865.
103. Acosta O, Bourgeat P, Zuluaga MA, Fripp J, Salvado O, Ourselin S. Automated voxel-based 3D cortical thickness measurement in a combined Lagrangian–Eulerian PDE approach using partial volume maps. *Medical Image Analysis.* 2009;13(5):730-743.
104. Dale AM, Fischl B, Sereno MI. Cortical surface-based analysis. I. Segmentation and surface reconstruction. *NeuroImage.* 1999;9(2):179-194.
105. Fischl B, Dale AM. Measuring the thickness of the human cerebral cortex from magnetic resonance images. *Proceedings of the National Academy of Sciences of the United States of America.* 2000;97(20):11050-11055.
106. Dale AM, Sereno MI. Improved Localizadon of Cortical Activity by Combining EEG and MEG with MRI Cortical Surface Reconstruction: A Linear Approach. *Journal of cognitive neuroscience.* 1993;5(2):162-176.
107. Fischl B, Liu A, Dale AM. Automated manifold surgery: constructing geometrically accurate and topologically correct models of the human cerebral cortex. *IEEE transactions on medical imaging.* 2001;20(1):70-80.
108. Fernandes MB, Maximino LP, Perosa GB, Abramides DV, Passos-Bueno MR, Yacubian-Fernandes A. Apert and Crouzon syndromes-Cognitive development, brain abnormalities, and molecular aspects. *American journal of medical genetics Part A.* 2016;170(6):1532-1537.
109. Maliepaard M, Mathijssen IM, Oosterlaan J, Okkerse JM. Intellectual, behavioral, and emotional functioning in children with syndromic craniosynostosis. *Pediatrics.* 2014;133(6):e1608-1615.
110. Spruijt B, Rijken BF, den Ottelander BK, et al. First Vault Expansion in Apert and Crouzon-Pfeiffer Syndromes: Front or Back? *Plastic and reconstructive surgery.* 2016;137(1):112e-121e.

CHAPTER 2

Intracranial Hypertension and Cortical Thickness in Syndromic Craniosynostosis

Wilson AT, den Ottelander BK, de Goederen R, van Veelen MLC, Dremmen MHG, Persing JA, Vrooman HA, Mathijssen IMJ

Developmental Medicine and Child Neurology, 2020

Abstract

Aim: This study evaluates the impact of ICH risk factors on cerebral cortex thickness in syndromic craniosynostosis.

Methods: ICH risk factors including papilledema, hydrocephalus, obstructive sleep apnea (OSA), cerebellar tonsillar position, occipitofrontal circumference curve deflection (OFC), age, and sex were collected from syndromic (Apert, Crouzon, Pfeiffer, Muenke, Saethre-Chotzen) craniosynostosis patient records and imaging. MRI scans were analyzed via FreeSurfer software and exported for statistical analysis. A linear mixed model was developed to determine effect on cerebral cortex thickness changes (significance $p < 0.05$).

Results: 107 patients (171 scans) were evaluated. Average cortical thickness in this cohort was 2.78 ± 0.17 mm with an average age of 8.88 years. Previous findings of papilledema ($p = 0.036$) and of hydrocephalus ($p = 0.007$) were independently associated with cortical thinning. Cortical thickness did not vary significantly by sex ($p = 0.534$), syndrome ($p = 0.896$), OSA ($p = 0.464$), OFC ($p = 0.375$), or tonsillar position ($p = 0.682$).

Interpretation: Detection of papilledema or hydrocephalus in syndromic craniosynostosis is associated with significant changes in cortical thickness supporting the need for preventative rather than reactive treatment strategies.

Introduction

Craniosynostosis is a congenital disease of premature fusion of calvarial sutures, which occurs in 1 / 2000 to 1 / 2500 births[1]. This results in craniocerebral disproportion and skull deformity based on the location and number of sutures involved. Syndromic variants of the disease (most commonly Apert, Crouzon, Pfeiffer, Muenke, and Saethre-Chotzen), which are attributable to single gene mutations or chromosomal abnormalities, comprise 20% of these cases and are characterized by additional defects such as limb, ear, or midface deformities[1,2]. Of particular concern in the syndromic population is the increased incidence of intracranial hypertension (ICH) which may lead to cognitive or visual impairment[3,4]. Previous studies have demonstrated a prevalence of 61-83% of ICH in syndromic patients prior to surgery with 35-47% developing recurrent ICH following a vault expansion procedure[4-8].

The detection of ICH is a frequent indication for surgical intervention in craniosynostosis patients. The gold-standard method of measurement is intraparenchymal pressure monitoring, which is too invasive for use as a screening tool. Therefore, less invasive methods are frequently utilized along with the clinical exam and history. In our center, these include fundoscopy, optical coherence tomography (OCT), and magnetic resonance imaging (MRI). Due to the complexity of the pathogenesis of ICH in syndromic patients, further evaluation of contributing factors is often necessary and may include polysomnography to assess for obstructive sleep apnea (OSA), occipitofrontal circumference (OFC) measurement to determine risk for craniocerebral disproportion, and radiographic assessment for hydrocephalus or Chiari type I malformation[9,10].

It remains unclear what effects ICH may have on structural neurological development in syndromic craniosynostosis. Cortical thickness is an important in vivo biomarker for cognitive ability and may provide valuable insight regarding potential changes due to ICH[11-15]. As a subcomponent of cortical volume, cortical thickness reflects neuronal density per column, dendritic arborization, and glial support[16]. Development of the cortex occurs rapidly during childhood and adolescence, and cortical thinning has been correlated with reductions in IQ making it an appropriate biomarker for evaluation in syndromic craniosynostosis patients[15,14,17]. Understanding structural sequelae from positive clinical and imaging evaluation for ICH will better inform clinical decision making and timing of surgical

intervention. The aim of this study is to evaluate the effect of ICH risk factors and markers on cortical thickness in syndromic craniosynostosis patients.

Methods

Participants

This is an IRB approved study (MEC-2014-461). Medical and imaging records of all patients with syndromic craniosynostosis (Apert, Crouzon, Pfeiffer, Muenke, Saethre-Chotzen) at the Dutch Craniofacial Center (Erasmus University Medical Center, Rotterdam, NL) were reviewed from 2008 - 2018. All MRI studies including a 3D T1-weighted FSPGR sequence from these patients were included in the study, often resulting in multiple scans per patient. Some of these scans, however, were finally excluded due to image processing failure. Children with isolated single suture synostosis were excluded. Additional clinical and demographic data were collected for further analysis. Clinical management of syndromic patients included scheduled vault expansion in the first year of life. Subsequent development of ICH was treated according to suspected cause (e.g. secondary vault expansion for growth restriction, CPAP/midface advancement for OSA).

Papilledema

Craniosynostosis patients were evaluated by fundoscopy at follow-up for evidence of papilledema indicating ICH[18]. All patients underwent fundoscopy one day prior to initial vault expansion, three months postoperatively, biannually until the age of four, and then annually until age six. Following age six, fundoscopy was only performed on clinical indication. When papilledema was detected it was followed up with confirmatory fundoscopy and imaging four to six weeks later. Patients were considered to have a finding of papilledema as noted in the medical chart from the funduscopic exam by an experienced pediatric ophthalmologist after clinical exclusion of pseudopapilledema due to hypermetropia.

Obstructive Sleep Apnea

A diagnosis of OSA was made by clinical and ambulatory sleep studies. Polysomnography data were analyzed and scored by a trained physician according to the AASM 2012 update on the guideline for scoring pediatric respiratory events[19] and subsequently the obstructive apnea-hypopnea index (oAHI) was calculated: the number of obstructive- and mixed apneas and obstructive hypopneas with

desaturation/arousal, divided by the total sleep time[10]. Patients with an oAHI ≥ 5 were considered to have moderate to severe sleep apnea, which may cause ICH[20]. Dates of sleep studies were recorded and any history of moderate to severe OSA prior to the date of MRI acquisition was considered positive in our analysis.

Occipitofrontal Circumference

OFC reliably predicts intracranial volume (ICV) in syndromic craniosynostosis. Therefore, OFC curve deflection is seen as a risk factor for ICH[9,20]. OFC was manually measured pre-operatively, every three months until the age of two, every six months until the age of four, and from then yearly until 18. Growth curve deflection was defined as ≥ 0.5 SD fall from baseline over two years.

Hydrocephalus

Ventricular size was manually assessed on MR images. All scans were reviewed on a 3D reformatting platform (AquariusNET; TeraRecon, Inc., Melbourne, Australia) to align scans in all planes. The size of the lateral ventricles was evaluated on axial planes using the frontal occipital horn ratio (FOHR), ventricles were considered enlarged when the FOHR was > 0.34 [21]. Hydrocephalus was considered present when ventricles were progressively enlarged on ≥ 2 consecutive MRI studies. Progressive hydrocephalus following vault expansion was treated with third ventriculostomy or ventriculoperitoneal shunting.

Cerebellum Tonsillar Position

Cerebellum tonsillar position was manually measured in the mid-sagittal and adjacent MR slices at the level of the lowest observable point as previously described[22]. The level of the foramen magnum was set as zero and measurements above this level were considered negative and those below as positive. All measurements were performed on 3D reformatting software (AquariusNET; TeraRecon, Inc., Melbourne, Australia) to align scans in all planes.

MRI Acquisition

All MRI scans were performed on a 1.5 T scanner (GE Healthcare, MR Signa Excite HD, Little Chalfont, UK) and the imaging protocol included a 3D FSPGR T1-weighted MR sequence. Imaging parameters for craniosynostosis patients were the following: 2 mm slice thickness, no slice gap; field of view (FOV)

22.4 cm; matrix size 224 × 224; in plane resolution of 1 mm; echo time (TE) 3.1 ms, and repetition time (TR) 9.9 ms[22].

Cortical Thickness

MRI dicom files were exported and converted to NIfTI-1 file format on a computer cluster with Scientific Linux as the operating system and containing preloaded FreeSurfer software modules (v6.0) (https://surfer.nmr.mgh.harvard.edu). FreeSurfer is a brain imaging software package developed by the Athinoula A. Martinos Center for Biomedical Imaging at Massachusetts General Hospital for analyzing magnetic resonance imaging (MRI) scan data. It is an important tool in functional brain mapping and facilitates the visualization of the functional regions of the highly folded cerebral cortex. FreeSurfer is a fully-automated image processing software package, which allows for surface-based registration analysis and has demonstrated some advantages over more traditional voxel-based morphometric techniques which are prone to partial voluming effects[23]. The processing methodologies used by FreeSurfer have previously been validated and described in detail[24-27].

All T1-weighted scans from our cohort were processed by the FreeSurfer v6.0 'auto-recon-all' pipeline. Quality of scans and surfaces generated by FreeSurfer were then inspected post-pipeline for accuracy and error logs were reviewed for scans which failed to complete the pipeline. Visual inspection is common practice in studies using automated tools like FreeSurfer to ensure that surfaces are not including the dura or excluding entire segments of cortex due to incorrect thresholding[17]. Error logs revealed uncorrectable topology errors due to excessive motion artifact or poor gray-white differentiation in younger patients. Scans which failed to complete the auto-recon-all pipeline, due to excessive motion artifacts and/or poor scan quality, or scans which demonstrated white matter or pial surface errors were excluded from further analysis. Vertex-wise cortical thickness estimates were then generated by the FreeSurfer package for successful scans and exported for statistical analysis.

Statistical Analysis

All acquired biomarker data were imported into R statistical software (R Core Team, R version 3.6.1, 2019, Vienna, Austria) and a multivariate linear mixed model was used to account for multiple measurements, age, and sex (nlme package). Subject identity was the only random effect term included. Syndrome, papilledema, OFC deflection, and hydrocephalus were all evaluated as potential

interaction terms, but were not found to improve model fit by Akaike information criterion, therefore no interaction terms were used. Necessary assumptions for linear mixed models were also evaluated. Linearity was assessed graphically (lattice package). Homogeneity of variance was evaluated with Levene's test (p = 0.90) and normal distribution of residuals was evaluated via *Q-Q* plot (car and stats packages). No transformation was necessary. Global cortical thickness was calculated as the average between left and right hemisphere outputs from FreeSurfer and was treated as the primary outcome. All variables except for age, tonsillar position, and cortical thickness were evaluated as categorical. *P*-values and 95% confidence intervals were calculated for each model variable and a significance level of 0.05 was considered in all tests. Graphs were created using ggplot2 package with a loess smoother.

Results

171 MRIs of 107 syndromic patients were successfully processed and included for analysis (see Supplemental Figure). Of those excluded, 83% were considered too young (< 2 years old) to expect consistent gray-white matter differentiation at a level suitable for FreeSurfer analysis. The final number of scans per syndrome were as follows: 38 Apert, 68 Crouzon, 25 Muenke, 18 Pfeiffer, and 22 Saethre-Chotzen (Table 1).

Mean global cortical thickness for the entire study population was 2.78 $\pm$ 0.17 mm (range: 2.34 - 3.25). Cortical thickness estimates generated by FreeSurfer are overlaid onto the pial surface of a patient with Crouzon syndrome in Figure 1. Average age at the time of scan was 8.88 years (range: 1.15 – 34.03). Our model demonstrated a significant association between a historical finding of papilledema and cortical thickness (p = 0.036) (Figure 2). Patients with a finding of hydrocephalus were also shown to have significantly thinner cortices (p = 0.007). History of OFC curve deflection (p = 0.375), moderate to severe obstructive sleep apnea (p = 0.464), or tonsillar position (p = 0.682) did not have a significant impact. Lastly, syndrome diagnosis and sex were both found to have non-significant influences on cortical thickness in our cohort.

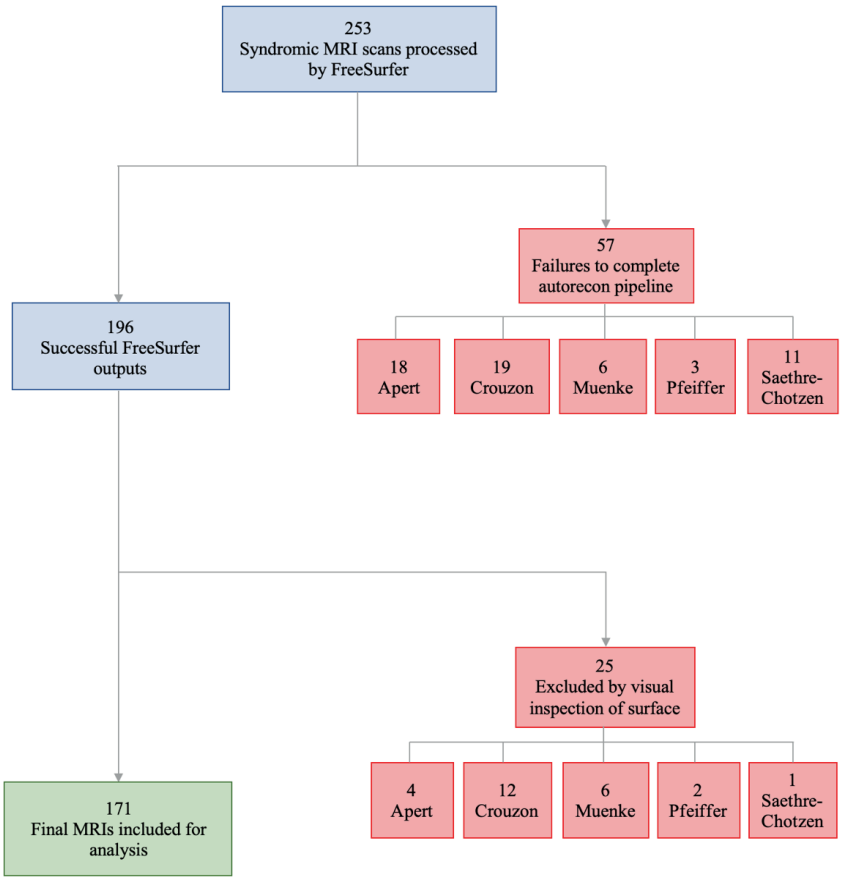

Supplemental Figure: Flow map of the inclusion of MRI scans.

Grouping	*n* (MRIs)	Mean Thickness (range)	*P*
(+) Hydrocephalus	25 (14.6%)	2.71 (2.34 – 3.22)	**0.007**
(+) Papilledema	83 (48.5%)	2.73 (2.34 – 3.22)	**0.036**
(+) OSA	30 (17.5%)	2.79 (2.51 – 3.01)	0.464
(+) OFC	66 (38.6%)	2.83 (2.49 – 3.25)	0.375
Tonsillar Position	-	-	0.682
Sex	-	-	0.534
Male	83 (48.5%)	2.80 (2.34 – 3.25)	-
Female	88 (51.5%)	2.78 (2.41 – 3.14)	-
Syndrome	-	-	0.832
Apert	38 (22.2%)	2.81 (2.52 – 3.13)	-
Crouzon	68 (39.8%)	2.77 (2.52 – 3.06)	-
Muenke	25 (14.6%)	2.84 (2.49 – 3.09)	-
Pfeiffer	18 (10.5%)	2.76 (2.51 – 3.03)	-
Saethre-Chotzen	22 (12.9%)	2.74 (2.37 – 3.09)	-
Age	-	-	**< 0.001**
Total MRIs	171	2.78 (2.34 – 3.25)	-

Table 1: Linear mixed model of the average global cortical thickness of 107 patients with syndromic craniosynostosis with 171 total MRIs, including repeated scans. Thickness values are reported in mm. OSA = Obstructive Sleep Apnea, OFC = Occipitofrontal Curve deflection.

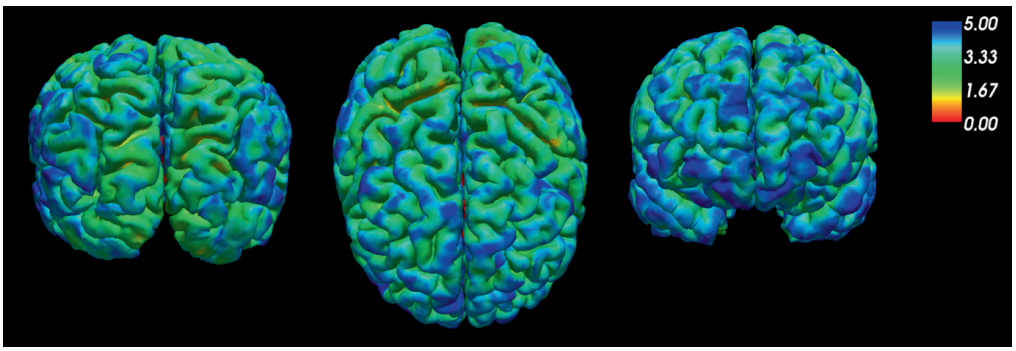

Figure 1: Cortical thickness color map overlaid on the pial surface of a 4-year-old patient with Crouzon syndrome. Occipital, axial, and frontal views are shown respectively from left to right with a 0-5mm color-coded scale.

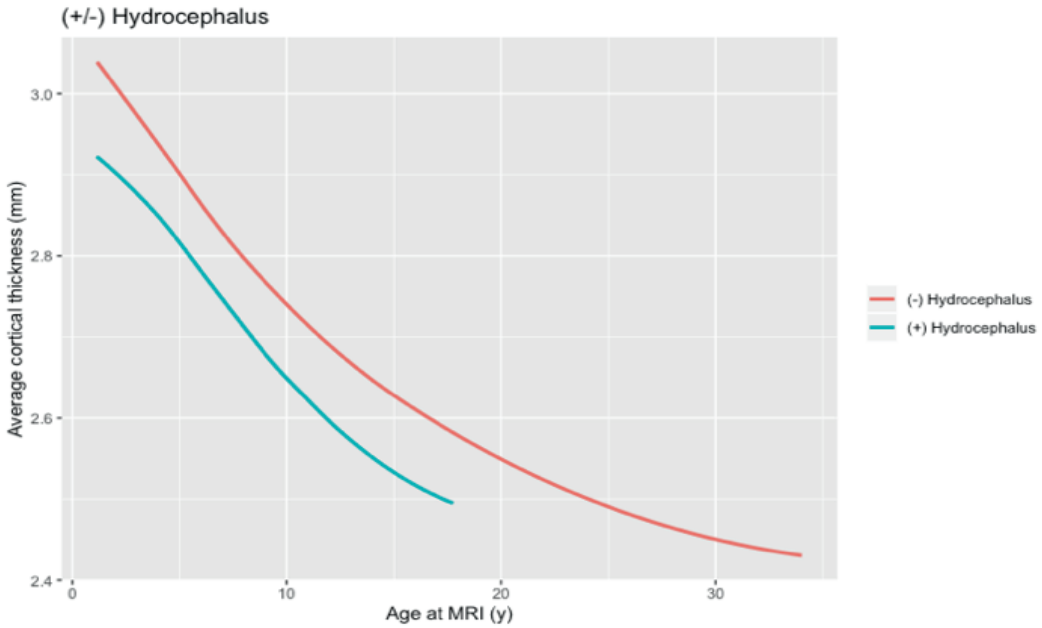
(+/-) Hydrocephalus
Average cortical thickness (mm)
3.0
2.8
2.6
2.4
0
10
20
30
Age at MRI (y)
(-) Hydrocephalus
(+) Hydrocephalus

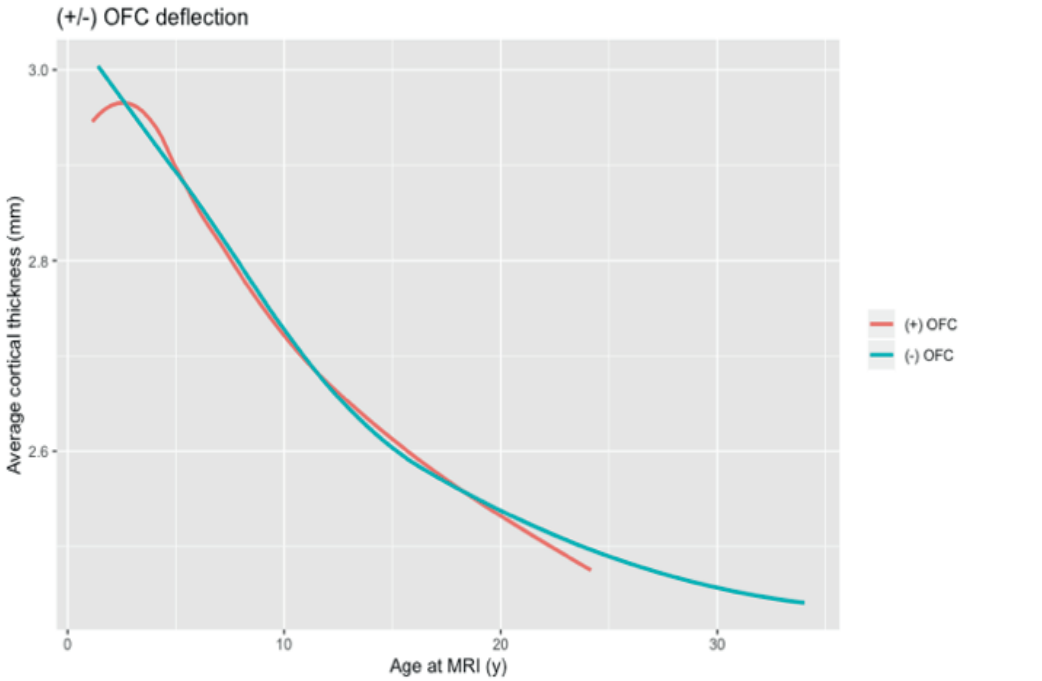
(+/-) OFC deflection
Average cortical thickness (mm)
3.0
2.8
2.6
0
10
20
30
Age at MRI (y)
(+) OFC
(-) OFC

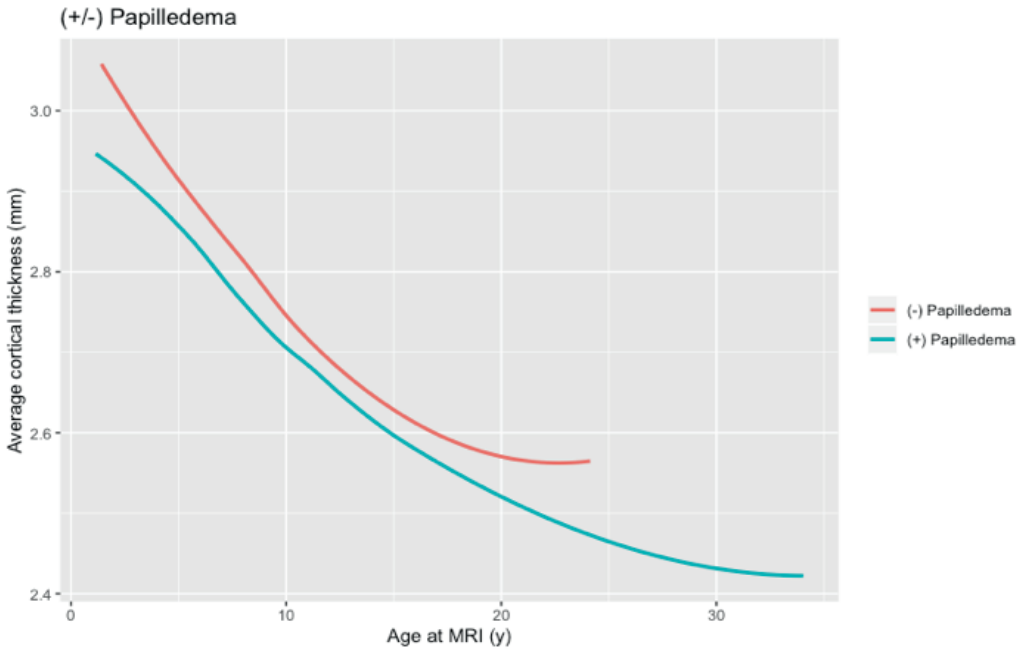
(+/-) Papilledema
Average cortical thickness (mm)
3.0
2.8
2.6
2.4
0
10
20
30
Age at MRI (y)
(-) Papilledema
(+) Papilledema

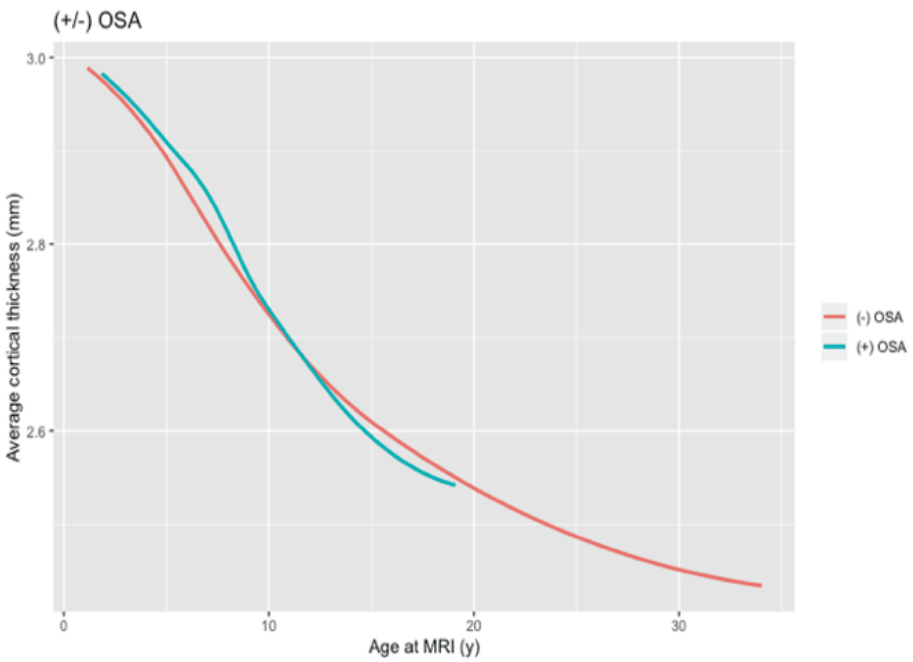
(+/-) OSA
Average cortical thickness (mm)
3.0
2.8
2.6
0
10
20
30
Age at MRI (y)
(-) OSA
(+) OSA

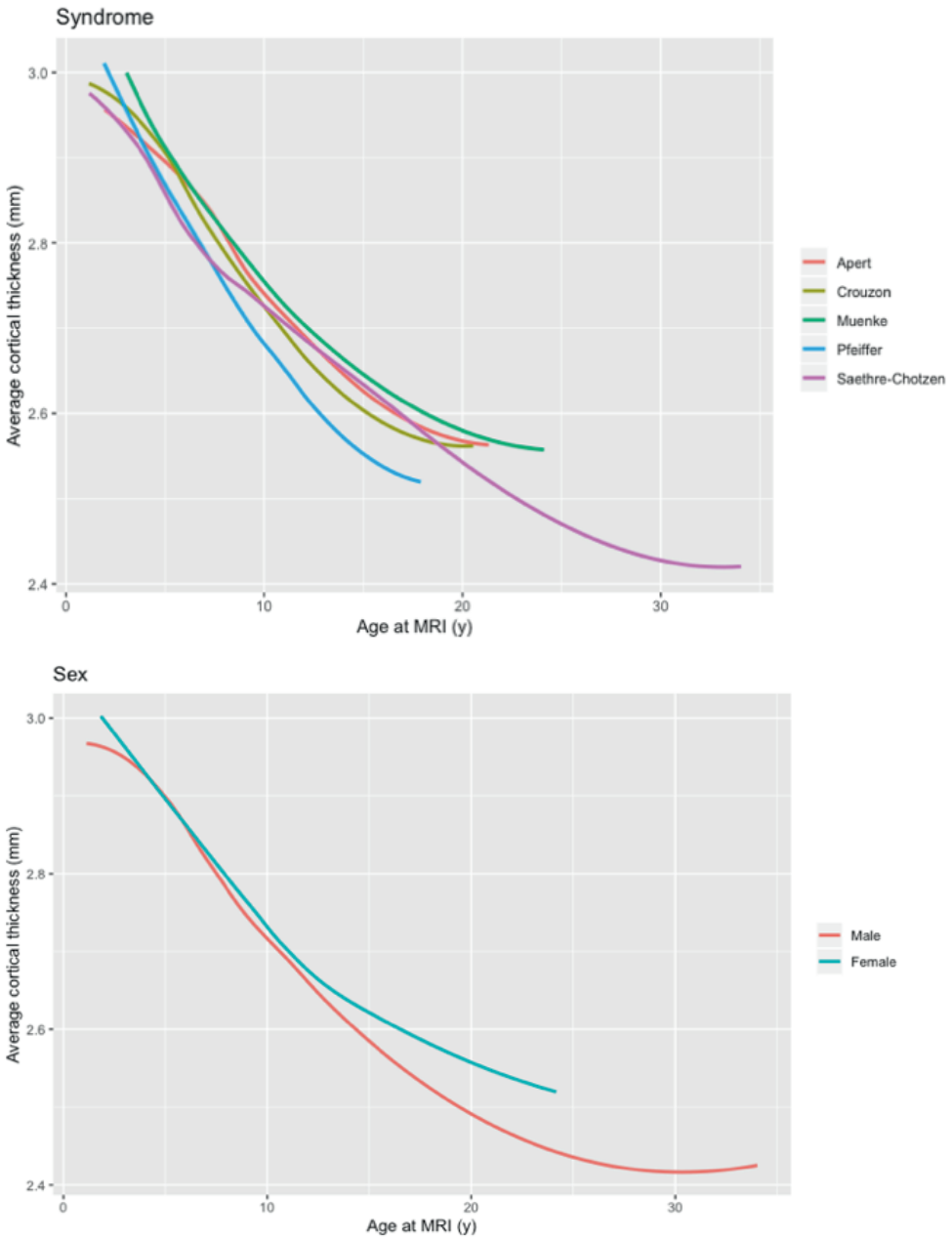

Figure 2: Effects of categorical variables on cortical thickness progression.

Discussion

In this study we evaluate the effect of various intracranial hypertension risk factors on cortical thickness in syndromic craniosynostosis. Historical findings of papilledema as well as hydrocephalus were found to result in a thinner cortex. Other factors associated with development of ICH were not correlated with cortical thickness changes. Lastly, syndrome diagnosis, independent of other detected indicators (e.g. hydrocephalus, papilledema), did not have an effect on cortical thickness.

In healthy children, natural development of the cerebral cortex results in a non-linear thinning pattern over time, with a significant rate increase occurring during adolescence[28]. This process can be understood as a natural decline in thickness driven by synaptic pruning and guided by stimulation level in critical periods of development[29-32]. Our study demonstrates a similar cortical maturation pattern in syndromic patients, with age correlating to a thinner cortex.

In the current study, we found presence of papilledema to be significantly correlated with global cortical thinning in syndromic patients. Previous work by Tuite et al demonstrated papilledema to be a reliable tool for the diagnosis of ICH in craniosynostosis patients, with an overall specificity of 98% but with an age-dependent sensitivity of 100% only for patients over the age of 8[18]. Furthermore, it has been shown that papilledema does not occur as a result of transient elevations in ICP but rather arises from prolonged exposure leading to axoplasmic flow stasis, neuronal swelling, and extracellular fluid accumulation[33]. The necessity of prolonged ICH exposure for papilledema detection could explain why it occurs in the context of accelerated cortical thinning and other metrics have not. By the time ICH is detectable as papilledema, cortical neurons may have already sustained sufficient stress to result in aberrant remodeling, thereby limiting neuronal density and dendritic arborization. This process is critical to establish normative cytoarchitecture of the cortex and disruption would explain the thinning pattern observed in this study. Furthermore, this pattern seems to mirror that of hydrocephalus, for which a causal relationship is generally accepted. It is possible that a causal relationship does exist between papilledema and cortical thinning, however, to prove this would require successful processing of the preoperative scans in neonates which are unavailable at present.

Our data suggest that once papilledema is clinically observable, its association with cortical thinning will continue throughout future radiographic evaluation of syndromic patients as evidenced by

sustained reductions as patients age (Figure 2). Given that structural neurologic change has already occurred at the time of papilledema detection, this calls into question whether or not waiting for evidence of sustained ICH exposure is the best course of action in treating syndromic patients. Although preventative surgery does not guarantee patients will not develop ICH during the following years of childhood, we do feel it offers a distinct advantage by alleviating skull growth restriction during a critical period of brain development within the first year of life. An aim of this study was to demonstrate that this is an important intervention given that at the time of detection (papilledema) cortical thinning has already occurred. Indeed, further investigation into alternative tests allowing for earlier detection and better risk stratification is warranted.

A finding of hydrocephalus was also shown to result in thinner cortices. This finding confirms previous studies demonstrating varying levels of cortical thinning and gray matter reduction according to severity of hydrocephalus in both children and animal models[34-36]. The pathogenesis of hydrocephalus in craniosynostosis is thought to be multifactorial. Primary causes are often considered to be impaired cerebrospinal fluid (CSF) reabsorption, overproduction of CSF at the choroid plexus, Chiari type I malformation, and/or increased venous outflow resistance from progressive crowding of the posterior fossa or at the level of third ventricle[37]. Microstructurally, this results in widespread neuronal swelling, increased extracellular space, and myelination delay[38]. It is not surprising then, that the shared cellular pathology of hydrocephalus and papilledema is reflected in similar changes to the cerebral cortex. Although patients with papilledema may also present with hydrocephalus, we report only 18 of 83 cases of this in our cohort. Furthermore, it is important to emphasize that hydrocephalus and papilledema were independently associated with cortical thinning in our model after accounting for such nested effects.

Although moderate to severe OSA has been shown to confer increased risk of ICH development in craniosynostosis[39,10], it has not resulted in cortical thickness changes in this study. The mechanism by which OSA is thought to contribute to ICH is through hypercapnia leading to altered cerebral hemodynamics[40]. OSA diagnosis may not be reflected in cortical changes because unlike papilledema and hydrocephalus, it does not appear to be a sequela of longstanding ICH but rather an etiology. Furthermore, the duration of OSA is often limited as parents are regularly coached regarding detection of symptoms and treatment is begun shortly after diagnosis. It seems prolonged exposure to ICH is

necessary to induce changes in cortical thickness, and transient OSA may be insufficient to produce such an effect.

OFC measurement is a reliable proxy for ICV in syndromic craniosynostosis and significant deflections in its progression have been linked to ICH development, especially in the postoperative period[9,41]. However, we did not observe any changes in cortical thickness as a result of OFC deflection in this cohort. Skull growth restriction as measured by OFC deflection is one factor among others that contribute to ICH in a complex pathophysiology which requires time to develop. Although a significant amount of time is required to develop both papilledema and OFC curve deflection, we attribute differences in significance observed in this study to variability in what these parameters indicate. Deflection of OFC curves indicate only skull growth restriction, which is one of multiple contributors to ICH in the syndromic patient. Conversely, papilledema reflects a state of ICH regardless of specific etiology. Although many patients with skull growth restriction go on to develop papilledema, it is not universally the case (32⁄56 patients with OFC deflection found to have papilledema in our cohort). This suggests that severity of ICH status, as determined by papilledema, rather than etiology is more important with regard to cortical thinning.

Lastly, cerebellum tonsillar position did not correlate with altered cortical thickness. The association of Chiari malformation type I with craniosynostosis is well established, but the causes for descent of the tonsils may result from sustained ICP elevation or may present as syndrome-specific anomalies. Differing etiologies of tonsillar position in our cohort could explain lack of significance with regard to cortical thickness.

There are several limitations to our study which should be considered when interpreting our results. First, a significant portion of our data is cross-sectional, which makes inferences concerning cortical development for patients without repeated MRI scans difficult. Additionally, patients who were excluded due to lack of successful thickness estimate outputs could unpredictably affect outcomes (107 of 147 patients were suitable for study), as a significant number may have pathology pertinent to cortical thickness development. Although excluded cases may potentially influence this analysis, an overwhelming majority (83%) of cases were too young (< 2 yrs) to expect consistent gray-white matter differentiation. Future efforts to evaluate potential differences in white matter maturation rates may

shed more light on why these patients were unable to be included. Lastly, cortical development is a complex process which may be impacted by additional socioeconomic or other factors not addressed in this study.

This study demonstrates that syndromic craniosynostosis patients with a previous finding of papilledema have reduced cerebral cortex thickness. This association is age-independent and is likely due to prolonged ICH exposure. Clinically, this supports the need for preventative rather than reactive treatment strategies. Although the effect of surgical intervention is not directly evaluated here, our craniofacial center recommends early vault expansion during this critical period of brain development. Future studies should investigate potential changes in cortical thickness for patients who undergo a first operation at an older age, improved methods of ICH detection in younger patients, as well as the effect of ICH on neuropsychological development.

References

1 Johnson D, Wilkie AOM. Craniosynostosis. *European journal of human genetics : EJHG* 2011; **19**: 369-76.

2 Sharma VP, Fenwick AL, Brockop MS, McGowan SJ, Goos JA, Hoogeboom AJ, Brady AF, Jeelani NO, Lynch SA, Mulliken JB, Murray DJ, Phipps JM, Sweeney E, Tomkins SE, Wilson LC, Bennett S, Cornall RJ, Broxholme J, Kanapin A, Johnson D, Wall SA, van der Spek PJ, Mathijssen IM, Maxson RE, Twigg SR, Wilkie AO. Mutations in TCF12, encoding a basic helix-loop-helix partner of TWIST1, are a frequent cause of coronal craniosynostosis. *Nature genetics* 2013; **45**: 304-7.

3 Christian EA, Imahiyerobo TA, Nallapa S, Urata M, McComb JG, Krieger MD. Intracranial hypertension after surgical correction for craniosynostosis: a systematic review. *Neurosurgical focus* 2015; **38**: E6.

4 Gault DT, Renier D, Marchac D, Jones BM. Intracranial pressure and intracranial volume in children with craniosynostosis. *Plastic and reconstructive surgery* 1992; **90**: 377-81.

5 Greene AK, Mulliken JB, Proctor MR, Meara JG, Rogers GF. Phenotypically unusual combined craniosynostoses: presentation and management. *Plastic and reconstructive surgery* 2008; **122**: 853-62.

6 Marucci DD, Dunaway DJ, Jones BM, Hayward RD. Raised intracranial pressure in Apert syndrome. *Plastic and reconstructive surgery* 2008; **122**: 1162-8; discussion 9-70.

7 Woods RH, Ul-Haq E, Wilkie AO, Jayamohan J, Richards PG, Johnson D, Lester T, Wall SA. Reoperation for intracranial hypertension in TWIST1-confirmed Saethre-Chotzen syndrome: a 15-year review. *Plastic and reconstructive surgery* 2009; **123**: 1801-10.

8 Abu-Sittah GS, Jeelani O, Dunaway D, Hayward R. Raised intracranial pressure in Crouzon syndrome: incidence, causes, and management. *Journal of neurosurgery. Pediatrics* 2016; **17**: 469-75.

9 Rijken BF, den Ottelander BK, van Veelen ML, Lequin MH, Mathijssen IM. The occipitofrontal circumference: reliable prediction of the intracranial volume in children with syndromic and complex craniosynostosis. *Neurosurgical focus* 2015; **38**: E9.

10 Spruijt B, Mathijssen IM, Bredero-Boelhouwer HH, Cherian PJ, Corel LJ, van Veelen ML, Hayward RD, Tasker RC, Joosten KF. Sleep Architecture Linked to Airway Obstruction and Intracranial Hypertension in Children with Syndromic Craniosynostosis. *Plast Reconstr Surg* 2016; **138**: 1019e-29e.

11 Steenwijk MD, Geurts JJ, Daams M, Tijms BM, Wink AM, Balk LJ, Tewarie PK, Uitdehaag BM, Barkhof F, Vrenken H, Pouwels PJ. Cortical atrophy patterns in multiple sclerosis are non-random and clinically relevant. *Brain : a journal of neurology* 2016; **139**: 115-26.

12 Kamson DO, Pilli VK, Asano E, Jeong JW, Sood S, Juhasz C, Chugani HT. Cortical thickness asymmetries and surgical outcome in neocortical epilepsy. *Journal of the neurological sciences* 2016; **368**: 97-103.

13 Romano A, Cornia R, Moraschi M, Bozzao A, Chiacchiararelli L, Coppola V, Iani C, Stella G, Albertini G, Pierallini A. Age-Related Cortical Thickness Reduction in Non-Demented Down's Syndrome Subjects. *Journal of neuroimaging : official journal of the American Society of Neuroimaging* 2016; **26**: 95-102.

14 Burgaleta M, Johnson W, Waber DP, Colom R, Karama S. Cognitive ability changes and dynamics of cortical thickness development in healthy children and adolescents. *NeuroImage* 2014; **84**: 810-9.

15 S K, Y AD, Rj H, Ij D, Oc L, C L, Ac E. Positive association between cognitive ability and cortical thickness in a representative US sample of healthy 6 to 18 year-olds. *Intelligence* 2009; **37**: 145-55.

16 Duncan NW, Gravel P, Wiebking C, Reader AJ, Northoff G. Grey matter density and GABAA binding potential show a positive linear relationship across cortical regions. *Neuroscience* 2013; **235**: 226-31.
17 Girault JB, Cornea E, Goldman BD, Jha SC, Murphy VA, Li G, Wang L, Shen D, Knickmeyer RC, Styner M, Gilmore JH. Cortical Structure and Cognition in Infants and Toddlers. *Cerebral cortex (New York, N.Y. : 1991)* 2019.
18 Tuite GF, Chong WK, Evanson J, Narita A, Taylor D, Harkness WF, Jones BM, Hayward RD. The effectiveness of papilledema as an indicator of raised intracranial pressure in children with craniosynostosis. *Neurosurgery* 1996; **38**: 272-8.
19 Berry RB, Budhiraja R, Gottlieb DJ, Gozal D, Iber C, Kapur VK, Marcus CL, Mehra R, Parthasarathy S, Quan SF, Redline S, Strohl KP, Davidson Ward SL, Tangredi MM. Rules for scoring respiratory events in sleep: update of the 2007 AASM Manual for the Scoring of Sleep and Associated Events. Deliberations of the Sleep Apnea Definitions Task Force of the American Academy of Sleep Medicine. *J Clin Sleep Med* 2012; **8**: 597-619.
20 Spruijt B, Joosten KF, Driessen C, Rizopoulos D, Naus NC, van der Schroeff MP, Wolvius EB, van Veelen ML, Tasker RC, Mathijssen IM. Algorithm for the Management of Intracranial Hypertension in Children with Syndromic Craniosynostosis. *Plastic and reconstructive surgery* 2015; **136**: 331-40.
21 Rijken BF, Lequin MH, Van Veelen ML, de Rooi J, Mathijssen IM. The formation of the foramen magnum and its role in developing ventriculomegaly and Chiari I malformation in children with craniosynostosis syndromes. *J Craniomaxillofac Surg* 2015; **43**: 1042-8.
22 Rijken BF, Lequin MH, van der Lijn F, van Veelen-Vincent ML, de Rooi J, Hoogendam YY, Niessen WJ, Mathijssen IM. The role of the posterior fossa in developing Chiari I malformation in children with craniosynostosis syndromes. *Journal of cranio-maxillo-facial surgery : official publication of the European Association for Cranio-Maxillo-Facial Surgery* 2015; **43**: 813-9.
23 Clarkson MJ, Cardoso MJ, Ridgway GR, Modat M, Leung KK, Rohrer JD, Fox NC, Ourselin S. A comparison of voxel and surface based cortical thickness estimation methods. *NeuroImage* 2011; **57**: 856-65.
24 Fischl B, Sereno MI, Dale AM. Cortical surface-based analysis. II: Inflation, flattening, and a surface-based coordinate system. *NeuroImage* 1999; **9**: 195-207.
25 Dale AM, Fischl B, Sereno MI. Cortical surface-based analysis. I. Segmentation and surface reconstruction. *NeuroImage* 1999; **9**: 179-94.
26 Fischl B, Dale AM. Measuring the thickness of the human cerebral cortex from magnetic resonance images. *Proceedings of the National Academy of Sciences of the United States of America* 2000; **97**: 11050-5.
27 Cardinale F, Chinnici G, Bramerio M, Mai R, Sartori I, Cossu M, Lo Russo G, Castana L, Colombo N, Caborni C, De Momi E, Ferrigno G. Validation of FreeSurfer-estimated brain cortical thickness: comparison with histologic measurements. *Neuroinformatics* 2014; **12**: 535-42.
28 Piccolo LR, Merz EC, He X, Sowell ER, Noble KG, Pediatric Imaging NGS. Age-Related Differences in Cortical Thickness Vary by Socioeconomic Status. *PloS one* 2016; **11**: e0162511-e.
29 Paus T. Mapping brain maturation and cognitive development during adolescence. *Trends in cognitive sciences* 2005; **9**: 60-8.
30 Hensch TK. Critical period regulation. *Annual review of neuroscience* 2004; **27**: 549-79.
31 Knudsen EI. Sensitive periods in the development of the brain and behavior. *Journal of cognitive neuroscience* 2004; **16**: 1412-25.

32 Petanjek Z, Judas M, Kostovic I, Uylings HB. Lifespan alterations of basal dendritic trees of pyramidal neurons in the human prefrontal cortex: a layer-specific pattern. *Cerebral cortex (New York, N.Y. : 1991)* 2008; **18**: 915-29.

33 Hayreh SS. Pathogenesis of optic disc edema in raised intracranial pressure. *Progress in retinal and eye research* 2016; **50**: 108-44.

34 Zhang S, Ye X, Bai G, Fu Y, Mao C, Wu A, Liu X, Yan Z. Alterations in Cortical Thickness and White Matter Integrity in Mild-to-Moderate Communicating Hydrocephalic School-Aged Children Measured by Whole-Brain Cortical Thickness Mapping and DTI. *Neural plasticity* 2017; **2017**: 5167973-.

35 Fletcher JM, McCauley SR, Brandt ME, Bohan TP, Kramer LA, Francis DJ, Thorstad K, Brookshire BL. Regional brain tissue composition in children with hydrocephalus. Relationships with cognitive development. *Archives of neurology* 1996; **53**: 549-57.

36 Olopade FE, Shokunbi MT, Siren AL. The relationship between ventricular dilatation, neuropathological and neurobehavioural changes in hydrocephalic rats. *Fluids and barriers of the CNS* 2012; **9**: 19.

37 Collmann H, Sorensen N, Krauss J. Hydrocephalus in craniosynostosis: a review. *Child's nervous system : ChNS : official journal of the International Society for Pediatric Neurosurgery* 2005; **21**: 902-12.

38 Castejon OJ. Submicroscopic pathology of human and experimental hydrocephalic cerebral cortex. *Folia neuropathologica* 2010; **48**: 159-74.

39 Inverso G, Brustowicz KA, Katz E, Padwa BL. The prevalence of obstructive sleep apnea in symptomatic patients with syndromic craniosynostosis. *International journal of oral and maxillofacial surgery* 2016; **45**: 167-9.

40 Gonsalez S, Hayward R, Jones B, Lane R. Upper airway obstruction and raised intracranial pressure in children with craniosynostosis. *The European respiratory journal* 1997; **10**: 367-75.

41 Breakey RWF, Knoops PGM, Borghi A, Rodriguez-Florez N, O'Hara J, James G, Dunaway DJ, Schievano S, Jeelani NUO. Intracranial Volume and Head Circumference in Children with Unoperated Syndromic Craniosynostosis. *Plastic and reconstructive surgery* 2018; **142**: 708e-17e.

CHAPTER 3

Cortical thickness in Crouzon-Pfeiffer syndrome: findings in relation to primary cranial vault expansion

Wilson AT, de Planque CA, Yang S, Tasker RC, van Veelen MLC, Dremmen MHG, Vrooman HA, Mathijssen IMJ

Plastic and Reconstructive Surgery Global Open, 2020

Abstract

Background: Episodes of intracranial hypertension are associated with reductions in cerebral cortical thickness (CT) in syndromic craniosynostosis. Here we focus on Crouzon–Pfeiffer syndrome patients to measure CT and evaluate associations with type of primary cranial vault expansion and synostosis pattern.

Methods: Records from 34 Crouzon–Pfeiffer patients were reviewed along with MRI data on CT and intracranial volume to examine associations. Patients were grouped according to initial cranial vault expansion (frontal/occipital). Data were analyzed by multiple linear regression controlled for age and brain volume to determine an association between global/lobar CT and vault expansion type. Synostosis pattern effect sizes on global/lobar CT were calculated as secondary outcomes.

Results: Occipital expansion patients demonstrated 0.02 mm thicker cortex globally (P = 0.81) with regional findings, including: thicker cortex in frontal (0.02 mm, P = 0.77), parietal (0.06 mm, P = 0.44) and occipital (0.04 mm, P = 0.54) regions; and thinner cortex in temporal (−0.03 mm, P = 0.69), cingulate (−0.04 mm, P = 0.785), and, insula (−0.09 mm, P = 0.51) regions. Greatest effect sizes were observed between left lambdoid synostosis and the right cingulate (d = −1.00) and right lambdoid synostosis and the left cingulate (d = −1.23). Left and right coronal synostosis yielded effect sizes of d = −0.56 and d = −0.42 on respective frontal lobes.

Conclusions: Both frontal and occipital primary cranial vault expansions correlate to similar regional CT in Crouzon–Pfeiffer patients. Lambdoid synostosis appears to be associated with cortical thinning, particularly in the cingulate gyri.

Introduction

The Crouzon-Pfeiffer syndrome is a common form of syndromic craniosynostosis (1) and mutations in the fibroblast growth factor receptor (*FGFR2*) gene are responsible for phenotypic severity in accelerated cranial suture fusion, facial anomalies, and exorbitism (2). Clinically, a severe sequela of Crouzon-Pfeiffer syndrome is intracranial hypertension (ICH), which may be due to factors such as cranial growth restriction, venous outflow obstruction, hydrocephalus and obstructive sleep apnea (3-5). Hence, cranial vault expansion is commonly performed and at our center has included procedures such as fronto-orbital advancement (FOA), biparietal out-fracturing, and occipital expansion (6). Compared to FOA, occipital expansion has produced greater gain in intracranial volume at our center while reducing the incidence of papilledema and tonsillar herniation (7).

Cerebral cortical thickness is an important *in vivo* biomarker for brain development and cognitive ability (8, 9). As a subcomponent of cortical volume, cortical thickness is a general measure of neuronal density, dendritic arborization, and glial support (10). Due to advancement in image processing techniques, its use in recent years across a variety of disciplines has risen and demonstrated it to be of increasing importance in establishing a morphologic link to various pathologic and non-pathologic neuropsychological outcomes (9, 11-15). More recently it has demonstrated sensitivity to evidence of ICH in the syndromic craniosynostosis population (16). Almost two-thirds of patients with Crouzon-Pfeiffer syndrome develop ICH and undergo cranial vault expansion(17), yet they exhibit – on average – global cortical thinning (16). Since most cases of Crouzon-Pfeiffer syndrome develop with normal intelligence (18, 19) we wondered whether the apparent discrepancy between evidence of global cortical thinning and development of normal intelligence could be resolved by a better understanding of lobar cortical findings proximate to skull regions involved in cranial vault expansion procedures. Hence, the primary aim of this study was to compare differences in cortical thickness following frontal versus occipital primary vault expansion in Crouzon-Pfeiffer syndrome patients. Our secondary aim was to determine if any relationship between synostosis pattern and cortical thickness exists.

Methods

The Institution Research Ethics Board (IRB) at Erasmus University Medical Center (MEC), Rotterdam, The Netherlands approved this study (MEC-2014-461), which is a part of ongoing work at the Dutch

Craniofacial Center and involves protocolized care, brain imaging, clinical assessment and data summary and evaluation (6, 20, 21). We reviewed the medical records of Crouzon-Pfeiffer syndrome patients who were managed at our center between 2008 and 2018. Our usual practice in such patients involves scheduled primary vault expansion in the first year of life. Patients were included in this study if they had cranial magnetic resonance imaging (MRI) data that could be extracted and analyzed from three-dimensional (3D) T1-weighted fast spoiled gradient echo (FSPGR) sequences. We excluded patients in whom the quality of imaging was not suitable for analysis.

Additional clinical and demographic data were collected including sex, age at the time of MRI, birth weight, age at the time of vault expansion, initial type of vault expansion, and synostosis pattern. Initial type of vault expansion was classified as frontal or occipital. Suture-specific synostosis was noted in each patient as a binary variable for each of the 6 major sutures. Partial involvement of a suture was considered as positive. Fundoscopy to assess for papilledema was also performed in all cases by a pediatric ophthalmologist prior to surgery, 3 months postoperatively, biannually until the age of 4, annually until the age of 6 and then upon indication in older patients. When papilledema was detected it was followed up with confirmatory fundoscopy and imaging 4-6 weeks later. Data from these examinations were collected to analyze the presence of ICH both pre and postoperatively.

MRI Acquisition

All MRI scans were performed on a 1.5 T scanner (GE Healthcare, MR Signa Excite HD, Little Chalfont, UK) with the imaging protocol including a 3D FSPGR T1-weighted MR sequence. Imaging parameters for craniosynostosis patients were the following: 2 mm slice thickness, no slice gap; field of view (FOV) 22.4 cm; matrix size 224 × 224; in plane resolution of 1 mm; echo time (TE) 3.1 ms, and repetition time (TR) 9.9 ms (22). MRI was the imaging modality of choice in this study because of its ability to adequately distinguish between tissue densities (white matter, grey matter, and dura) critical to the calculation of cerebral cortical thickness.

Cortical Thickness and Brain Volume

MRI dicom files were exported and converted to neuroimaging informatics technology initiative (NIfTI)-1 file format on a computer cluster with Scientific Linux as the operating system before analysis with FreeSurfer software modules (v6.0, see https://surfer.nmr.mgh.harvard.edu; developed by the

Athinoula A. Martinos Center for Biomedical Imaging, Massachusetts General Hospital) (23). The processing methodologies used by FreeSurfer have previously been validated and described in detail (24-26). Maps produced by FreeSurfer are not restricted by voxel resolution of the original data and are therefore able to detect submillimeter changes in cortical thickness as demonstrated by validation against histological analysis (within 0.07 mm and statistically indistinguishable from standard neuropathologic techniques) and manual measurements (27-30). All T1-weighted images from the cohort were processed using the 'auto-recon-all' pipeline in FreeSurfer. Estimates of vertex-wise cortical thickness were then generated by hemisphere and by cerebral lobes (i.e., frontal, temporal, parietal, occipital, cingulate, insula) as specified by the '--lobes' argument within the 'mris_annotation2label' command. Left and right hemisphere thickness outputs were averaged to generate a value for global cortical thickness. Similarly, lobar outputs from left and right hemispheres were averaged to generate a whole lobe thickness. Whole brain volume excluding ventricular volume was exported from FreeSurfer as 'BrainSegVolNotVent' via the 'mri_segstats' command.

Statistical Analysis

All data were imported into R statistical software (R Core Team, R version 3.6.1, 2019, Vienna, Austria) for analysis. Multivariate linear regression was first used to determine the level of variance in global thickness attributable to age at the time of MRI, sex, and whole brain volume. Multivariate analysis of covariance (MANCOVA) was then performed to assess these effects by lobe. Finally, multiple linear regression was used to determine associations between type of initial cranial vault expansion and lobar thickness while controlling for age and brain volume. A post-hoc power analysis was also performed to assess the quantitative limits of our current dataset. Cohen's *d* with 95% confidence intervals were calculated as a secondary analysis to determine effect of suture-specific synostosis on underlying cortical lobes. Homogeneity of variance among suture-specific groups was evaluated by Levene's test for age and chi squared for sex.

Results

Patient cohort

Following review of medical and imaging records, 43 Crouzon-Pfeiffer patients were identified. Six patients were excluded from further analysis since they did not undergo any primary vault expansion; either because they did not have synostosis (*n* = 2) or because of late referral and/or incomplete

records (*n* = 4). An additional 3 patients underwent primary biparietal expansion and were also excluded. In total, 34 Crouzon-Pfeiffer patients (19 male, 15 female) were therefore included in our cohort (mean ± SD age at the time of MRI of 8.9 $\pm$ 4.5 years). The interval between initial vault expansion and MRI was 7.1 $\pm$ 4.7 years. ICH was present in 8 (23.5%) patients preoperatively alone, 8 (23.5%) patients postoperatively alone, and 6 (17.6%) patients both pre and postoperatively. In 12 (35.3%) patients no ICH was present. Birth weight data (range: 2920 g – 4460 g; SD : 408 g) were also collected and no patients were found to be of low enough weight (< 1500 g) to impact thickness development as reported in previous studies (31, 32). Additionally, birth weight was found to be evenly distributed between both treatment groups and among all sutural involvement subgroups.

Frontal	df	sum sq	mean sq	F statistic	η2
Age	1	0.37174	0.37174	13.7338	0.30632442
Sex	1	0.02775	0.02775	1.0252	0.0228668
BrainVol	1	0.00204	0.00204	0.0756	0.00168102
Residuals	30	0.81202	0.02707		

Temporal	df	sum sq	mean sq	F statistic	η2
Age	1	0.27837	0.278374	17.8413	0.37158609
Sex	1	0.00245	0.00245	0.157	0.00327042
BrainVol	1	0.00024	0.000242	0.0155	0.00032037
Residuals	30	0.46808	0.015603		

Parietal	df	sum sq	mean sq	F statistic	η2
Age	1	0.15166	0.151659	7.5828	0.2017265
Sex	1	0.00006	0.000056	0.0028	7.98E-05
BrainVol	1	0.00008	0.000083	0.0042	0.00010641
Residuals	30	0.60001	0.02		

Occipital	df	sum sq	mean sq	F statistic	η2
Age	1	0.57963	0.57963	33.9775	0.50018553
Sex	1	0.01966	0.01966	1.1522	0.01696539
BrainVol	1	0.04776	0.04776	2.7999	0.04121398
Residuals	30	0.51178	0.01706		

Cingulate	df	sum sq	mean sq	F statistic	η2
Age	1	0.64805	0.64805	10.7218	0.25127664
Sex	1	0.00488	0.00488	0.0807	0.00189218
BrainVol	1	0.11283	0.11283	1.8667	0.04374901
Residuals	30	1.81327	0.06044		

Insula	df	sum sq	mean sq	F statistic	η2
Age	1	1.30516	1.30516	21.2218	0.38340486
Sex	1	0.22115	0.22115	3.5959	0.0649652
BrainVol	1	0.03279	0.03279	0.5331	0.00963242
Residuals	30	1.84503	0.0615		

Tale 1: Univariate results from MANCOVA test to assess variability attributable to age, sex, and brain volume. BrainVol = whole brain volume; df = degrees of freedom; sum sq = sum of squares; mean sq = mean square; η2 = eta squared.

	Global			Frontal			Temporal		
Predictors	*Estimates*	*CI*	*p*	*Estimates*	*CI*	*p*	*Estimates*	*CI*	*p*
(Intercept)	2.92	2.55 – 3.29	**<0.001**	3.06	2.56 – 3.55	**<0.001**	3.21	2.84 – 3.57	**<0.001**
Age at MRI	-0.02	-0.04 – -0.00	**0.012**	-0.02	-0.04 – -0.00	**0.036**	-0.02	-0.04 – -0.01	**0.004**
Brain volume	0.00	-0.00 – 0.00	0.917	0.00	-0.00 – 0.00	0.937	0.00	-0.00 – 0.00	0.788
Occipital expansion	0.02	-0.12 – 0.15	0.815	0.02	-0.15 – 0.20	0.778	-0.03	-0.16 – 0.10	0.680
Observations	34			34			34		
R^2 / R^2 adjusted	0.387 / 0.326			0.308 / 0.239			0.377 / 0.314		

	Parietal			Occipital		
Predictors	*Estimates*	*CI*	*p*	*Estimates*	*CI*	*p*
(Intercept)	2.66	2.25 – 3.07	**<0.001**	2.70	2.31 – 3.10	**<0.001**
Age at MRI	-0.01	-0.03 – 0.01	0.211	-0.02	-0.04 – -0.01	**0.008**
Brain volume	0.00	-0.00 – 0.00	0.991	-0.00	-0.00 – 0.00	0.245
Occipital expansion	0.06	-0.09 – 0.20	0.444	0.05	-0.10 – 0.19	0.511
Observations	34			34		
R^2 / R^2 adjusted	0.217 / 0.139			0.528 / 0.481		

	Cingulate			Insula		
Predictors	*Estimates*	*CI*	*p*	*Estimates*	*CI*	*p*
(Intercept)	3.51	2.79 – 4.24	**<0.001**	3.34	2.60 – 4.09	**<0.001**
Age at MRI	-0.03	-0.06 – 0.00	0.062	-0.06	-0.09 – -0.03	**0.001**
Brain volume	-0.00	-0.00 – 0.00	0.254	0.00	-0.00 – 0.00	0.193
Occipital expansion	-0.04	-0.29 – 0.22	0.783	-0.09	-0.36 – 0.17	0.482
Observations	34			34		
R^2 / R^2 adjusted	0.286 / 0.215			0.426 / 0.368		

Table 2: Linear regression results for global and lobar cortical thickness. CI = 95% confidence interval.

Primary cranial vault expansion

Before assessing any effect of primary cranial vault expansion type on cortical thickness we determined the level of variance explained by age, sex, and brain volume. Multivariate linear regression showed that these three variables accounted for 40% of the variance in cortical thickness (R^2 = 0.40), with univariate analyses yielding R^2 for age, sex and brain volume as 0.39, 0.01, and 0.06, respectively. Further evaluation by lobe using MANCOVA yielded a Pillai trace test statistic of 0.64, 0.17, and 0.24 for age, sex, and brain volume respectively. Univariate results of the MANCOVA test by lobe are available in Table 1.

Of the 34 patients, 13 (7 male, 6 female, median age at MRI 5.1 yrs) underwent occipital expansion as a primary procedure. 21 patients (12 male, 9 female, median age at MRI 11.5) underwent primary frontal expansion. Multiple linear regression did not find a correlation between global cortical thickness and primary cranial vault expansion type (Table 2). Primary occipital expansion was associated with a 0.02 mm thicker cortex globally (β = 0.02, 95% CI -0.12 – 0.15, p = 0.82), as well as thicker frontal (β = 0.02, 95% CI -0.15 – 0.20, p = 0.78), parietal (β = 0.06, 95% CI -0.09 – 0.20, p = 0.44) , and occipital (β = 0.05, 95% CI -0.10 – 0.19, p = 0.51) lobar cortices. Also, in the occipital expansion group, there was an association with thinner temporal (β = -0.03, 95% CI -0.16 – 0.10, p = 0.68), cingulate (β = -0.04, 95% CI -0.29 – 0.22, p = 0.78), and insular (β = -0.09, 95% CI -0.36 – 0.17, p = 0.48) cortices. β-coefficients and 95% confidence intervals for each region are shown in figure 1. Lastly, power analysis revealed the need for a cohort size of 59 patients in order to detect a 0.2 mm change in thickness at a level of 80%. Our cohort in this study was 80% powered to detect a 0.37 mm difference between surgical treatment groups.

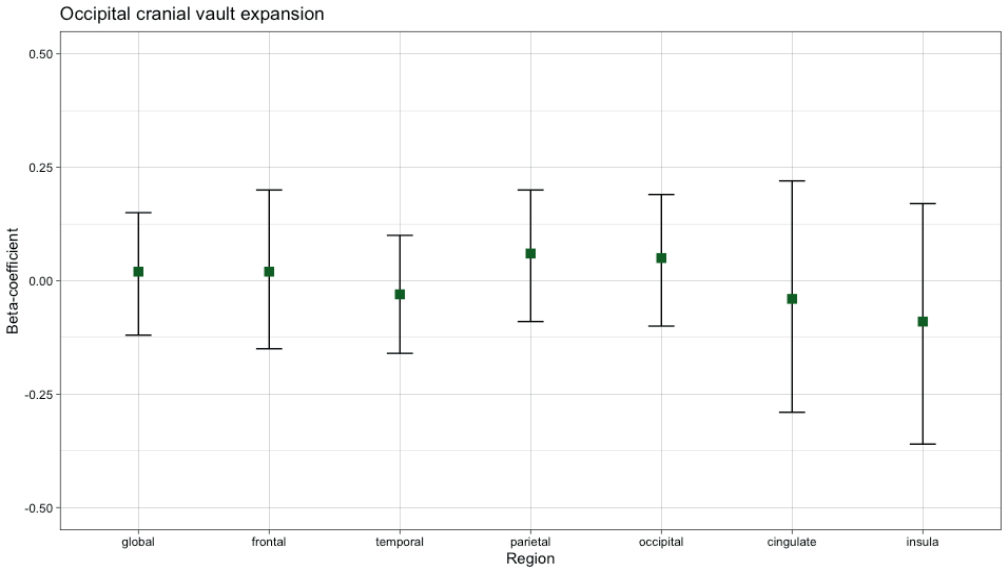

Figure 1: *ß*-coefficients with 95% confidence intervals associated with occipital cranial vault expansion extracted from linear mixed models of each lobe as well as globally.

Synostosis pattern

Of the 34 patients, 14 suffered from pansynostosis, 7 had bicoronal involvement, 6 had bilambdoid involvement, 4 had isolated sagittal synostosis, and 3 had additional combinations involving multiple sutures. Cohen's *d* effect sizes and 95% confidence intervals for independent involvement of 5 major sutures are shown in table 3 along with demographic data for each subgroup. Homogeneity of variance was found to be adequate in each subgroup as assessed by Levene's test for age (left coronal $p = 0.49$; right coronal $p = 0.57$; sagittal $p = 0.19$; left lambdoid $p = 0.89$; right lambdoid $p = 0.77$) and chi squared test for sex (left coronal $p = 0.68$; right coronal $p = 0.64$; sagittal $p = 0.63$; left lambdoid $p = 0.98$; right lambdoid $p = 0.98$). For matched synostosis pattern to underlying cortical thickness, the largest effect was observed between coronal sutures and the frontal cortex, with left coronal synostosis yielding an effect size of $d = -0.56$ (95% CI -1.4 – 0.27) and $d = -0.65$ (95% CI -1.49 – 0.19) and right coronal synostosis yielding $d = -0.31$ (95% CI -1.22 – 0.61) and $d = -0.42$ (95% CI -1.34 – 0.50) for left and right frontal lobes respectively. The overall largest effect sizes were observed between lambdoid suture involvement and the cingulate cortex, with left lambdoid synostosis corresponding

to *d* = -0.87 (95% CI -1.65 – -0.10) and *d* = -1.00 (95% CI -1.78 – -0.21) and right lambdoid synostosis corresponding to *d* = -1.23 (95% CI -2.08 – -0.38) and *d* = -1.05 (95% CI -1.88 – -0.22) for left and right cingulate cortices respectively. These effects are demonstrated in figure 2.

	Left coronal	Right coronal	Sagittal	Left lambdoid	Right lambdoid
n	26	28	23	23	25
Male (%)	14 (54%)	15 (54%)	14 (61%)	13 (57%)	14 (56%)
Female (%)	12 (46%)	13 (46%)	9 (39%)	10 (43%)	11 (44%)
Median age (SD)	8.0 (4.7)	8.6 (4.7)	10.7 (3.6)	8.0 (4.6)	8.0 (4.6)
Left frontal					
cohen's *d*	-0.56	-0.31	0.03	-0.48	-0.65
sd	0.20	0.20	0.20	0.20	0.19
conf.int.lower	-1.40	-1.22	-0.71	-1.24	-1.46
conf.int.upper	0.27	0.61	0.78	0.28	0.16
Right frontal					
cohen's *d*	-0.65	-0.42	0.23	-0.53	-0.59
sd	0.19	0.19	0.19	0.19	0.19
conf.int.lower	-1.49	-1.34	-0.52	-1.28	-1.40
conf.int.upper	0.19	0.50	0.98	0.23	0.21
Left temporal					
cohen's *d*	-0.52	-0.06	0.11	-0.56	-0.32
sd	0.15	0.15	0.15	0.15	0.15
conf.int.lower	-1.36	-0.98	-0.64	-1.32	-1.12
conf.int.upper	0.31	0.85	0.85	0.20	0.47
Right temporal					
cohen's *d*	-0.24	-0.01	-0.09	-0.43	-0.24
sd	0.16	0.16	0.16	0.16	0.16
conf.int.lower	-1.07	-0.92	-0.83	-1.18	-1.04
conf.int.upper	0.58	0.91	0.66	0.32	0.55
Left parietal					
cohen's *d*	-0.42	-0.25	-0.37	-0.05	-0.24
sd	0.15	0.15	0.15	0.15	0.15
conf.int.lower	-1.25	-1.17	-1.13	-0.80	-1.03
conf.int.upper	0.41	0.66	0.38	0.70	0.56

Right parietal					
cohen's *d*	-0.37	-0.20	-0.12	-0.30	-0.50
sd	0.16	0.16	0.16	0.16	0.16
conf.int.lower	-1.20	-1.11	-0.87	-1.05	-1.30
conf.int.upper	0.46	0.72	0.63	0.45	0.30
Left occipital					
cohen's *d*	-0.34	-0.10	0.70	-0.07	-0.30
sd	0.19	0.20	0.19	0.20	0.19
conf.int.lower	-1.17	-1.02	-0.07	-0.82	-1.10
conf.int.upper	0.49	0.81	1.47	0.68	0.49
Right occipital					
cohen's *d*	-0.31	-0.06	0.78	-0.09	-0.22
sd	0.19	0.20	0.18	0.20	0.20
conf.int.lower	-1.13	-0.97	0.01	-0.84	-1.01
conf.int.upper	0.52	0.86	1.55	0.66	0.58
Left cingulate					
cohen's *d*	-0.43	-0.36	0.16	-0.87	-1.23
sd	0.27	0.27	0.27	0.25	0.24
conf.int.lower	-1.26	-1.28	-0.59	-1.65	-2.08
conf.int.upper	0.40	0.56	0.90	-0.10	-0.38
Right cingulate					
cohen's *d*	-0.32	-0.11	0.49	-1.00	-1.05
sd	0.33	0.33	0.32	0.30	0.30
conf.int.lower	-1.14	-1.03	-0.27	-1.78	-1.88
conf.int.upper	0.51	0.81	1.25	-0.21	-0.22
Left insula					
cohen's *d*	-0.57	-0.27	0.21	-0.30	-0.31
sd	0.33	0.34	0.34	0.34	0.34
conf.int.lower	-1.40	-1.19	-0.53	-1.05	-1.10
conf.int.upper	0.27	0.64	0.96	0.45	0.49
Right insula					
cohen's *d*	-0.66	-0.20	0.24	-0.46	-0.30
sd	0.32	0.33	0.33	0.33	0.33
conf.int.lower	-1.50	-1.12	-0.51	-1.22	-1.09
conf.int.upper	0.18	0.72	0.99	0.29	0.50

Table 3: Cohen's *d* effect sizes with standard deviation and 95% confidence intervals for suture involvement on cortical thickness by lobe and hemisphere.

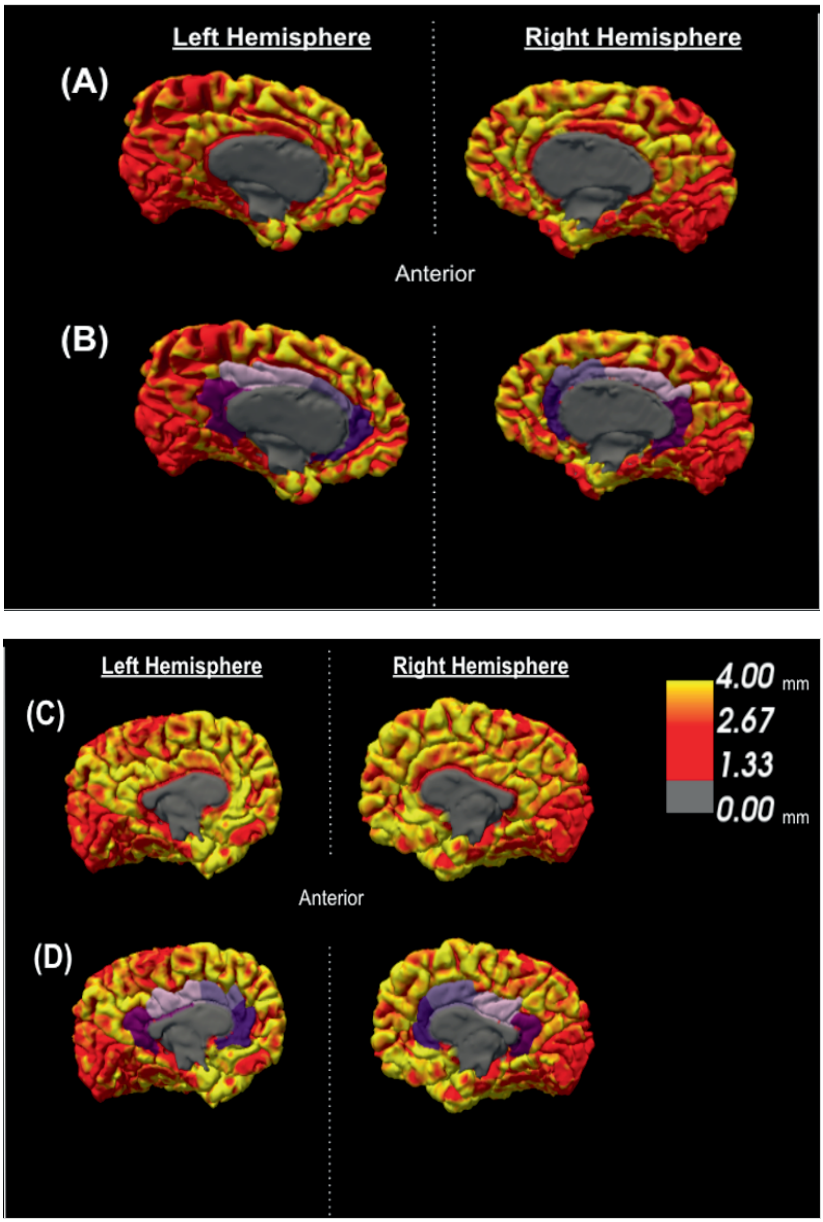

Figure 2: Pial surface heat maps extracted from Freesurfer with 0-4 mm cortical thickness scale. A) Left and right hemispheres of a 9 year-old Crouzon-Pfeiffer patient with bilateral lambdoid synostosis, B) Hemispheres of the same patient in A with cingulate gyri identified in purple, C) Left and right hemispheres of a 7 year-old Crouzon-Pfeiffer patient with bicoronal synostosis, D) Hemispheres of the same patient in C with cingulate gyri identified in purple.

Discussion

The primary aim of this study was to determine any association between cortical thickness and frontal versus occipital primary vault expansion in Crouzon-Pfeiffer syndrome patients. Our secondary aim was to determine any relationship between synostosis pattern and cortical thickness. We hypothesized that cortical lobes beneath growth-restricted regions of the calvarium may be at increased risk for thinning in Crouzon-Pfeiffer patients and that targeted vault expansion may confer a protective advantage to these regions. This study failed to find any difference in effect between frontal and occipital primary vault expansions on global or lobar cerebral cortical thickness. In regard to synostosis pattern and cortical thickness we found that lambdoid synostosis was associated with thinning across all brain regions, but particularly within the cingulate and frontal cortices. This leads us to question our hypothesis of localized growth restriction affecting proximate cortical lobes and consider how cranial shape contributes to pressure elevations and subsequent thinning in distant regions of the brain.

Both frontal and occipital cranial vault procedures resulted in similar cortical thicknesses in this study. Previous work by Spruijt et al evaluated the effect of frontal versus occipital primary vault expansions on occipitofrontal head circumference (OFC) in an Apert and Crouzon cohort and found that occipital-first expansion resulted in greater circumferences and reduced postoperative incidence of papilledema (7). A recent study has highlighted the importance of papilledema in syndromic craniosynostosis patients, demonstrating an association with global thinning of the cortex (16). The failure to find a direct association between primary cranial vault expansion type and cortical thickness in this study is most likely due to insufficient power. It is possible that occipital expansion resulted in fewer cases of papilledema than would otherwise be observed, however, the effect of surgery type alone was insufficient to result in detectable cortical thinning. This study was adequately powered to detect only a large difference in cortical thickness (0.37 mm), far exceeding that previously reported as a result of papilledema, between surgical treatment groups. With improved power we would expect more subtle cortical thickness changes to emerge, congruent with previous findings.

Our secondary analysis showed lambdoid synostosis to result in thinning across all brain regions, with pronounced effects in the cingulate and frontal cortices. We expected to observe greater effect sizes

between synostoses and corresponding cortical lobes, (e.g. coronal/frontal, lambdoid/occipital) but interestingly lambdoid involvement was associated with more thinning in the frontal cortex than the occipital. The largest effect sizes observed were those of lambdoid synostoses on the cingulate gyri. To date, lambdoid synostoses have been shown to result in localized brain dysmorphology such as increased rates of cerebellar tonsillar herniation (33, 34). This is likely due to the disproportionate cerebellar growth, which normally occurs in the first 2 years of life, in the context of posterior fossa maldevelopment (35). It may be that the association between lambdoid craniosynostosis and cortical thinning is related to increased ICH rates, which then differentially affects more susceptible cortical regions such as the cingulate gyri. The explanation for why ICH rates may be elevated in lambdoid synostosis is crowding of the posterior fossa leading to venous outflow obstruction and/or accessory venous drainage pathways which are common in Crouzon-Pfeiffer syndrome (36). Furthermore, contralateral growth restriction of the occiput may result in a cranial distortion mirrored by that of the pericallosal artery supplying the cingulate cortex, however, further study is needed to evaluate this possibility.

Coronal suture involvement was also associated with cortical thinning across all brain regions measured, however, its effects were generally small (cohen's $d < 0.5$) except for frontal lobes. But even in frontal lobes, the effect was not definitive as 95% confidence intervals included zero at their outer limits. Despite this, it seems that some localized influence does exist and a more comprehensive explanation is required to resolve these apparent discrepancies. Due to the fact that lambdoid and coronal synostosis both result in significant skull distortion including flattening of the occiput, scoliosis of the face and turribrachycephaly, dependent upon specific suture combinations, we must consider the influence of overall cranial shape and its contribution to ICH and subsequent cortical changes. It may be that turribrachycephaly contributes to frontal cortical thinning which occurs in bicoronal and bilambdoid synostosis, while isolated lambdoid suture involvement contributes more heavily to ICH development disproportionately impacting the cingulate gyri. The idea that cranial shape influences neurodevelopment is supported by previous study in non-syndromic craniosynostosis patients who experienced worse developmental and linguistic outcomes than healthy children or patients with varying forms of single suture synostosis(37-40). Our results similarly show cortical thickness effect sizes corresponding to these outcomes, with sagittal synostosis resulting in increased cortical thickness across various brain regions, most notably in the occipital lobes.

When interpreting the results of our study several limitations should be considered. First, 34 patients were included for analysis which limits the power of our study to draw negative inferences and could explain our failure to discover any cortical changes associated with type of primary cranial vault expansion. Almost all scans were postoperative in this study. Ideally, cortical thickness data pre and postoperatively would be obtained from serial imaging studies, however this was not possible due to the early age of surgery (median 1.27 years) and the lack of adequate tissue contrast inherent in infant brains on MRI(41). Additionally, it is possible that other variables unaccounted for in our analysis, which may influence cortical development, could have resulted in reverse confounding, thereby masking any effect of surgical intervention type. Lastly, the precision of Freesurfer processing methodologies may be influenced by cranial dysmorphology. Freesurfer generates maps using spatial intensity gradients across tissue classes on MRI data which allow for greater resolution than voxel size. Previous validation of Freesurfer has demonstrated cortical thickness measurement to be statistically indistinguishable from traditional neuropathology techniques on histological analysis(26, 27, 30). Furthermore, Freesurfer analysis has been applied with accuracy to a variety of neuropathologies, across a variety of ages(27, 29, 42). In this study we confirmed successful processing through manual inspection of all surfaces generated by the Freesurfer pipeline on each scan to ensure the reliability of our data.

Despite variable effects of synostosis pattern on regional cortical thickness seen in this study, we observed similar global and regional thicknesses in both frontal-first and occipital-first cranial vault expansion groups. Evaluation of effect size due to suture involvement showed frontal lobe thinning in coronal and lambdoid synostosis cases, suggesting that turribrachycephaly may adversely influence frontal cortex development. Lambdoid synostosis was also associated with a pronounced thinning effect in the cingulate gyri, likely attributable to increased ICH rates due to crowding of the posterior fossa. This explanation seems most likely given the buried nature of the cingulate cortex as well as its associations with the cerebellum, and frequent tonsillar herniation seen in lambdoid Crouzon-Pfeiffer cases(43, 44). Future studies should evaluate the effect of primary cranial vault expansion type as well as synostosis pattern on neuropsychological and functional outcomes such as hearing as well as investigate potential vascular causes of cingulate thinning observed in this study.

References:

1. Cohen, M. M., Jr., Kreiborg, S. Birth prevalence studies of the Crouzon syndrome: comparison of direct and indirect methods. *Clin Genet* 1992;41:12-15.
2. Rutland, P., Pulleyn, L. J., Reardon, W., et al. Identical mutations in the FGFR2 gene cause both Pfeiffer and Crouzon syndrome phenotypes. *Nat Genet* 1995;9:173-176.
3. Ghali, G. Z., Zaki Ghali, M. G., Ghali, E. Z., et al. Intracranial Venous Hypertension in Craniosynostosis: Mechanistic Underpinnings and Therapeutic Implications. *World Neurosurg* 2019;127:549-558.
4. Spruijt, B., Mathijssen, I. M., Bredero-Boelhouwer, H. H., et al. Sleep Architecture Linked to Airway Obstruction and Intracranial Hypertension in Children with Syndromic Craniosynostosis. *Plastic and reconstructive surgery* 2016;138:1019e-1029e.
5. Cinalli, G., Sainte-Rose, C., Kollar, E. M., et al. Hydrocephalus and craniosynostosis. *Journal of neurosurgery* 1998;88:209-214.
6. Spruijt, B., Joosten, K. F., Driessen, C., et al. Algorithm for the Management of Intracranial Hypertension in Children with Syndromic Craniosynostosis. *Plastic and reconstructive surgery* 2015;136:331-340.
7. Spruijt, B., Rijken, B. F., den Ottelander, B. K., et al. First Vault Expansion in Apert and Crouzon-Pfeiffer Syndromes: Front or Back? *Plast Reconstr Surg* 2016;137:112e-121e.
8. Burgaleta, M., Johnson, W., Waber, D. P., Colom, R., Karama, S. Cognitive ability changes and dynamics of cortical thickness development in healthy children and adolescents. *Neuroimage* 2014;84:810-819.
9. S, K., Y, A. D., Rj, H., et al. Positive association between cognitive ability and cortical thickness in a representative US sample of healthy 6 to 18 year-olds. *Intelligence* 2009;37:145-155.
10. Duncan, N. W., Gravel, P., Wiebking, C., Reader, A. J., Northoff, G. Grey matter density and GABAA binding potential show a positive linear relationship across cortical regions. *Neuroscience* 2013;235:226-231.
11. Williams, V. J., Juranek, J., Cirino, P., Fletcher, J. M. Cortical Thickness and Local Gyrification in Children with Developmental Dyslexia. *Cerebral cortex (New York, NY : 1991)* 2018;28:963-973.
12. Gautam, P., Anstey, K. J., Wen, W., Sachdev, P. S., Cherbuin, N. Cortical gyrification and its relationships with cortical volume, cortical thickness, and cognitive performance in healthy mid-life adults. *Behav Brain Res* 2015;287:331-339.
13. Alvarez, I., Parker, A. J., Bridge, H. Normative cerebral cortical thickness for human visual areas. *NeuroImage* 2019;201:116057.
14. Zink, D. N., Miller, J. B., Caldwell, J. Z. K., Bird, C., Banks, S. J. The relationship between neuropsychological tests of visuospatial function and lobar cortical thickness. *J Clin Exp Neuropsychol* 2018;40:518-527.
15. Menary, K., Collins, P. F., Porter, J. N., et al. Associations between cortical thickness and general intelligence in children, adolescents and young adults. *Intelligence* 2013;41:597-606.
16. Wilson, A. T., Den Ottelander, B. K., De Goederen, R., et al. Intracranial hypertension and cortical thickness in syndromic craniosynostosis. *Dev Med Child Neurol* 2020.
17. Abu-Sittah, G. S., Jeelani, O., Dunaway, D., Hayward, R. Raised intracranial pressure in Crouzon syndrome: incidence, causes, and management. *Journal of neurosurgery Pediatrics* 2016;17:469-475.
18. Fernandes, M. B., Maximino, L. P., Perosa, G. B., Abramides, D. V., Passos-Bueno, M. R., Yacubian-Fernandes, A. Apert and Crouzon syndromes-Cognitive development, brain abnormalities, and molecular aspects. *American journal of medical genetics Part A* 2016;170:1532-1537.

19. Maliepaard, M., Mathijssen, I. M., Oosterlaan, J., Okkerse, J. M. Intellectual, behavioral, and emotional functioning in children with syndromic craniosynostosis. *Pediatrics* 2014;133:e1608-1615.
20. Rijken, B. F., Leemans, A., Lucas, Y., van Montfort, K., Mathijssen, I. M., Lequin, M. H. Diffusion Tensor Imaging and Fiber Tractography in Children with Craniosynostosis Syndromes. *AJNR American journal of neuroradiology* 2015;36:1558-1564.
21. Mathijssen, I. M. Guideline for Care of Patients With the Diagnoses of Craniosynostosis: Working Group on Craniosynostosis. *The Journal of craniofacial surgery* 2015;26:1735-1807.
22. Rijken, B. F., Lequin, M. H., van der Lijn, F., et al. The role of the posterior fossa in developing Chiari I malformation in children with craniosynostosis syndromes. *Journal of cranio-maxillo-facial surgery : official publication of the European Association for Cranio-Maxillo-Facial Surgery* 2015;43:813-819.
23. Clarkson, M. J., Cardoso, M. J., Ridgway, G. R., et al. A comparison of voxel and surface based cortical thickness estimation methods. *NeuroImage* 2011;57:856-865.
24. Fischl, B., Sereno, M. I., Dale, A. M. Cortical surface-based analysis. II: Inflation, flattening, and a surface-based coordinate system. *NeuroImage* 1999;9:195-207.
25. Dale, A. M., Fischl, B., Sereno, M. I. Cortical surface-based analysis. I. Segmentation and surface reconstruction. *NeuroImage* 1999;9:179-194.
26. Fischl, B., Dale, A. M. Measuring the thickness of the human cerebral cortex from magnetic resonance images. *Proceedings of the National Academy of Sciences of the United States of America* 2000;97:11050-11055.
27. Rosas, H. D., Liu, A. K., Hersch, S., et al. Regional and progressive thinning of the cortical ribbon in Huntington's disease. *Neurology* 2002;58:695-701.
28. Kuperberg, G. R., Broome, M. R., McGuire, P. K., et al. Regionally localized thinning of the cerebral cortex in schizophrenia. *Arch Gen Psychiatry* 2003;60:878-888.
29. Salat, D. H., Buckner, R. L., Snyder, A. Z., et al. Thinning of the cerebral cortex in aging. *Cerebral cortex (New York, NY : 1991)* 2004;14:721-730.
30. Cardinale, F., Chinnici, G., Bramerio, M., et al. Validation of FreeSurfer-estimated brain cortical thickness: comparison with histologic measurements. *Neuroinformatics* 2014;12:535-542.
31. Martinussen, M., Fischl, B., Larsson, H. B., et al. Cerebral cortex thickness in 15-year-old adolescents with low birth weight measured by an automated MRI-based method. *Brain : a journal of neurology* 2005;128:2588-2596.
32. Bjuland, K. J., Løhaugen, G. C., Martinussen, M., Skranes, J. Cortical thickness and cognition in very-low-birth-weight late teenagers. *Early human development* 2013;89:371-380.
33. Chivoret, N., Arnaud, E., Giraudat, K., et al. Bilambdoid and sagittal synostosis: Report of 39 cases. *Surg Neurol Int* 2018;9:206.
34. Fearon, J. A., Dimas, V., Ditthakasem, K. Lambdoid Craniosynostosis: The Relationship with Chiari Deformations and an Analysis of Surgical Outcomes. *Plastic and reconstructive surgery* 2016;137:946-951.
35. Cinalli, G., Renier, D., Sebag, G., Sainte-Rose, C., Arnaud, E., Pierre-Kahn, A. Chronic tonsillar herniation in Crouzon's and Apert's syndromes: the role of premature synostosis of the lambdoid suture. *Journal of neurosurgery* 1995;83:575-582.
36. Hayward, R. Venous hypertension and craniosynostosis. *Child's nervous system : ChNS : official journal of the International Society for Pediatric Neurosurgery* 2005;21:880-888.
37. Korpilahti, P., Saarinen, P., Hukki, J. Deficient language acquisition in children with single suture craniosynostosis and deformational posterior plagiocephaly. *Child's Nervous System* 2012;28:419-425.

38. Andrews, B. T., Fontana, S. C. Correlative vs. Causative Relationship between Neonatal Cranial Head Shape Anomalies and Early Developmental Delays. *Front Neurosci* 2017;11:708.
39. Renier, D., Lajeunie, E., Arnaud, E., Marchac, D. Management of craniosynostoses. *Child's nervous system : ChNS : official journal of the International Society for Pediatric Neurosurgery* 2000;16:645-658.
40. Da Costa, A. C., Anderson, V. A., Savarirayan, R., et al. Neurodevelopmental functioning of infants with untreated single-suture craniosynostosis during early infancy. *Child's nervous system : ChNS : official journal of the International Society for Pediatric Neurosurgery* 2012;28:869-877.
41. Wang, F., Lian, C., Wu, Z., et al. Developmental topography of cortical thickness during infancy. *Proceedings of the National Academy of Sciences of the United States of America* 2019;116:15855-15860.
42. Nickel, K., Tebartz van Elst, L., Manko, J., et al. Inferior Frontal Gyrus Volume Loss Distinguishes Between Autism and (Comorbid) Attention-Deficit/Hyperactivity Disorder-A FreeSurfer Analysis in Children. *Front Psychiatry* 2018;9:521.
43. Badura, A., Verpeut, J. L., Metzger, J. W., et al. Normal cognitive and social development require posterior cerebellar activity. *Elife* 2018;7.
44. Herrojo Ruiz, M., Maess, B., Altenmuller, E., Curio, G., Nikulin, V. V. Cingulate and cerebellar beta oscillations are engaged in the acquisition of auditory-motor sequences. *Hum Brain Mapp* 2017;38:5161-5179.

CHAPTER 4

Intracranial hypertension and corpus callosum volume in syndromic craniosynostosis: a retrospective cohort study

Wilson AT, Ottelander BK, Tasker RC, van Veelen MLC, Dremmen MHG, Vrooman HA, Mathijssen IMJ

Child's Nervous System, *(submitted)*

Abstract

Introduction: Intracranial hypertension (ICH) in syndromic craniosynostosis is associated with reduced cortical thickness. In this study we have assessed the association between ICH, ventriculomegaly and corpus callosum volume.

Methods: We reviewed the clinical records and imaging data of 100 syndromic craniosynostosis patients and 36 control patients. A total of 188 magnetic resonance imaging (MRI) studies were analyzed for whole and segmented corpus callosum volumes, as well as total brain tissue volumes. Clinical data including syndrome type (Apert, Crouzon-Pfeiffer, Muenke, Saethre-Chotzen) and presence of papilledema, stable and progressive ventriculomegaly, age at MRI and sex were collated. Clinical and imaging data were analyzed using a linear mixed effects model to control for age, brain volume, sex, and syndrome, as well as repeated measurements.

Results: Mean (± SD) age at the time of MRI was 8.9 (± 5.2) years. Progressive ventriculomegaly was independently associated with a 469 mm^3 reduction of total corpus callosum volume (95% CI -809.7 – -129.1, p = 0.009). Papilledema was not associated with total corpus callosum volume (β = 70.5, 95% CI -130.7 – 271.7, p = 0.498). Segmental analysis revealed strong negative correlations with volume due to progressive ventriculomegaly in central (β = -109.6, 95% CI -180.8 – -38.4), mid-anterior (β = -106.9, 95% CI -194.8 – -18.9), and mid-posterior (β = -107.5, 95% CI -180.3 – -34.7) regions. Stable ventriculomegaly also resulted in reduced central (β = -54.4, 95% CI -94.8 – -14.0), mid-anterior (β = -59.5, 95% CI -105.3 – -13.7), and mid-posterior (β = -24.0, 95% CI -66.2 – 18.2) volumes. Reduced central segment volumes were observed across all syndromes, the greatest of which were in Apert (β = -96.9, 95% CI -160.1 – -33.8) and Muenke (β = -57.7, 95% CI -116.2 – 0.7) patients despite larger average total brain volume.

Conclusions: Syndromic craniosynostosis with progressive ventriculomegaly is associated with decreased total corpus callosum volume. Papilledema was not associated with reduced callosal volume. Syndromic status was correlated with regional volume loss in the callosal body, indicative of abnormal development.

Introduction

Craniosynostosis (CS) is a congenital disease of premature fusion of calvarial sutures, resulting in skull deformity and craniocerebral disproportion. Syndromic CS (sCS) variants comprise up to 20% of these cases and are associated with additional findings including limb, midface, or ear deformities[1,2]. The development of intracranial hypertension (ICH) in sCS cases is more common than in isolated CS and is a frequent justification for surgical intervention[3-5]. Although management differs among craniofacial surgical centers, at our institution cranial vault expansion is preferred in sCS cases in the first year of life, in an effort to reduce any sequelae associated with ICH.

Our recent study in sCS patients shows that ICH is associated with global thinning of the cerebral cortex[6]. Specifically, historical finding of papilledema and hydrocephalus were both independently associated with cortical thinning after controlling for known contributing factors such as age. Clinically, this supports treatment strategies aimed at preventing the development of ICH rather than a more conservative reactionary approach. In light of these previous findings, we now wonder whether a reduction in white matter volume may also result from ICH, further supporting our treatment protocol.

White matter development has been well characterized in the corpus callosum (CC), demonstrating a steady increase in callosal posterior and mid-body volume throughout childhood in typically developing children[7]. Radiographically, its size is positively correlated with intelligence and negatively correlated with disorders such as attention deficit hyperactivity disorder (ADHD), making it suitable for study as a biomarker for development in craniosynostosis patients[8,9]. Therefore, the primary aim of this study is to determine if ICH in sCS patients is associated with reduced total callosal volume. A secondary aim is to identify at-risk regions of the corpus callosum by assessing segmental volumes and the association with ICH.

Methods

Participants

The Institution Research Ethics Board (IRB) at Erasmus University Medical Center (MEC), Rotterdam, The Netherlands, approved this study (MEC-2014-461). This report is part of ongoing work at the Dutch Craniofacial Center, which is a center that adheres to protocolized care with brain imaging,

serial clinical assessment, data summary and evaluation[10]. Medical records of all sCS patients (Apert, Crouzon-Pfeiffer, Muenke, and Saethre-Chotzen) managed at our center (2008 to 2018) were reviewed and demographic data were collected. Patients were included in the study if they had cranial magnetic resonance imaging (MRI) data that could be extracted and analyzed from 3-dimensional T1-weighted fast spoiled gradient echo (FSPGR) sequences. Patients in whom the quality of scans were not suitable for analysis were excluded. Additionally, recent imaging reports were reviewed to identify age and sex matched control patients with appropriate MR sequences selected from hospital cases undergoing investigation for headache, head trauma, single seizure episode, early menstruation, hypoglycemia, and heat intolerance. Indications for imaging were reviewed by a pediatric neurosurgeon and deemed suitable for comparison to our sCS cohort. Clinical management of sCS patients included scheduled cranial vault expansion in the first year of life. Subsequent development of ICH was treated according to suspected cause (e.g., secondary vault expansion for recurrent cranial growth restriction, continuous positive airway pressure/midface advancement for obstructive sleep apnea).

Papilledema

Fundoscopy was performed on all sCS patients to assess for papilledema indicating ICH[11]. This screening examination occurred the day before primary cranial vault expansion, 3 months after operation, and then annually until the age of 6 years. Additional fundoscopy was then performed if clinically indicated. Upon identification of papilledema, follow up confirmatory fundoscopy was performed 4-6 weeks later. Patients were scored as positive for previously identified papilledema by a pediatric ophthalmologist (making sure to exclude pseudopapilledema from hypermetropia).

Ventriculomegaly

Ventricular size was manually assessed on MR images. All scans were reviewed on a 3D reformatting platform (AquariusNET; TeraRecon, Inc., Melbourne, Australia) to align scans in all planes. The size of the lateral ventricles was evaluated on axial planes using the frontal occipital horn ratio (FOHR), ventricles were considered enlarged when the FOHR was > 0.34[12]. A distinction was made between stable and progressive ventriculomegaly (PV), with the former considered present in isolated scans and the latter when ventricles were progressively enlarged on ≥ 2 consecutive MRI studies. PV in the

setting of ICH following vault expansion was treated with third ventriculostomy or ventriculoperitoneal shunting.

MRI Acquisition

All MRI scans were performed on a 1.5 Tesla scanner (GE Healthcare, MR Signa Excite HD, Little Chalfont, UK) with the imaging protocol including a 3D fast spoiled gradient echo (FSPGR) T1-weighted MR sequence. Imaging parameters for sCS patients were the following: 2 mm slice thickness, no slice gap; field of view (FOV) 22.4 cm; matrix size 224 × 224; in plane resolution of 1 mm; echo time (TE) 3.1 ms, and repetition time (TR) 9.9 ms[13]. MRIs in this study were performed following primary cranial vault expansion as well as after any cerebrospinal fluid diversion procedure (e.g., ventriculoperitoneal shunt) which may have been performed.

Corpus callosum volumes

MRI dicom files were exported and converted to neuroimaging informatics technology initiative (NIfTI) file format on a computer cluster with Scientific Linux as the operating system and preloaded Freesurfer software (version 6.0, see https://surfer.nmr.mgh.harvard.edu; developed by the Athinoula A. Martinos Center for Biomedical Imaging, Massachusetts General Hospital). All corpus callosum and total brain volumes were derived from Freesurfer software modules which have been previously validated and described in detail[14-16]. All patients underwent the 'auto-recon-all' pipeline which generates pial and white matter surface maps as well as auto-segments subcortical structures, including the corpus callosum. In this process, anatomical structures are segmented and labeled based on intensity gradients and spatial information from probabilistic atlases[17]. Surfaces and segmentation results were then inspected to confirm accuracy relative to the original T1 images. No manual editing was performed and scans with inaccurate segmentation of the corpus callosum were excluded from further analysis. In Freesurfer, corpus callosum volumes are automatically partitioned into 5 distinct regions along the primary eigenaxis (posterior, mid-posterior, central, mid-anterior, anterior). These volumes were exported via the 'mri_segstats' command and summed to calculate total corpus callosum volume. Total brain volume values were exported from FreeSurfer as 'BrainSegVolNotVent' via the 'mri_segstats' command.

Statistical analysis

All clinical, demographic and biomarker data were analyzed in R statistical software (R Core Team, R version 3.6.1, 2019, Vienna, Austria). A multivariate linear mixed model was used with total corpus callosum volume as the dependent variable and age, sex, syndromic status, total brain volume, papilledema, stable ventriculomegaly and PV as covariates (nlme package). Subject identity was the only random term included. PV and papilledema were both considered as potential interaction terms but ultimately not included as they failed to improve model fit based on Akaike information criterion (AIC). Linearity was assessed graphically (lattice package) and also demonstrated improved fit by AIC over logarithmic conversion of age. Multicollinearity was evaluated via variance inflation factor (VIF) and found to be less than 1.5 for each variable in the model (car and stats packages). Normality of residuals was assessed by *Q-Q* plot (car and stats packages). For the primary aim, *ß*-coefficients, 95% confidence intervals, and *p*-values are reported. For secondary regional analysis of callosal segment volumes, *ß*-coefficients and 95% confidence intervals are reported.

Results

A total of 188 MRIs (86 male, 102 female) were successfully processed by Freesurfer and included for analysis. Mean (± SD) age at the time of MRI was 8.9 (± 5.2) years. Number of scans per syndrome as well as stable ventriculomegaly, PV, previous papilledema, brain volume, total callosal volume, and ratio of callosal volume to brain volume are shown in Table 1. Stable ventriculomegaly was present in 11 (33%) Apert, 24 (32%) Crouzon-Pfeiffer, and 8 (32%) Muenke patients. Notably, PV was only present in Apert (12%) and Crouzon-Pfeiffer (11%) syndrome subgroups. Only 6 patients underwent a CSF diversion procedure (5 ventriculoperitoneal shunts in Crouzon patients and 1 ventriculostomy in an Apert patient), all of which occurred prior to imaging. Papilledema was observed in 48%-59% of all syndromic patients except for those diagnosed with Muenke syndrome (4%). All syndromic groups yielded smaller callosal/total brain volume ratios than controls (2.65) with the lowest values observed in Apert (2.29) and Muenke (2.34) syndromes (Table 1).

	Control	Apert	Crouzon-Pfeiffer	Muenke	Saethre-Chotzen
Stable VM (*n*)	0 (0%)	11 (33%)	24 (32%)	8 (32%)	0 (0%)
Progressive VM (*n*)	0 (0%)	4 (12%)	8 (11%)	0 (0%)	0 (0%)
Papilledema (*n*)	0 (0%)	16 (48%)	44 (59%)	1 (4%)	10 (53%)
Age (mean ± SD, yrs)	9.6 ± (5.1)	8.9 ± (5.1)	8.8 ± (4.8)	7.6 ± (4.5)	9.7 ± (7.8)
Brain volume (mean ± SD, mL)	1118.0 ± (107.4)	1368 ± (150.1)	1173.4 ± (147.9)	1297 ± (126.7)	1088 ± (124.2)
Corpus callosum volume (mean ± SD, mm^3)	2962 ± (590.2)	3136 ± (528.5)	2919 ± (637.0)	3038 ± (598.9)	2743 ± (502.5)
CC / Brain volume	2.65	2.29	2.49	2.34	2.52
Total MRIs (*n*)	36	33	75	25	19

Table 1. Patient characteristics shown by total number of MRI scans. Stable VM = stable ventriculomegaly; Progressive VM = progressive ventriculomegaly; CC/Brain volume = corpus callosum volume to brain volume ratio.

For patients with PV, a reduction of 469 mm^3 in total callosal volume was observed (β = -469.4, 95% CI -809.7 – -129.1, p = 0.009) while controlling for syndromic status, age, sex, and brain volume (Table 2). Historical finding of papilledema was not associated with any change in whole callosal volume (β = 70.5, 95% CI -130.7 – 271.7, p = 0.498), and neither was syndromic status or sex (β = -38.0, 95% CI -208.6 – 132.7, p = 0.670). Both age at the time of MRI (β = 49.5, 95% CI 35.5 – 63.5, p = < 0.001) and brain volume (β = 1.3, 95% CI 0.7 – 1.9, p = < 0.001) demonstrated positive correlation with whole callosal volume. Whole callosal volumes of patients with and without ventriculomegaly and papilledema are shown in Figure 1. Segmental volumes by age for both groups are shown in Figure 2.

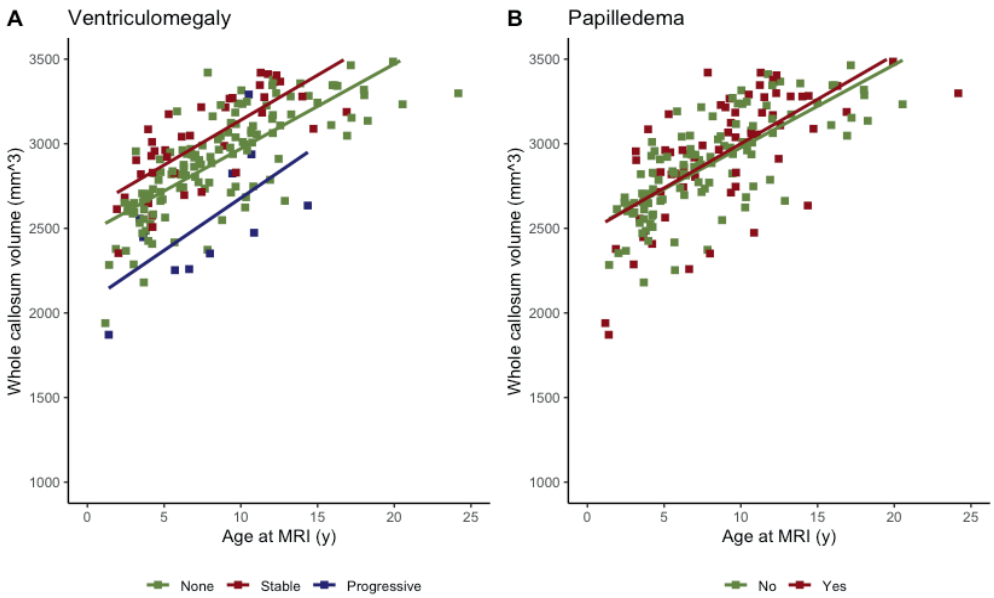

Figure 1. Whole corpus callosum volume shown by age for all patients. Subjects are categorized 437 by ventriculomegaly status on the left and by historical finding of papilledema on the right.

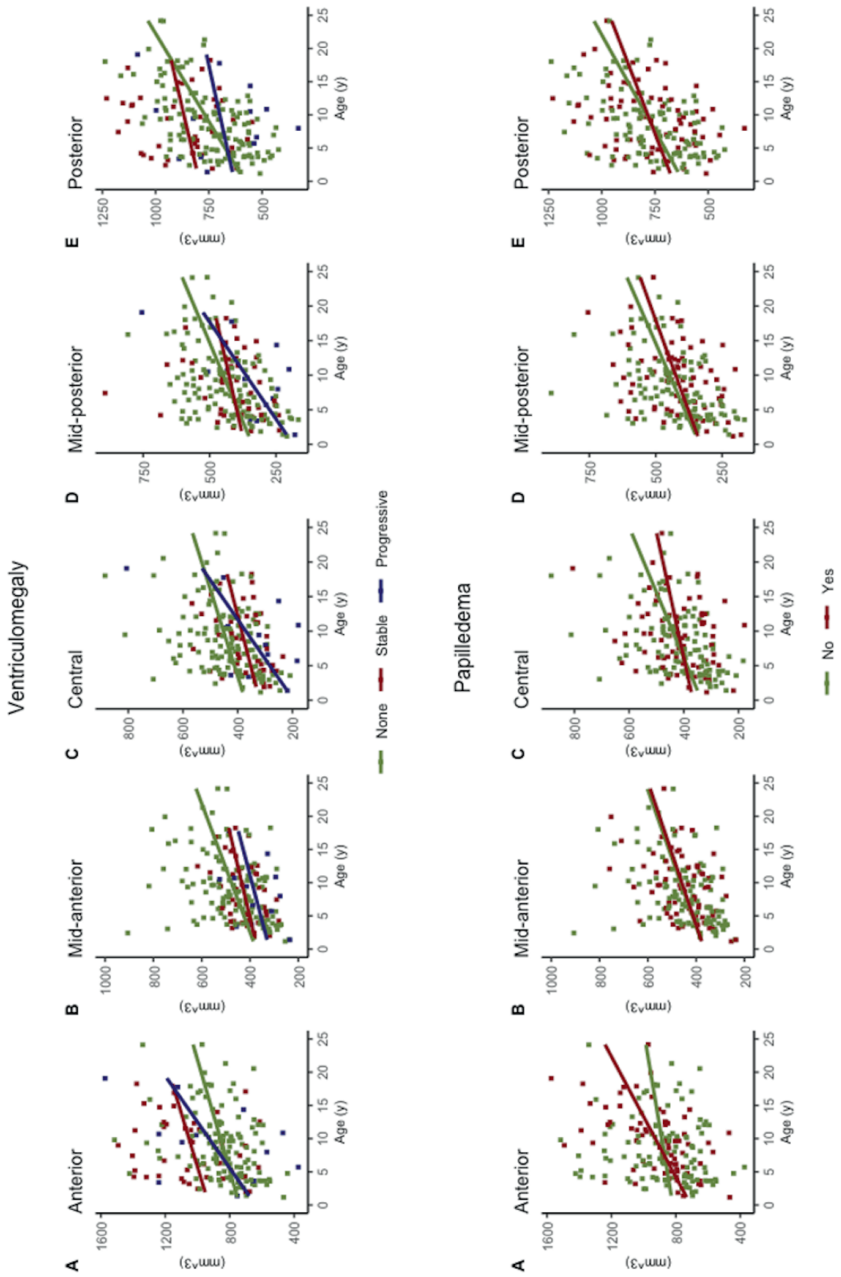

Figure 2. Regional corpus callosum volume shown by age for all patients grouped by ventriculomegaly and papilledema status. Regions are A = anterior, B = mid-anterior, C = central, D = mid-posterior, E = posterior, for both ventriculomegaly and papilledema plots.

Whole corpus callosum volume model

		Whole callosum	
Predictors	*Estimates*	*CI*	*p*
(Intercept)	1103.2	422.9 – 1783.5	**0.002**
Papilledema	70.5	-130.7 – 271.7	0.498
Stable VM	14.8	-170.2 – 199.8	0.877
Progressive VM	-469.4	-809.7 – -129.1	**0.009**
Apert	-173.9	-474.7 – 127.0	0.269
Crouzon-Pfeiffer	-48.1	-297.5 – 201.2	0.712
Muenke	-118.2	-395.5 – 159.2	0.415
Saethre-Chotzen	-234.0	-537.2 – 69.2	0.141
Sex: Female	-38.0	-208.6 – 132.7	0.670
Age	49.5	35.5 – 63.5	**<0.001**
Brain volume	1.3	0.7 – 1.9	**<0.001**
$N_{Subject\_ID}$	135		
Observations	188		

Table 2. Results of linear mixed effects model for whole corpus callosum volume. Brain volume reported in cm^3 and age reported in years. CI = 95% confidence interval; VM = ventriculomegaly.

Segmental analysis by multivariate multiple mixed regression modeling revealed a negative correlation between PV and callosal volumes across regions with greatest effects observed in the central (*ß* = -109.6, 95% CI -180.8 – -38.4), mid-anterior (*ß* = -106.9, 95% CI -194.8 – -18.9), and mid-posterior (*ß* = -107.5, 95% CI -180.3 – -34.7) segments (Table 3). Stable ventriculomegaly resulted in reduced central (*ß* = -54.4, 95% CI -94.8 – -14.0), mid-anterior (*ß* = -59.5, 95% CI -105.3 – -13.7), and mid-posterior (*ß* = -24.0, 95% CI -66.2 – 18.2) volumes. Historical finding of papilledema did not result in any significant segmental changes in volume. Syndromic status did, however, correlate with various segmental volume reductions which are demonstrated in Figure 3. Reduced central segment volumes were observed across all syndromes, the greatest of which were in Apert (*ß* = -96.9, 95% CI -160.1 – -

33.8) and Muenke (*ß* = -57.7, 95% CI -116.2 – 0.7) patients. A diagnosis of Muenke syndrome was also associated with lower callosal volume in the posterior segment (*ß* = -117.3, 95% CI -203.6 – -31.0). Finally, Saethre-Chotzen diagnosis was correlated with reduced mid-posterior volume (*ß* = -71.1, 95% CI -136.2 – -6.0) in addition to reduction of the central callosal segment. Age at the time of MRI was strongly correlated with CC volume across all segments, as was brain volume. Sex was not associated with any significant differences in segmental CC volumes.

Regional corpus callosum models

	Posterior		**Mid-posterior**		**Central**	
Predictors	*Estimates*	*CI*	*Estimates*	*CI*	*Estimates*	*CI*
(Intercept)	403.0	196.9 – 609.1	218.7	66.8 – 370.5	178.2	31.8 – 324.6
Papilledema	2.6	-59.7 – 65.0	4.7	-38.7 – 48.2	9.6	-32.8 – 52.0
Stable VM	69.0	13.9 – 124.0	-24.0	-66.2 – 18.2	-54.4	-94.8 – -14.0
Progressive VM	-75.4	-182.0 – 31.2	-107.5	-180.3 – -34.7	-109.6	-180.8 – -38.4
Apert	-40.7	-134.5 – 53.2	-58.0	-122.7 – 6.8	-96.9	-160.1 – -33.8
Crouzon-Pfeiffer	3.6	-74.3 – 81.5	-26.1	-79.6 – 27.4	-50.4	-102.7 – 1.9
Muenke	-117.3	-203.6 – -31.0	8.5	-51.6 – 68.5	-57.7	-116.2 – 0.7
Saethre-Chotzen	-49.5	-144.3 – 45.4	-71.1	-136.2 – -6.0	-40.0	-103.5 – 23.5
Sex: female	-45.1	-98.5 – 8.3	-17.8	-54.4 – 18.7	18.0	-17.8 – 53.7
Age	16.4	12.3 – 20.6	9.3	6.1 – 12.5	6.2	3.2 – 9.3
Brain volume	0.2	0.0 – 0.4	0.1	0.0 – 0.3	0.2	0.1 – 0.3
N	135 Subjects		135 Subjects		135 Subjects	
Observations	188		188		188	

	Mid-Anterior		Anterior	
Predictors	*Estimates*	*CI*	*Estimates*	*CI*
(Intercept)	149.8	-21.2 – 320.7	173.0	-80.0 – 425.9
Papilledema	18.4	-33.1 – 70.0	36.9	-39.6 – 113.3
Stable VM	-59.5	-105.3 – -13.7	66.7	-0.9 – 134.3
Progressive VM	-106.9	-194.8 – -18.9	-73.3	-204.0 – 57.3
Apert	-28.8	-106.3 – 48.6	61.8	-53.2 – 176.9
Crouzon-Pfeiffer	-15.4	-79.7 – 48.9	46.7	-48.8 – 142.2
Muenke	-35.0	-106.2 – 36.3	94.4	-11.4 – 200.2
Saethre-Chotzen	-50.4	-128.6 – 27.9	-23.4	-139.7 – 92.9
Sex: female	14.2	-29.8 – 58.3	-12.0	-77.4 – 53.4
Age	7.3	3.8 – 10.7	10.8	5.6 – 15.9
Brain volume	0.2	0.1 – 0.4	0.5	0.2 – 0.7
N	135 Subjects		135 Subjects	
Observations	188		188	

Table 3. Results of linear mixed effects models for each region of the corpus callosum. Brain volume reported in cm^3 and age reported in years. CI = 95% confidence interval; VM = ventriculomegaly.

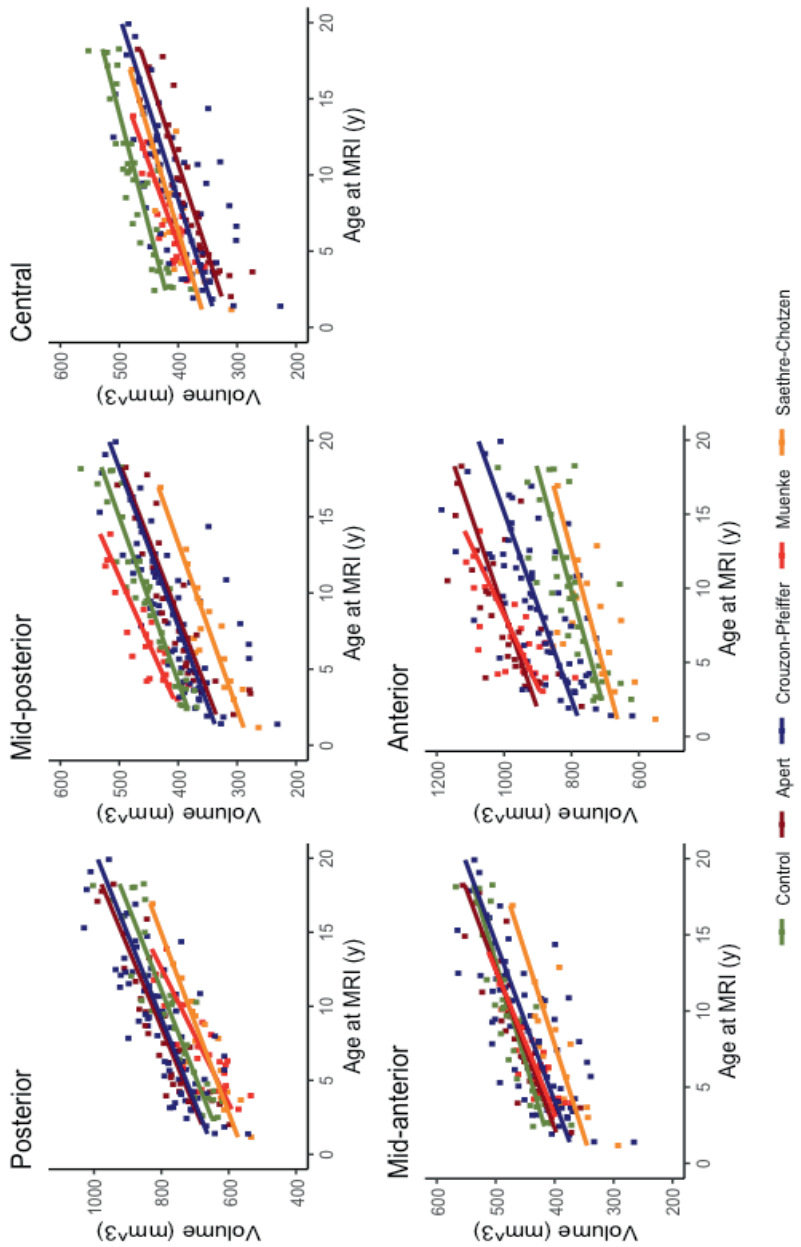

Figure 3. Regional corpus callosum volumes shown by age and grouped by syndromic status. Regions are A = anterior, B = mid-anterior, C = central, D = mid-posterior, E = posterior.

Discussion

We have previously described a correlation between papilledema, PV, and global cerebral cortical thinning in sCS patients[6]. The primary aim of this study was to determine if ICH in sCS is associated with white matter volume loss in the CC. We found that PV resulted in significantly reduced whole CC volume but failed to detect a correlation with papilledema. The secondary aim was to evaluate segmental volumes of the CC in relation to syndromic status or markers of ICH. This analysis revealed central thinning in the majority of sCS patients compared to controls with syndrome-specific variability in the posterior and mid-posterior regions. Greatest reduction in CC volume due to PV was also observed in the central segment. Overall, these findings may be explained by atypical strain on the callosum from both ventriculomegaly and cranial deformity.

Corpus callosum size is typically related to hemispheric volume in children and has demonstrated sensitivity to a variety of pathological processes including hydrocephalus and microcephaly[18]. White matter damage has previously been investigated in children with hydrocephalus via diffusion tensor imaging (DTI) and decreased continuity in tracts subjected to greater mechanical distortion has been described[19]. Here we show that reduced total volume of the CC is present in syndromic cases with PV. Notably, only 12 scans with previous PV were identified in our cohort and all carry a diagnosis of either Apert or Crouzon-Pfeiffer syndrome. Despite few patients with confirmed PV, we were able to detect significant callosal volume reductions of 469 mm^3, corresponding to loss of 15.0% and 16.1% for each respective syndrome. This is congruent with a previous report of reduced CC area in non-syndromic cases with lateral ventricular enlargement[20].

Due to our previous findings of cerebral cortical thinning following papilledema in syndromic patients, we expected to find commensurate whole callosum volumetric changes in this study, but none were observed. Failure to detect an association with papilledema may be due to differences in sensitivities of white and grey matter to intracranial pressure elevations[21]. Furthermore, intensive screening and timely treatment of ICH once detected likely reduces the development of morphologic sequelae from prolonged elevations in intracranial pressure.

Regional callosal development in healthy patients has been well described in the literature.[7,22-25] Progressive thickening of the body throughout childhood is typically observed. Lack of adherence to

this growth pattern occurs in various neuropsychiatric disorders and is concerning for atypical development[9,26,27]. Analysis of regional CC volumes in this study revealed a negative correlation between PV and volume across all regions with the greatest reductions occurring in the body (central, mid-anterior, and mid-posterior segments). These regions have previously been shown to bear the greatest amount of mechanical stress due to hydrocephalus. Hofmann et al showed that in both communicating and non-communicating hydrocephalus, the body of the CC rises and impingement by the free edge of the falx cerebri occurs at its dorsal aspect[28]. Stable ventriculomegaly resulted in a pattern of CC volume similar to that of PV with negative correlations observed in the central, mid-anterior, and mid-posterior segments. Due to similar focal growth deficits of the callosal body observed in both progressive and stable ventriculomegaly, a mechanical explanation is probable.

Callosal body volume reductions were also mirrored in syndromic patients without ventriculomegaly. A mechanical explanation exists for these patients as well. The posterior mid-body of the CC has demonstrated susceptibility following traumatic brain injury (TBI), likely due to axonal shear strain produced by the falx and tentorium cerebri[29-31]. In TBI, white matter atrophy is attributed to both immediate traumatic axonal injury as well as hypoxia-ischemia occurring in the post-injury phase[31]. Although all patients in this study were atraumatic, a similar but non-ballistic stress may be produced by asymmetric cranial deformity due to sCS, resulting in the focal loss of volume observed in this study.

Clinically, the prevention of hydrocephalus, ICH, and prolonged cranial distortion remain primary goals in the treatment for sCS patients. Current strategies to achieve this vary among craniofacial centers, with some advocating for prophylactic vault expansion (spring-assisted, distraction osteogenesis, and/or whole vault remodeling) and others opting for a more conservative approach, reserving early surgery for those with confirmed ICH[32]. At our center, prophylactic vault expansion is preferred due to the high rate of ICH and its negative sequelae known to occur in sCS[33,34]. Authentic hydrocephalus has been reported in up to 7% of Apert patients and 64% of Crouzon-Pfeiffer patients and is associated with worse neuropsychiatric outcomes[35-37]. Although the effect of surgical intervention was not directly evaluated here, evidence of focal growth reduction of the CC body supports the rationale for early operative intervention in attempt to relieve cranial growth restriction and its potential effects on neuromorphologic development.

Our findings must be interpreted with the following limitations. First, not every patient included underwent serial imaging which makes longitudinal interpretation of our data more difficult. We have attempted to maximize use of the data we do have by including all available scans and indexing them by patient through mixed effects modeling. Secondly, the PV patients included were few in number and relegated to only two syndromes, therefore conclusions regarding the effect of PV on CC volume must be limited to Apert and Crouzon-Pfeiffer patients. Thirdly, development of the CC occurs over an extended period of time beginning in the anterior segment in childhood and ending posteriorly in adulthood[23]. Due to the age of the majority of our cohort, it is likely that final development of the posterior segments has not yet occurred and could potentially normalize over time. However, the age of our patients is well-distributed across subgroups and therefore underdevelopment should be equally shared among syndromic and control patients alike.

In this study we have shown that PV, specifically in Apert and Crouzon-Pfeiffer syndrome, results in reduced whole CC volume. Regionally, syndromic diagnosis and stable ventriculomegaly both resulted in reduced growth of the callosal body which is consistent with abnormal development. Both intrinsic strain from ventriculomegaly and extrinsic strain from cranial deformity are expected to contribute to this phenomenon. Clinical management of syndromic patients includes the normalization of these forces through CSF diversion procedures for hydrocephalus and surgical correction of skull deformities. Prophylactic cranial vault expansion in the first year of life is the preferred treatment at our center in attempt to prevent prolonged mechanical stress from cranial deformity and its focal effects on the CC. Future studies should investigate regional callosal tractography and the effect of different treatment protocols on structural brain development in syndromic patients.

References

1. Sharma VP, Fenwick AL, Brockop MS, et al. Mutations in TCF12, encoding a basic helix-loop-helix partner of TWIST1, are a frequent cause of coronal craniosynostosis. *Nature genetics.* 2013;45(3):304-307.
2. Johnson D, Wilkie AOM. Craniosynostosis. *European journal of human genetics : EJHG.* 2011;19(4):369-376.
3. Marucci DD, Dunaway DJ, Jones BM, Hayward RD. Raised intracranial pressure in Apert syndrome. *Plastic and reconstructive surgery.* 2008;122(4):1162-1168; discussion 1169-1170.
4. Abu-Sittah GS, Jeelani O, Dunaway D, Hayward R. Raised intracranial pressure in Crouzon syndrome: incidence, causes, and management. *Journal of neurosurgery Pediatrics.* 2016;17(4):469-475.
5. Cornelissen MJ, Loudon SE, van Doorn FE, Muller RP, van Veelen MC, Mathijssen IM. Very Low Prevalence of Intracranial Hypertension in Trigonocephaly. *Plastic and reconstructive surgery.* 2017;139(1):97e-104e.
6. Wilson AT, Den Ottelander BK, De Goederen R, et al. Intracranial hypertension and cortical thickness in syndromic craniosynostosis. *Dev Med Child Neurol.* 2020.
7. Luders E, Thompson PM, Toga AW. The development of the corpus callosum in the healthy human brain. *The Journal of neuroscience : the official journal of the Society for Neuroscience.* 2010;30(33):10985-10990.
8. Luders E, Narr KL, Bilder RM, et al. Positive correlations between corpus callosum thickness and intelligence. *NeuroImage.* 2007;37(4):1457-1464.
9. Luders E, Narr KL, Hamilton LS, et al. Decreased callosal thickness in attention-deficit/hyperactivity disorder. *Biol Psychiatry.* 2009;65(1):84-88.
10. Mathijssen IM. Guideline for Care of Patients With the Diagnoses of Craniosynostosis: Working Group on Craniosynostosis. *The Journal of craniofacial surgery.* 2015;26(6):1735-1807.
11. Tuite GF, Chong WK, Evanson J, et al. The effectiveness of papilledema as an indicator of raised intracranial pressure in children with craniosynostosis. *Neurosurgery.* 1996;38(2):272-278.
12. Rijken BF, Lequin MH, Van Veelen ML, de Rooi J, Mathijssen IM. The formation of the foramen magnum and its role in developing ventriculomegaly and Chiari I malformation in children with craniosynostosis syndromes. *Journal of cranio-maxillo-facial surgery : official publication of the European Association for Cranio-Maxillo-Facial Surgery.* 2015;43(7):1042-1048.
13. Rijken BF, Lequin MH, van der Lijn F, et al. The role of the posterior fossa in developing Chiari I malformation in children with craniosynostosis syndromes. *Journal of cranio-maxillo-facial surgery : official publication of the European Association for Cranio-Maxillo-Facial Surgery.* 2015;43(6):813-819.
14. Dale AM, Fischl B, Sereno MI. Cortical surface-based analysis. I. Segmentation and surface reconstruction. *NeuroImage.* 1999;9(2):179-194.
15. Fischl B, Dale AM. Measuring the thickness of the human cerebral cortex from magnetic resonance images. *Proceedings of the National Academy of Sciences of the United States of America.* 2000;97(20):11050-11055.
16. Fischl B, Sereno MI, Dale AM. Cortical surface-based analysis. II: Inflation, flattening, and a surface-based coordinate system. *NeuroImage.* 1999;9(2):195-207.
17. Fischl B, Salat DH, Busa E, et al. Whole Brain Segmentation: Automated Labeling of Neuroanatomical Structures in the Human Brain. *Neuron.* 2002;33(3):341-355.

18. Andronikou S, Pillay T, Gabuza L, et al. Corpus callosum thickness in children: an MR pattern-recognition approach on the midsagittal image. *Pediatr Radiol.* 2015;45(2):258-272.
19. Rajagopal A, Shimony JS, McKinstry RC, et al. White matter microstructural abnormality in children with hydrocephalus detected by probabilistic diffusion tractography. *AJNR American journal of neuroradiology.* 2013;34(12):2379-2385.
20. Aldridge K, Collett BR, Wallace ER, et al. Structural brain differences in school-age children with and without single-suture craniosynostosis. *Journal of neurosurgery Pediatrics.* 2017;19(4):479-489.
21. Lafrenaye AD, McGinn MJ, Povlishock JT. Increased intracranial pressure after diffuse traumatic brain injury exacerbates neuronal somatic membrane poration but not axonal injury: evidence for primary intracranial pressure-induced neuronal perturbation. *J Cereb Blood Flow Metab.* 2012;32(10):1919-1932.
22. Giedd JN, Rumsey JM, Castellanos FX, et al. A quantitative MRI study of the corpus callosum in children and adolescents. *Brain Res Dev Brain Res.* 1996;91(2):274-280.
23. Tanaka-Arakawa MM, Matsui M, Tanaka C, et al. Developmental changes in the corpus callosum from infancy to early adulthood: a structural magnetic resonance imaging study. *PLoS One.* 2015;10(3):e0118760.
24. Giedd JN, Blumenthal J, Jeffries NO, et al. Development of the human corpus callosum during childhood and adolescence: a longitudinal MRI study. *Prog Neuropsychopharmacol Biol Psychiatry.* 1999;23(4):571-588.
25. Keshavan MS, Diwadkar VA, DeBellis M, et al. Development of the corpus callosum in childhood, adolescence and early adulthood. *Life Sci.* 2002;70(16):1909-1922.
26. Freitag CM, Luders E, Hulst HE, et al. Total brain volume and corpus callosum size in medication-naïve adolescents and young adults with autism spectrum disorder. *Biol Psychiatry.* 2009;66(4):316-319.
27. Boger-Megiddo I, Shaw DW, Friedman SD, et al. Corpus callosum morphometrics in young children with autism spectrum disorder. *J Autism Dev Disord.* 2006;36(6):733-739.
28. Hofmann E, Becker T, Jackel M, et al. The corpus callosum in communicating and noncommunicating hydrocephalus. *Neuroradiology.* 1995;37(3):212-218.
29. Gentry LR, Thompson B, Godersky JC. Trauma to the corpus callosum: MR features. *AJNR Am J Neuroradiol.* 1988;9(6):1129-1138.
30. Mendelsohn DB, Levin HS, Harward H, Bruce D. Corpus callosum lesions after closed head injury in children: MRI, clinical features and outcome. *Neuroradiology.* 1992;34(5):384-388.
31. Tasker RC. Changes in white matter late after severe traumatic brain injury in childhood. *Dev Neurosci.* 2006;28(4-5):302-308.
32. O'Hara J, Ruggiero F, Wilson L, et al. Syndromic Craniosynostosis: Complexities of Clinical Care. *Mol Syndromol.* 2019;10(1-2):83-97.
33. Spruijt B, Joosten KF, Driessen C, et al. Algorithm for the Management of Intracranial Hypertension in Children with Syndromic Craniosynostosis. *Plast Reconstr Surg.* 2015;136(2):331-340.
34. de Jong T, Bannink N, Bredero-Boelhouwer HH, et al. Long-term functional outcome in 167 patients with syndromic craniosynostosis; defining a syndrome-specific risk profile. *J Plast Reconstr Aesthet Surg.* 2010;63(10):1635-1641.
35. Collmann H, Sörensen N, Krauss J. Hydrocephalus in craniosynostosis: a review. *Childs Nerv Syst.* 2005;21(10):902-912.

36. Noetzel MJ, Marsh JL, Palkes H, Gado M. Hydrocephalus and mental retardation in craniosynostosis. *J Pediatr.* 1985;107(6):885-892.
37. Coll G, El Ouadih Y, Abed Rabbo F, Jecko V, Sakka L, Di Rocco F. Hydrocephalus and Chiari malformation pathophysiology in FGFR2-related faciocraniosynostosis: A review. *Neurochirurgie.* 2019;65(5):264-268.

CHAPTER 5

Disappointing results of spring-assisted cranial vault expansion in Crouzon patients presenting with sagittal synostosis

Wilson AT, Gaillard L, Versnel SL, Spoor JK, van Veelen MLC, Mathijssen IMJ

Neurosurgical Focus, 2021

Abstract

The aim of this study is to report on our center's experience with spring-assisted cranial vault expansion (SAE) in Crouzon patients with sagittal suture synostosis. Strip craniotomy with SAE in patients with isolated scaphocephaly has resulted in successful outcomes with low complication and revision rates. However, recent experience suggests that the outcome in Crouzon patients with sagittal synostosis undergoing SAE is less favorable compared to frontobiparietal (FBP) expansion. We reviewed both operations performed at our center and noticed an upward expansion of the skull which may be related to ventriculomegaly, with concurrent intracranial hypertension and poor aesthetic outcome. All SAE treated sagittal synostosis patients diagnosed with Crouzon syndrome have required a revision FBP operation. Based on this outcome we consider Crouzon syndrome a contraindication for correcting sagittal synostosis with springs.

Introduction

Spring-assisted cranial vault expansion (SAE) was first described by Lauritzen in 1998 and has since been widely adopted by various craniofacial centers globally, including our own starting in 2010[1-3]. Advantages of this technique include early operative intervention, minimized blood loss and operative time, resulting in an improved morbidity profile compared to traditional whole vault remodeling techniques[4]. A drawback is the need for a second operation for device removal. Overall, spring-mediated cranial vault expansion yields good functional and aesthetic results in the treatment of isolated sagittal craniosynostosis[5].

Preferred management of sagittal synostosis (SS) at our center involves scheduled SAE prior to 6 months of age. Prior to 2010, frontobiparietal (FBP) remodeling was performed, at the age of 6 to 9 months. This switch in protocol was recently reviewed and showed SAE to be safe and effective with reduced operative time, reduced blood loss, and a lower incidence of postoperative intracranial hypertension (ICH)[5]. However, recent observation suggests that SAE may be less effective in SS patients diagnosed with Crouzon syndrome. We therefore evaluated surgical treatment in all Crouzon patients with scaphocephaly due to sagittal synostosis.

Methods

Medical records of all Crouzon patients treated at our center were reviewed. Only those with sagittal synostosis confirmed by computed tomography (CT) were included for analysis. The management of patients with Crouzon syndrome at our institution includes, regular occipitofrontal head circumference (OFC) measurements, fundoscopy, polysomnography (PSG), and magnetic resonance imaging (MRI) of the brain. Data from all of these assessments were evaluated along with postoperative aesthetic outcome (Table 1). Obstructive sleep apnea (OSA) was diagnosed by an obstructive apneic-hypopneic index (oAHI) greater than 1 for mild and greater than 5 for moderate to severe disease. Skull growth restriction was considered to have occurred as indicated by a drop of 0.5 standard deviations (SD) in OFC measurements indexed to each patient's own progression curve over 2 years. Cranial index (CI) was also calculated pre and postoperatively at the earliest date of imaging available from x-ray, CT, or MRI by dividing maximum skull breadth by maximum skull length and multiplying by 100.

Patient	Sex	Primary operation (age)	Additional vault operation (age, indication)	OSA	OFC growth arrest	Ventriculomegaly (progressive +/-)
#1	M	FBP (39 mo)	-	mild	no	no, (-)
#2	M	FBP (11 mo)	-	no	no	yes, (-)
#3	M	FBP (9 mo)	-	no	no	no, (-)
#4	F	SAE (5 mo)	FBP (27 mo, skull deformity, raised ICP)	no	no	yes, (+)
#5	M	SAE (5 mo)	FBP (19 mo, skull deformity)	mild	no	no, (-)
#6	M	SAE (4 mo)	FBP (16 mo, raised ICP), Biparietal remodeling (51 mo, skull deformity)	mild	yes	yes, (-)

Patient	Papilledema (age)	Progressive synostosis (age)	Cranial index (age)	Aesthetic outcome following primary operation	Aesthetic outcome following secondary operation
#1	no	yes, (74 mo)	68.7 (37 mo) 77.4 (59 mo)	good	-
#2	no	yes, (110 mo)	71.9 (98 mo)	acceptable, mild narrowing and increased height	-
#3	no	yes, (20 mo)	75.5 (111 mo)	good	-
#4	yes, (25 mo)	yes, (28 mo)	66.5 (2 mo) 82.2 (22 mo) 81.6 (28 mo)	mild narrowing with turricephaly	suboptimal, with some residual turricephaly
#5	yes, (19 mo)	no	63.5 (2 mo) 67.0 (11 mo) 80.0 (28 mo)	narrow, persistent scaphocephaly	good
#6	yes, (10 mo)	yes, (16 mo)	61.3 (3 mo) 67.2 (15 mo) 75.3 (52 mo)	narrow, with turricephaly	suboptimal, with some residual turricephaly

Table 1: Clinical and demographic data for each patient are shown. OSA = obstructive sleep apnea; OFC = occipitofrontal circumference; FBP = frontobiparietal expansion; SAE = spring-assisted expansion. Age in months shown in parentheses.

Operative Technique

Osteotomies varied significantly between techniques. Two parasagittal osteotomies were performed in SAE with a bone strip left in place to avoid damage to the sagittal sinus. Width of the osteotomies were tailored to the shape of each patient's skull but always within 3 to 4 cm. Springs used in each case were 9N with a maximal width of 8.9 cm (BS 2056, grade 316S42; 1.22-mm thick; The Active Spring Co., Essex, United Kingdom). In each case spring removal was scheduled 12 weeks following placement[5]. Osteotomies made during FBP also included parasagittal cuts but the bone strip overlying the sagittal sinus was rotated 90 degrees to achieve biparietal widening (Figure 1). The remaining bone graft was used to close the vault as much as possible. This technique has previously been described in detail[6].

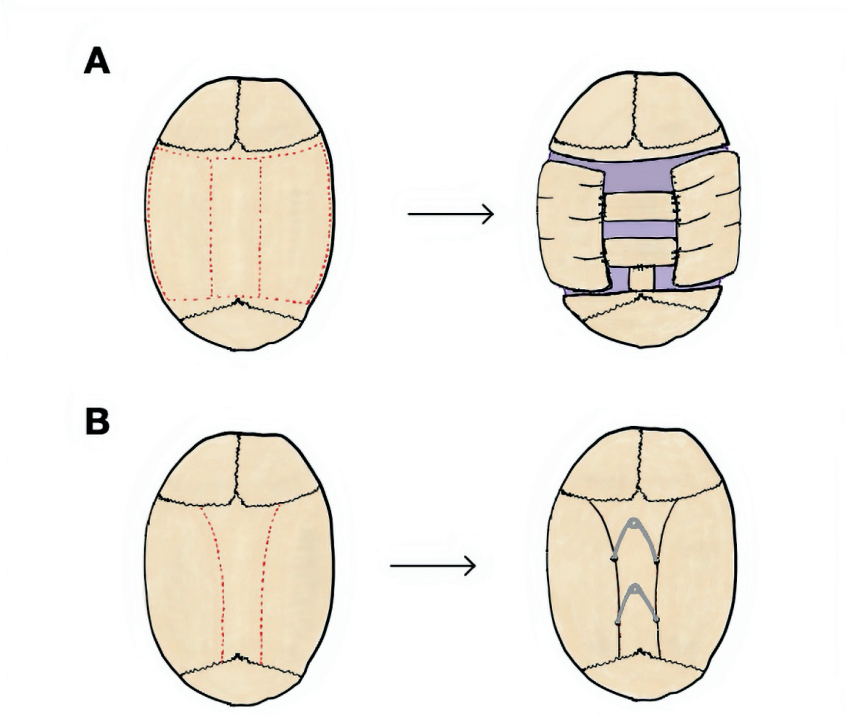

Figure 1: A) Frontobiparietal expansion. Osteotomies are shown as dashed red lines and bone flap design is shown to the right. B) Spring-assisted expansion. Osteotomies are shown as dashed red lines and subsequent spring placement is shown to the right.

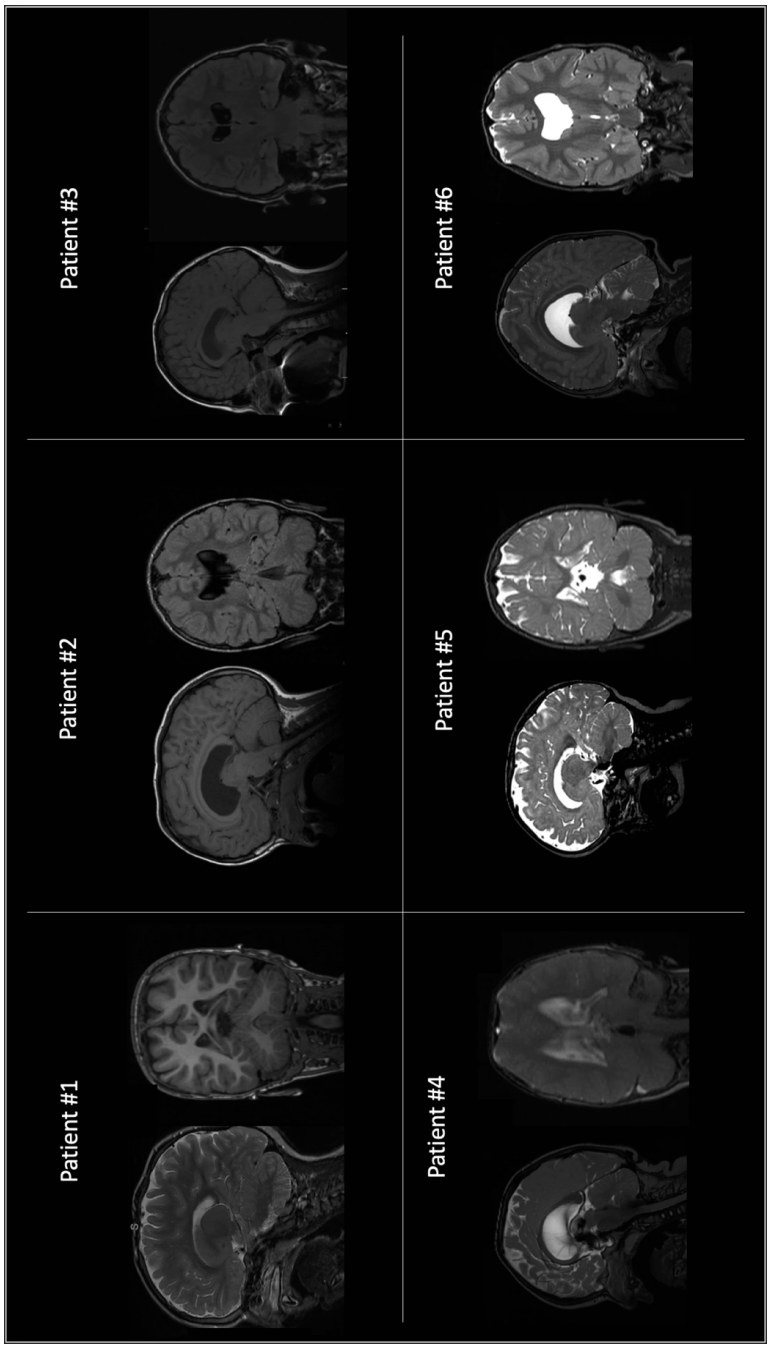

Figure 2: Postoperative magnetic resonance imaging of each patient (patients 1-6 labeled).

Results

In total, six Crouzon patients were identified (1999-2018) to have undergone surgical treatment for SS. Three underwent a traditional FBP technique, and three were treated by SAE. None of the FBP-treated patients required additional vault expansion or revision (Table 1). All of the SAE patients required a secondary FBP operation and one (patient 6) required tertiary biparietal remodeling. The indication for revision surgery was poor aesthetic outcome in each case with additional concerns for raised intracranial pressure (ICP) in some patients based on fundoscopy and MRI. Ventriculomegaly occurred in two patients undergoing SAE and one FBP patient. Only one of these patients (patient 4) demonstrated progressive ventriculomegaly over one year following initial cranial vault expansion. Cranial indices were similar in both FBP and SAE treated patients (Table 1). Progressive synostosis, which is common in Crouzon syndrome[7], occurred in four patients at varying time intervals following vault expansion, but did not appear to affect surgical outcome. Average time to progressive synostosis, when present, was 36 months and average time to surgical revision in SAE patients was 16 months.

Turricephalic growth and ventriculomegaly were observed in patients from both treatment groups (patients 2, 4, and 6), but only those treated by SAE required revision surgery. In patient 4, ventriculomegaly was noted prior to surgery and subsequent expansion occurred most dramatically in a cranial direction, with an upward lift of the sagittal bone strip. Good correction of the occiput was observed postoperatively but biparietal narrowing and elevation of the vertex contributed to a suboptimal aesthetic outcome. Hydrocephalus was then diagnosed on subsequent imaging and confirmed by direct ICP monitoring 17 months following spring removal. FBP was performed and biparietal widening was achieved with some residual turricephaly. No treatment (e.g. shunt placement) for ventriculomegaly was performed prior to the FBP operation.

In patient 5, Crouzon features were not evident at the time of SAE. Intraoperatively, the parietal bones were observed to be thicker and less pliable than normal, perhaps limiting lateral expansion. A de novo unclassified variant in FGFR2 was then detected (c.931G>T, p.Val311Phe). Residual occipital bulleting was observed following SAE and parents mentioned difficulty in maintaining supine positioning according to postoperative protocol. In the following months, non-specific signs of raised ICP were noted (elongated optic nerve, large amount of cerebrospinal fluid in the optic nerve sheath,

globe flattening bilaterally) along with papilledema. Ultimately FBP was performed for definitive correction of persistent skull narrowing and raised ICP. The final aesthetic outcome was good with notable biparietal widening and normalization of ICP.

Adequate correction of the occiput was achieved in patient 6 with a fair amount of biparietal widening following initial SAE. Shortly thereafter upward growth of the skull through the parasagittal osteotomies was noted resulting in severe turricephaly along with signs of raised ICP, ventriculomegaly, and papilledema. Subsequently FBP was performed with biparietal narrowing still observed postoperatively. This was followed by additional biparietal remodelling 3 years later in an attempt to further correct the turricephalic shape. The final aesthetic result remains suboptimal due to residual turricephaly. Postoperative MRIs of each patient are shown in Figure 2.

Discussion

Of the six Crouzon patients with SS reviewed here, all three who had a primary SAE procedure before the age of six months underwent secondary cranial vault surgery. The indication for reoperation was inadequate skull deformity correction and the development of ICH in the follow-up period. Although the benefit of SAE in isolated SS has been reduction of ICH, good aesthetic correction, and less blood loss, the revision rate in this initial cohort suggests that SAE is suboptimal in Crouzon patients with SS. The underlying tendency toward ventricular expansion and progressive synostosis known to occur in Crouzon syndrome, as well as younger age at operation in SAE-treated patients may explain these findings.

Ventriculomegaly occurs in nearly half of all Crouzon patients and may be a benign dilation or progress into hydrocephalus requiring shunt placement[8-10]. Progressive ventriculomegaly was only seen in one patient (patient 4) who was later confirmed to have hydrocephalus and raised ICP shown by direct measurement. Ventricular dilation following cranial vault expansion has previously been reported in patients with no preoperative evidence of hydrocephalus and attributed to a subclinical elevation in ICP which is decompressed during surgery[8,11]. Since postoperative ventricular dilation may occur, it seems plausible that the direction of its expansion, when present, might be influenced by type of operation.

Following cranial vault expansion, subsequent brain growth likely encounters differential resistance bi-parietally and vertically in the case of SAE due to fewer osteotomies and reliance on progressive expansion. This dynamic approach retains physiologic resistance at uninvolved sutures (e.g. squamosal) where parietal bones are anchored but the difference between physiologic resistance and that of newly expanding osteotomies may direct brain growth upward toward the path of least resistance. In patients treated by FBP, cranial vault expansion is immediate and fixed, resulting in a relatively equal distribution of resistance by reconstructing the cranial vault in a mosaic fashion following the complete elevation of parietal bone flaps. A greater degree of uniform resistance may be especially important in patients prone to postoperative ventricular dilation such as those with Crouzon syndrome. In this way, if postoperative dilation occurs it may result in a uniform ventriculomegaly (as seen in patient 2) rather than one marked by distortion of both the ventricles and calvarium necessitating additional surgical correction (patients 4 and 6).

Additionally, dural attachments may play a role. Removal of these attachments to the central bone strip overlying the superior sagittal sinus only occurs in FBP as this segment is rotated ninety degrees to achieve biparietal widening. In SAE, these attachments are left in place with no change in position of the strip. If abnormal flow through the superior sagittal sinus is present preoperatively due to cranial distortion, SAE would not address this and FBP would untether it, potentially resulting in a more physiologic state.

Another factor which must be considered is the high rate of progressive synostosis in Crouzon syndrome which has been reported in up to 76.5% of cases[7]. Postoperative lambdoid synostosis could result in occipital flattening and elevation of the vertex, explaining the turricephaly observed in this study. In our cohort, lambdoid synostosis was noted in all FBP patients and two of three SAE patients. Notably, the best aesthetic outcome in the SAE group was observed in patient 5, who experienced no progressive synostosis. However, if progressive lambdoid involvement were the only reason for differences in outcomes between SAE and FBP groups we would expect higher rates of progressive synostosis in the SAE group as compared to the FBP group, which is not the case. Therefore, it seems unlikely that progressive suture involvement fully explains the differences observed between FBP and SAE patients.

Lastly, age at surgical intervention may also influence these outcomes as SAE and FBP were performed at 4-5 months and 9-39 months of age respectively. Skull growth occurs more rapidly in the first months of life making it more difficult to achieve definitive correction early in development due to less predictable changes in postoperative growth. However, improved neuropsychological outcomes in patients treated before the age of 6 months have been reported[12]. Therefore, we now prefer an FBP operation at the age of 6 months in all SS Crouzon patients to provide timely relief of skull growth restriction while attempting definitive correction of scaphocephaly.

Conclusions

We have briefly described our experience with SAE and FBP operations in SS patients with Crouzon syndrome and observed poor outcomes following SAE, both relating to development of ICH during follow-up as well as the head shape. Potential explanations for worse outcomes observed in SAE include ventriculomegaly, progressive synostosis, and age at the time of operation. Isolated sagittal synostosis rarely occurs in Crouzon syndrome, therefore the size of our cohort in this study is small. Further investigation of patients treated by both SAE and whole-vault remodeling techniques should continue in larger cohorts to elucidate the optimal treatment protocol for these patients. Based on our preliminary results we have changed our protocol to FBP at 6 months of age for Crouzon patients with sagittal synostosis and recommend against the use of springs in these select cases.

References:

1. Lauritzen C, Sugawara Y, Kocabalkan O, Olsson R. Spring mediated dynamic craniofacial reshaping. Case report. *Scand J Plast Reconstr Surg Hand Surg.* 1998;32(3):331-338.
2. David LR, Plikaitis CM, Couture D, Glazier SS, Argenta LC. Outcome analysis of our first 75 spring-assisted surgeries for scaphocephaly. *The Journal of craniofacial surgery.* 2010;21(1):3-9.
3. Taylor JA, Maugans TA. Comparison of spring-mediated cranioplasty to minimally invasive strip craniectomy and barrel staving for early treatment of sagittal craniosynostosis. *The Journal of craniofacial surgery.* 2011;22(4):1225-1229.
4. Arko Lt, Swanson JW, Fierst TM, et al. Spring-mediated sagittal craniosynostosis treatment at the Children's Hospital of Philadelphia: technical notes and literature review. *Neurosurgical focus.* 2015;38(5):E7.
5. van Veelen MC, Kamst N, Touw C, et al. Minimally Invasive, Spring-Assisted Correction of Sagittal Suture Synostosis: Technique, Outcome, and Complications in 83 Cases. *Plastic and reconstructive surgery.* 2018;141(2):423-433.
6. Veelen M-LCv, Mihajlović D, Dammers R, Lingsma H, Adrichem LNAv, Mathijssen IMJ. Frontobiparietal remodeling with or without a widening bridge for sagittal synostosis: comparison of 2 cohorts for aesthetic and functional outcome. 2015;16(1):86.
7. Connolly JP, Gruss J, Seto ML, et al. Progressive postnatal craniosynostosis and increased intracranial pressure. *Plastic and reconstructive surgery.* 2004;113(5):1313-1323.
8. Cinalli G, Sainte-Rose C, Kollar EM, et al. Hydrocephalus and craniosynostosis. *Journal of neurosurgery.* 1998;88(2):209-214.
9. Noetzel MJ, Marsh JL, Palkes H, Gado M. Hydrocephalus and mental retardation in craniosynostosis. *J Pediatr.* 1985;107(6):885-892.
10. Proudman TW, Clark BE, Moore MH, Abbott AH, David DJ. Central nervous system imaging in Crouzon's syndrome. *The Journal of craniofacial surgery.* 1995;6(5):401-405.
11. Collmann H, Sörensen N, Krauss J, Mühling J. Hydrocephalus in craniosynostosis. *Child's nervous system : ChNS : official journal of the International Society for Pediatric Neurosurgery.* 1988;4(5):279-285.
12. Patel A, Yang JF, Hashim PW, et al. The impact of age at surgery on long-term neuropsychological outcomes in sagittal craniosynostosis. *Plastic and reconstructive surgery.* 2014;134(4):608e-617e.

CHAPTER 6

Cerebral cortex maldevelopment in syndromic craniosynostosis: An allometric study

Wilson AT, Ottelander BK, van Veelen MLC, Dremmen MHG, Persing JA, Vrooman HA, Mathijssen IMJ, Tasker RC

Developmental Medicine and Child Neurology, 2021

Abstract

Aim: Our aim is to assess the relationship of surface area of the cerebral cortex to intracranial volume in syndromic craniosynostosis.

Methods: Syndromic craniosynostosis patient records were reviewed to include clinical and imaging data. 204 total MRIs were evaluated in this study (148 of *FGFR* patients, 19 of *TWIST1* patients, and 37 controls). MRIs were processed via FreeSurfer pipeline to determine total intracranial volume (ICV) and cortical surface area (CSA). Scaling coefficients were calculated from log-transformed data via mixed regression to account for multiple measurements, sex, syndrome, and age. Educational outcomes were reported by syndrome.

Results: Mean (SD) ICV was greater in *FGFR* patients (1519 ± 269 cm^3, $p = 0.016$) than in *TWIST1* (1304 ± 145 cm^3) or controls (1405 ± 158 cm^3). CSA was related to ICV by a scaling law with an exponent of 0.68 (95% CI 0.61 – 0.76) in *FGFR* patients compared to 0.81 (95% CI 0.50 – 1.12) in *TWIST1* patients and 0.77 (95% CI 0.61 – 0.93) in controls. Lobar analysis revealed reduced scaling in the parietal (0.50, 95% CI 0.42 – 0.59) and occipital (0.67, 95% CI 0.54 – 0.80) lobes of *FGFR* patients compared with controls. Modified learning environments were needed more often in *FGFR* patients.

Conclusion: Despite adequate ICV in *FGFR*-mediated craniosynostosis, CSA development is reduced, indicating maldevelopment, particularly in parietal and occipital lobes. Modified education is also more common in *FGFR* patients.

Introduction

Craniosynostosis is a congenital disorder characterized by premature fusion of calvarial sutures resulting in cranial shape deformity specific to the sutures involved. This shape is governed by Virchow's law which states that growth is enhanced parallel to affected sutures and is arrested orthogonally. Invariably, every pattern of true cranial growth restriction poses a risk to the developing brain and is treated accordingly with various surgical interventions. Multiple suture involvement often occurs in syndromic variants of the disease attributable to mutations in fibroblast growth factor receptor (*FGFR*) (Apert, Crouzon-Pfeiffer, and Muenke syndromes) and *TWIST1* (Saethre-Chotzen syndrome) genes which play important roles in cortical and mesodermal development respectively (1, 2). Thus, cranial growth restriction as well as genetic mutation may play a role in neurodevelopmental outcomes in syndromic craniosynostosis.

Allometry can be broadly defined as the relative change in proportion of one attribute compared to another during organismal growth. In general, human brain growth exhibits a power-law scaling relationship between surface area and volume as overall brain size increases, with larger brains showing disproportionally greater surface area than smaller ones (3-6). This is achieved through primary, secondary, and tertiary cortical folding driven by grey matter volume expansion and white matter tension in the second and third trimesters (7, 8). Disruption of this critical process, through prematurity or intrauterine growth restriction, results in reduced surface area to volume scaling and predictable impairment in neurobehavioral development (9).

Due to the increased frequency of neurodevelopmental issues in syndromic craniosynostosis and the pathognomonic cranial growth restriction characteristic of the disease, we wondered if there might exist a morphometric neural substrate for the developmental pathology in these cases. Thus, our primary aim is to evaluate the effect of syndromic craniosynostosis diagnosis on intracranial volume, while controlling for age and sex. A secondary aim is to evaluate the scaling relationship between intracranial volume (ICV) and cortical surface area (CSA). Finally, exploratory analyses of this relationship in distinct cortical lobes.

Methods

Participants

The Institution Research Ethics Board (IRB) at Erasmus University Medical Center (MEC), Rotterdam, the Netherlands approved this study (MEC-2014-461), which is part of ongoing work at the Dutch Craniofacial Center involving protocolized care, brain imaging, clinical assessment and data summary and evaluation. Medical records of all syndromic (Apert, Crouzon-Pfeiffer, Muenke, and Saethre-Chotzen) craniosynostosis patients treated at our center from 2008-2018 were reviewed and demographic data were collected. Patients were included if they had undergone 3-dimensional T1-weighted cranial magnetic resonance imaging (MRI) with fast spoiled gradient echo (FSPGR) which could be successfully processed via FreeSurfer 'auto-recon' pipeline. Patients with imaging not suitable for processing were excluded from further analysis. All available imaging data was utilized including multiple MRIs of the same patient at different time points. All syndromic patients underwent cranial vault expansion surgery prior to any MRIs included in this study. Control patients of a similar age and sex with appropriate MRI sequences were also identified and included for analysis. Indications for imaging included headache, head trauma, single seizure episode, early menstruation, hypoglycemia, and heat intolerance. Indications for imaging were reviewed by a pediatric neurosurgeon and deemed suitable for comparison to our syndromic cohort.

MRI Acquisition

All MRI scans were performed on a 1.5 T scanner (GE Healthcare, MR Signa Excite HD, Little Chalfont, UK) with the imaging protocol including a 3D FSPGR T1-weighted MR sequence. Imaging parameters for craniosynostosis patients were the following: 2 mm slice thickness, no slice gap; field of view (FOV) 22.4 cm; matrix size 224 × 224; in plane resolution of 1 mm; echo time (TE) 3.1 ms, and repetition time (TR) 9.9 ms.

Cortical volume, cortical surface area, and intracranial volume

MRI dicom files were exported and converted to neuroimaging informatics technology initiative (NIfTI) file format on a computer cluster with Scientific Linux as the operating system and preloaded Freesurfer software (version 6.0, see https://surfer.nmr.mgh.harvard.edu; developed by the Athinoula A. Martinos Center for Biomedical Imaging, Massachusetts General Hospital). All cortical

volume, cortical surface area, and intracranial volume values were obtained from FreeSurfer software modules which have previously been validated and described in detail (10-12). Each MRI underwent processing via the 'auto-recon-all' pipeline which generates pial and white matter surfaces and allows for accurate estimation of cortical volume, surface area, and intracranial volume values. Following initial processing, all surfaces generated by FreeSurfer were inspected visually to ensure accuracy. No manual editing or alteration of the generated surfaces was performed. Lobar cortical volume and surface area estimates were generated via the '--lobes' argument within the 'mris_annotation2label' command. A total of 6 lobes (frontal, temporal, parietal, occipital, cingulate, insula) in each hemisphere are included in the FreeSurfer parcellation. Left and right hemispheric outputs were summed to generate whole lobe values for statistical analysis. Total intracranial volume was exported from FreeSurfer as 'eTIV' via the 'mri_segstats' command. These techniques have previously been applied with success in the craniosynostosis population (13, 14).

Scaling coefficient

Objects of invariant shape but variable size demonstrate a geometric scaling relationship which can be expressed as:

$$s = kv^{\alpha}$$

where s = surface area, v = volume, k = constant, and $\alpha = 2/3$ is a scaling exponent(5). The coefficient α can be obtained by log transformation yielding:

$$log(s) = \alpha\, log(v) + log(k)$$

Therefore, plotting *log(v)* and *log(s)* by linear regression, the slope of the line is equal to α with the intercept equal to *log(k).* Deviations from $\alpha = 2/3$ would then provide information regarding accelerated ($\alpha > 2/3$) or retarded ($\alpha < 2/3$) surface area to volume scaling than otherwise expected from geometric principles. This technique has previously been demonstrated as a measure for cortical development sensitive to environmental effects and has been correlated to neurocognitive outcomes in neonates(5). An additional advantage is that the resulting exponent is unitless and may be compared across cohorts.

Education level

In an attempt to evaluate long-term functional outcome, data regarding educational placement were gathered from medical chart review in readily available cases. Educational placement in the Netherlands has varying levels of organization aimed at preparation for individuals pursuing a variety of career paths. Placement is made by both examination and recommendation by primary school teachers. For simplification, patients were organized into 3 distinct groups, 1) those requiring modified instruction or expanded services to complete their primary/secondary schooling, 2) those completing standard coursework without impairment, 3) those completing coursework in preparation for university study. For those in group 1, additional data regarding the nature of services provided were gathered and the following subgroups used, 1a) visual impairment, 1b) hearing or speech impairment, 1c) motor or intellectual disability, 1d) psychological or behavioral problems, 1e) mild learning problems.

Statistical analysis

All data were imported into R statistical software (R Core Team, R version 3.6.1, 2019, Vienna, Austria) for analysis. To assess inter-group differences in intracranial volume, a linear mixed effects regression ('nlme' package) was used while controlling for sex, age, and repeated measurements within the same subject (fit by maximum likelihood). Independent variables included age at the time of MRI, sex, and genetic group. The dependent variable was intracranial volume. The only random effect term included was subject identity which served as an index for each MRI included. Although repeated measurements were not available for every subject, the 'lme' function in R eliminates complete-case bias while incorporating all available data. Model assumptions were also checked. Linearity was assessed graphically ('lattice' package). Normality of residuals was verified via *Q-Q* plot ('stats' package). Similarly, log-transformed mixed regression models were used for evaluating CSA to ICV scaling relationships by genetic status. Patients were organized into control, *TWIST1*, and *FGFR* groups initially and later split into specific syndromes for subgroup analysis. Exploratory analysis was performed to evaluate potential regional differences in CSA to ICV scaling by lobe via linear mixed regression. Last, frequency tables were generated by syndrome for educational placement data. For the primary aim (global model), coefficents, 95% confidence intervals, and *p* values are reported. For the secondary aim and exploratory analysis, coefficients and 95% confidence intervals are reported.

	Control	FGFR	TWIST1
Age (years)	9.28 ± 5.38	8.76 ± 4.87	10.58 ± 7.78
Sex: F	21 (58.3%)	74 (50%)	13 (68.4%)
ICV (cm^3)	1405 ± 158	1519 ± 270	1304 ± 145
CSA (cm^2)	1744 ± 176	1945 ± 281	1764 ± 192
n (MRI)	36	148	19
N (subjects)	36	89	15

Table 1. Subject characteristics from MRIs shown grouped by mutation status. For age, ICV, and CSA mean (SD) are reported. F = female; ICV = intracranial volume; CSA = cortical surface area; n= number of MRIs; N = number of subjects; SD = standard deviation. Numeric values are calculated from total MRIs.

Results

In total, 203 MRIs from 140 subjects were included for analysis in this study. 4 outlier MRIs were excluded with ICV < 1000 cm^3 including 1 control and 3 Saethre-Chotzen patients which appeared to negatively skew ICV results in the *TWIST1* group. Prior to removal of outliers, mean ± SD *TWIST1* ICV was 1250 ± 195 cm^3 compared to final mean ± SD *TWIST1* ICV of 1304 ± 145 cm^3. Mean (SD) control ICV was 1393 ± 170 cm^3 compared to final control mean ICV of 1405 ± 158 cm^3 following outlier exclusion. In the final dataset there were 37 cases of Apert syndrome, 86 Crouzon-Pfeiffer, 25 Muenke, 19 Saethre-Chotzen, and 36 typically-developing controls. A summary of the final dataset is shown in Table 1. Average age (mean ± SD) at the time of MRI was 9.02 ± 5.29 yrs. For the primary aim, mean ± SD ICV was 1519 ± 270 cm^3 in *FGFR* patients, which was greater than that observed in controls (p = 0.016). In patients with *TWIST1* mutations, ICV was no different from controls (mean = 1251 cm^3, p = 0.080). As expected, age was positively associated with ICV (p < 0.001) and female sex was negatively correlated (p < 0.001). Complete results of the primary model are shown in Table 2.

Intracranial Volume

Predictors	*Estimates*	*95% CI*	*p*
Intercept	1338.72	1247.85 – 1429.59	**<0.001**
Age	17.20	12.26 – 22.13	**<0.001**
Sex:Female	-160.06	-229.11 – -91.01	**<0.001**
FGFR	101.27	20.15 – 182.38	**0.016**
TWIST1	-114.00	-240.14 – 12.14	0.080
$N_{Subject\_ID}$	140		
Observations	203		

Table 2. Linear mixed effects model evaluating differences in intracranial volume associated with *FGFR* and *TWIST1* mutations compared to controls. Model is fit by maximum likelihood. Random effect intercept = 188.77 and residual = 89.10. 95% CI = 95% confidence interval; FGFR = fibroblast growth factor receptor.

For the secondary aim, CSA to ICV scaling coefficients were obtained by log transformation. Genetic groupings were maintained for analysis but further subdivided into specific syndromic diagnosis as well (Figure 1). *FGFR* patients collectively yielded a scaling coefficient α_{FGFR} = 0.68 (95% CI 0.61 – 0.76) with syndromic subgroup coefficients α_{apert} = 0.53 (95% CI 0.38 – 0.69), $\alpha_{crouzon\text{-}pfeiffer}$ = 0.69 (95% CI 0.59 – 0.79), and α_{muenke} = 0.56 (95% CI 0.38- 0.74) compared to *TWIST1*/Saethre-Chotzen patients $\alpha_{saethre\text{-}chotzen}$ = 0.81 (95% CI 0.50 – 1.12) and controls $\alpha_{control}$ = 0.77 (95% CI 061 – 0.93). Lobar analysis (shown in Table 3) revealed smaller scaling coefficients in the parietal lobes of both *TWIST1* ($\alpha_{parietal}$ = 0.39, 95% CI -0.24 – 1.03) and *FGFR* ($\alpha_{parietal}$ = 0.50, 95% CI 0.42 – 0.59) patients compared to controls ($\alpha_{parietal}$ = 0.71, 95% CI 0.50 – 0.93). The occipital lobes of *FGFR* patients also demonstrated reduced CSA/ICV scaling ($\alpha_{occipital}$ = 0.67, 95% CI 0.54 – 0.80) compared to controls ($\alpha_{occipital}$ = 0.83, 95% CI 0.53 – 1.13). Brain surfaces of patients from each syndrome are shown in figure 2.

Of the 104 syndromic patients included in the study, educational data were available in 103. Frequency tables for education level are shown in Table 4. All but one patient requiring modified education were from the *FGFR* group. The majority (74%) of Apert syndrome patients required modified education, with 6 (26%) completing standard coursework without assistance. Of the patients requiring modified education, subgroup analysis revealed none were due to blindness/vision impairment, 2 (1 Crouzon-Pfeiffer, 1 Muenke) were due to hearing impairment, 19 (10 Apert, 8 Crouzon-Pfeiffer, 1 Muenke) were from motor or intellectual disability, 4 (2 Crouzon-Pfeiffer, 2 Muenke) were due to psychological or behavioral problems, and 11 (7 Apert, 1 Crouzon-Pfeiffer, 2 Muenke, 1 Saethre-Chotzen) had mild learning problems.

	Control (n = 36)			FGFR (n = 148)			TWIST (n = 19)		
	slope	95% CI	intercept	slope	95% CI	intercept	slope	95% CI	intercept
Frontal	0.76	0.56 – 0.95	2.07	0.73	0.62 – 0.84	2.16	0.81	0.33 – 1.30	1.91
Temporal	0.86	0.66 – 1.04	1.51	0.80	0.69 – 0.92	1.72	0.70	0.24 – 1.17	1.99
Parietal	0.71	0.50 – 0.93	2.10	0.50	0.42 – 0.59	2.79	0.39	-0.24 – 1.03	3.13
Occipital	0.83	0.53 – 1.13	1.42	0.67	0.54 – 0.80	1.94	1.18	0.71 – 1.65	0.37
Cingulate	0.94	0.66 – 1.22	0.56	0.79	0.61 – 0.96	1.06	1.11	0.69 – 1.53	0.07
Insula	0.87	0.61 – 1.13	0.61	0.75	0.60 – 0.90	1.00	0.98	0.46 – 1.50	0.28

Table 3. Linear mixed regression models of log-transformed data for each lobe, organized by genetic status. *m* = slope, 95% CI = 95 % confidence intervals for each slope given, *b* = intercept. $\log_{10}[CSA] = m \log_{10}[ICV] + b$. Dependent variable is CSA. Independent variable is ICV. CSA = cortical surface area; ICV = intracranial volume.

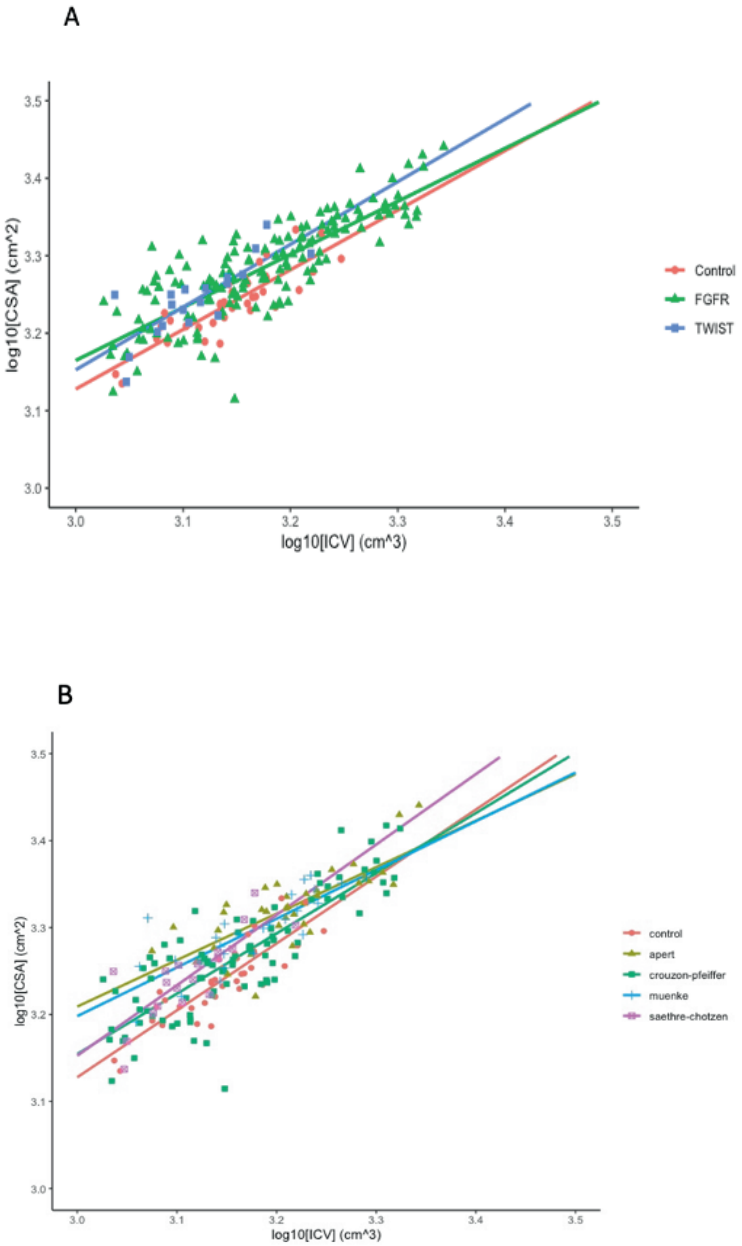

Figure 1. Cortical surface area plotted against intracranial volume in log-log space for each genetic grouping (A) as well as by syndrome (B). Slopes are equal to scaling coefficients.

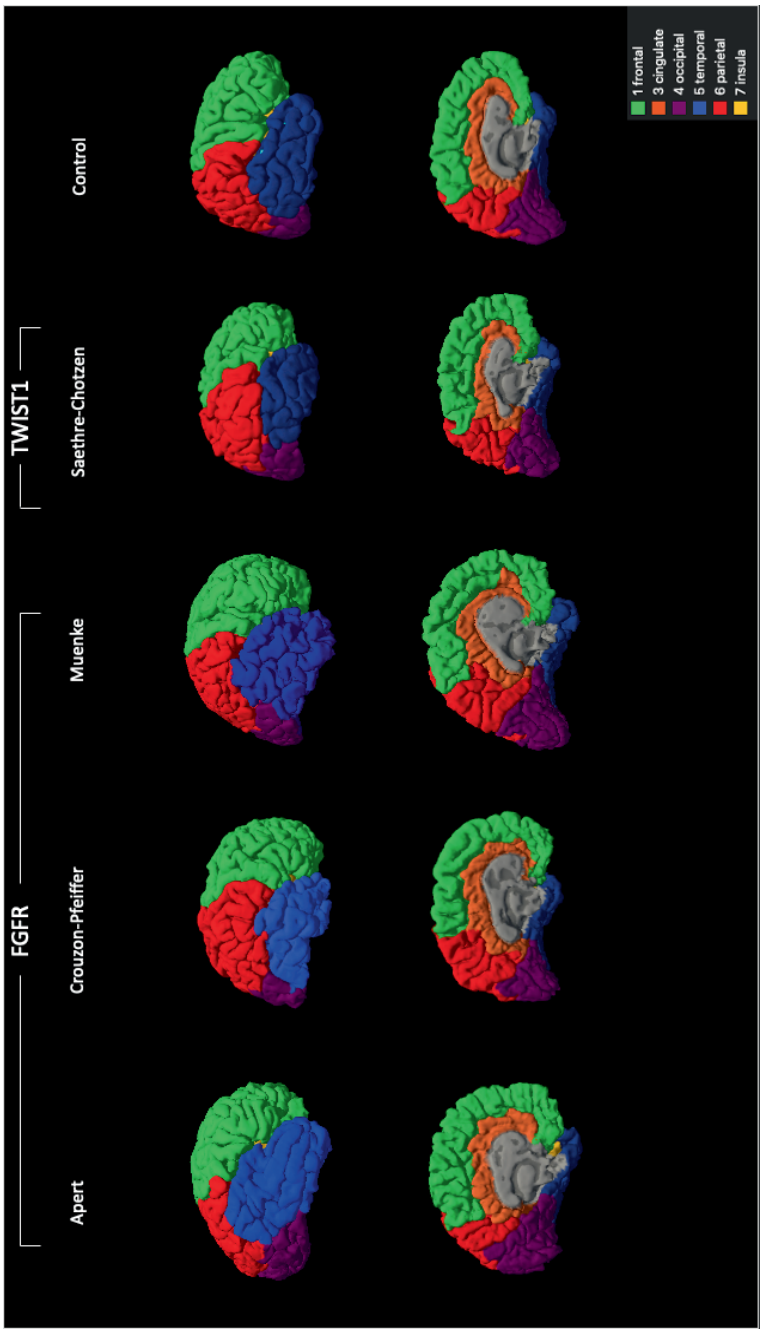

Figure 2. Brain surfaces with lobar parcellation shown for each syndrome and genetic grouping.

	FGFR			TWIST
	Apert	Crouzon-Pfeiffer	Muenke	Saethre-Chotzen
Group 1	17 (74%)	12 (27%)	6 (27%)	1 (7%)
Group 2	6 (26%)	27 (61%)	16 (73%)	9 (64%)
Group 3	0	5 (11%)	0	4 (29%)
Total	23	44	22	14

Table 4. Educational placement by genetic status/syndrome. Group 1 patients required special schooling or accommodation during their primary education years. Group 2 patients completed standard coursework at a regular school. Group 3 patients completed coursework in preparation for university study.

Discussion

The purpose of this study was to evaluate neuromorphologic development in syndromic craniosynostosis as it relates to cranial growth. Since ICV is a marker of cranial growth and its expansion often the aim of surgical intervention, it serves as a useful metric in the syndromic population(15, 16). Our primary analysis revealed larger ICV values in craniosynostosis patients with FGFR mutations compared to controls, but despite these larger volumes, a commensurate increase in cerebral cortical surface area was not observed. Further analysis indicates that reduced scaling of CSA to ICV is most severe in the parietal and occipital lobes for FGFR patients. Given the high rate of neuropsychiatric and developmental issues in this population, these findings may provide a morphometric neural substrate for such outcomes (17).

Craniocerebral disproportion is a hallmark of craniosynostosis resulting from inadequate ICV for the developing brain. Targeted volume expansion through surgical intervention seeks to improve this and clinical measurements such as occipitofrontal circumference are even made as a proxy for ICV

growth(15, 18-20). Previous data support our findings of elevated ICV in *FGFR*-mediated craniosynostosis, as larger volumes have been reported in Apert, Muenke, and Crouzon patients compared with typically developing controls (16, 21-24). ICV data is limited regarding Muenke syndrome, but Rijken et al have shown increased posterior fossa and cerebellar volumes in these patients (25). Lastly, in a study by Breakey et al, ICV and head circumference were measured in a series of syndromic children and similar values in Saethre-Chotzen patients and controls were observed, which also coincides with our current findings.

Despite larger ICV, *FGFR* patients did not demonstrate normative CSA development. Growth of the cerebral cortex is primarily driven by an increase in CSA which scales disproportionally as brain size increases (5). Disruptions to surface area maturation have been associated with various developmental pathologies common to the syndromic population including cognitive impairment and neurobehavioral disorders (5, 26, 27). Regional analysis revealed that scaling was most drastically reduced in the parietal and occipital lobes for *FGFR* patients. Although no reduction in global scaling coefficient was detected for *TWIST1* patients, lobar analysis showed similar reductions in parietal lobe CSA to ICV scaling. Previous work by Skranes et al demonstrated an association between reduced CSA in preterm infants and reductions in intelligence quotient (IQ) (28). In that study, the parietal cortex was implicated in multiple measures of intelligence including working memory, processing speed, and perceptual organization. Occcipital cortex development is important for visual processing ability which, if impaired, could manifest as a reading disability or be otherwise detrimental to scholastic achievement (29-31). Interestingly, Rachle et al showed that children with reading disability demonstrated reduced surface area in posterior regions of the brain without compensatory changes in the frontal lobe typical of adults with the disorder (31). Lack of early surface area maturation in the syndromic brain may explain some developmental issues observed in these patients.

Although detailed neuropsychological data were unavailable in our cohort, evaluation of educational data showed that all patients requiring modified placement had an *FGFR*-mediated form of craniosynostosis. Further subgroup analysis showed that the majority of Apert patients requiring modified education suffered from motor or intellectual disability, while psychological or behavioral issues were more common in Muenke syndrome. Crouzon-Pfeiffer placement was highly variable and Saethre-Chotzen patients all undertook normal or advanced coursework which is congruent with our

neuromorphometric findings. Previous neuropsychological outcomes in the syndromic population show a similar pattern of intellectual disability in Apert patients and higher prevalence of social or behavioral problems in Muenke syndrome (17).

The link between cortical maldevelopment and neuropsychological issues in syndromic craniosynostosis appears likely, however, the specific cause remains elusive. Due to different genetic mechanisms among the various syndromes, inborn errors of cortical folding or maturation may exist and may vary significantly among syndrome and subtype. For example, *FGFR* genes are critical in cortical development processes including neuronal migration and stabilization of dendritic patterning and *TWIST1* is involved in cranial mesodermal development (32-34). Other factors may also influence cortical development including craniocerebral disproportion, intracranial hypertension, surgical intervention and associated anesthesia burden. Future studies with consistent serial imaging and detailed neuropsychological assessment may provide greater insight regarding specific causes of the cortical maldevelopment described here.

When interpreting the findings of this study several limitations should be considered. First, serial MRIs were not available for each patient limiting the utility of longitudinal inferences regarding cortical maturation. For those patients in whom multiple MRIs were available, all scans were included via mixed effects regression modeling to fully utilize available data. We also considered the possibility of selection bias in both our syndromic population and controls. All syndromic patients are systematically evaluated by MRI as a part of standardized protocol and control patients were carefully selected based on indication so as to remove any with pathology pertinent to our analysis. Lastly, 1 control and 3 Saethre-Chotzen patients were excluded as outliers with significantly reduced intracranial volumes that appeared to negatively skew ICV results in the *TWIST1* group. Prior to removal of outliers, mean *TWIST1* ICV was 1250 cm^3 compared to final mean *TWIST1* ICV of 1304 cm^3 and mean control ICV was 1393 cm^3 compared to final control mean ICV of 1405 cm^3. Regarding development, 2/3 of the Saethre-Chotzen patients excluded based on outlier position had normal education outcomes so it is unlikely that we introduce a bias.

In this study we documented the paradoxical increase in ICV from cranial growth restriction in *FGFR*-mediated syndromic craniosynostosis. We also established that despite adequate volume, cerebral

cortex development remains abnormal in this patient population. Specifically, we identified reduced scaling of CSA to ICV in the parietal and occipital lobes and observed corresponding deficits in scholastic achievement primarily in Apert syndrome. Explanations for these findings include genetic influences on cortex folding, physical constraints on the expanding cerebral cortex, intracranial hypertension, and sequelae from surgical intervention. Further study is needed to elucidate precise mechanisms of cortical development in craniosynostosis and their link to neuropsychiatric outcomes. Clinically, identification of *in vivo* biomarkers sensitive to treatment variation and functional outcomes would help in optimizing care protocols for craniosynostosis patients. With further study, CSA/ICV scaling may prove useful as such.

References:

1. Stevens HE, Smith KM, Maragnoli ME, Fagel D, Borok E, Shanabrough M, et al. Fgfr2 is required for the development of the medial prefrontal cortex and its connections with limbic circuits. The Journal of neuroscience : the official journal of the Society for Neuroscience. 2010;30(16):5590-602.
2. Qin Q, Xu Y, He T, Qin C, Xu J. Normal and disease-related biological functions of Twist1 and underlying molecular mechanisms. Cell Res. 2012;22(1):90-106.
3. Hofman MA. Size and shape of the cerebral cortex in mammals. I. The cortical surface. Brain Behav Evol. 1985;27(1):28-40.
4. Hofman MA. On the evolution and geometry of the brain in mammals. Prog Neurobiol. 1989;32(2):137-58.
5. Kapellou O, Counsell SJ, Kennea N, Dyet L, Saeed N, Stark J, et al. Abnormal cortical development after premature birth shown by altered allometric scaling of brain growth. PLoS medicine. 2006;3(8):e265-e.
6. Hofman MA. Design principles of the human brain: an evolutionary perspective. Prog Brain Res. 2012;195:373-90.
7. Garcia KE, Robinson EC, Alexopoulos D, Dierker DL, Glasser MF, Coalson TS, et al. Dynamic patterns of cortical expansion during folding of the preterm human brain. Proceedings of the National Academy of Sciences of the United States of America. 2018;115(12):3156-61.
8. Dubois J, Benders M, Cachia A, Lazeyras F, Ha-Vinh Leuchter R, Sizonenko SV, et al. Mapping the Early Cortical Folding Process in the Preterm Newborn Brain. Cerebral Cortex. 2007;18(6):1444-54.
9. Dubois J, Benders M, Borradori-Tolsa C, Cachia A, Lazeyras F, Ha-Vinh Leuchter R, et al. Primary cortical folding in the human newborn: an early marker of later functional development. Brain : a journal of neurology. 2008;131(Pt 8):2028-41.
10. Dale AM, Fischl B, Sereno MI. Cortical surface-based analysis. I. Segmentation and surface reconstruction. NeuroImage. 1999;9(2):179-94.
11. Fischl B, Dale AM. Measuring the thickness of the human cerebral cortex from magnetic resonance images. Proceedings of the National Academy of Sciences of the United States of America. 2000;97(20):11050-5.
12. Fischl B, Sereno MI, Dale AM. Cortical surface-based analysis. II: Inflation, flattening, and a surface-based coordinate system. NeuroImage. 1999;9(2):195-207.
13. Wilson AT, de Planque CA, Yang SS, Tasker RC, van Veelen MC, Dremmen MHG, et al. Cortical Thickness in Crouzon-Pfeiffer Syndrome: Findings in Relation to Primary Cranial Vault Expansion. Plast Reconstr Surg Glob Open. 2020;8(10):e3204.
14. Wilson AT, Den Ottelander BK, De Goederen R, Van Veelen MC, Dremmen MHG, Persing JA, et al. Intracranial hypertension and cortical thickness in syndromic craniosynostosis. Dev Med Child Neurol. 2020;62(7):799-805.
15. Spruijt B, Rijken BF, den Ottelander BK, Joosten KF, Lequin MH, Loudon SE, et al. First Vault Expansion in Apert and Crouzon-Pfeiffer Syndromes: Front or Back? Plast Reconstr Surg. 2016;137(1):112e-21e.
16. Breakey RWF, Knoops PGM, Borghi A, Rodriguez-Florez N, O'Hara J, James G, et al. Intracranial Volume and Head Circumference in Children with Unoperated Syndromic Craniosynostosis. Plast Reconstr Surg. 2018;142(5):708e-17e.
17. Maliepaard M, Mathijssen IM, Oosterlaan J, Okkerse JM. Intellectual, behavioral, and emotional functioning in children with syndromic craniosynostosis. Pediatrics. 2014;133(6):e1608-15.

18. Rijken BF, den Ottelander BK, van Veelen ML, Lequin MH, Mathijssen IM. The occipitofrontal circumference: reliable prediction of the intracranial volume in children with syndromic and complex craniosynostosis. Neurosurg Focus. 2015;38(5):E9.
19. Hashmi A, Cahill GL, Zaldana M, Davis G, Cronin BJ, Brandel MG, et al. Can Head Circumference Be Used as a Proxy for Intracranial Volume in Patients With Craniosynostosis? Ann Plast Surg. 2019;82(5S Suppl 4):S295-s300.
20. Serlo WS, Ylikontiola LP, Lähdesluoma N, Lappalainen OP, Korpi J, Verkasalo J, et al. Posterior cranial vault distraction osteogenesis in craniosynostosis: estimated increases in intracranial volume. Childs Nerv Syst. 2011;27(4):627-33.
21. Sgouros S, Hockley AD, Goldin JH, Wake MJ, Natarajan K. Intracranial volume change in craniosynostosis. J Neurosurg. 1999;91(4):617-25.
22. Posnick JC, Armstrong D, Bite U. Crouzon and Apert syndromes: intracranial volume measurements before and after cranio-orbital reshaping in childhood. Plast Reconstr Surg. 1995;96(3):539-48.
23. Muenke M, Gripp KW, McDonald-McGinn DM, Gaudenz K, Whitaker LA, Bartlett SP, et al. A unique point mutation in the fibroblast growth factor receptor 3 gene (FGFR3) defines a new craniosynostosis syndrome. Am J Hum Genet. 1997;60(3):555-64.
24. Moloney DM, Wall SA, Ashworth GJ, Oldridge M, Glass IA, Francomano CA, et al. Prevalence of Pro250Arg mutation of fibroblast growth factor receptor 3 in coronal craniosynostosis. Lancet. 1997;349(9058):1059-62.
25. Rijken BF, Lequin MH, van der Lijn F, van Veelen-Vincent ML, de Rooi J, Hoogendam YY, et al. The role of the posterior fossa in developing Chiari I malformation in children with craniosynostosis syndromes. J Craniomaxillofac Surg. 2015;43(6):813-9.
26. Sarkar S, Daly E, Feng Y, Ecker C, Craig MC, Harding D, et al. Reduced cortical surface area in adolescents with conduct disorder. Eur Child Adolesc Psychiatry. 2015;24(8):909-17.
27. Batty MJ, Palaniyappan L, Scerif G, Groom MJ, Liddle EB, Liddle PF, et al. Morphological abnormalities in prefrontal surface area and thalamic volume in attention deficit/hyperactivity disorder. Psychiatry Res. 2015;233(2):225-32.
28. Skranes J, Løhaugen GC, Martinussen M, Håberg A, Brubakk AM, Dale AM. Cortical surface area and IQ in very-low-birth-weight (VLBW) young adults. Cortex. 2013;49(8):2264-71.
29. Kaiser D, Cichy RM. Typical visual-field locations enhance processing in object-selective channels of human occipital cortex. J Neurophysiol. 2018;120(2):848-53.
30. Pleisch G, Karipidis, II, Brauchli C, Röthlisberger M, Hofstetter C, Stämpfli P, et al. Emerging neural specialization of the ventral occipitotemporal cortex to characters through phonological association learning in preschool children. Neuroimage. 2019;189:813-31.
31. Raschle NM, Zuk J, Gaab N. Functional characteristics of developmental dyslexia in left-hemispheric posterior brain regions predate reading onset. Proc Natl Acad Sci U S A. 2012;109(6):2156-61.
32. Huang JY, Lynn Miskus M, Lu HC. FGF-FGFR Mediates the Activity-Dependent Dendritogenesis of Layer IV Neurons during Barrel Formation. J Neurosci. 2017;37(50):12094-105.
33. Huang JY, Krebs BB, Miskus ML, Russell ML, Duffy EP, Graf JM, et al. Enhanced FGFR3 activity in postmitotic principal neurons during brain development results in cortical dysplasia and axonal tract abnormality. Sci Rep. 2020;10(1):18508.
34. Bildsoe H, Fan X, Wilkie EE, Ashoti A, Jones VJ, Power M, et al. Transcriptional targets of TWIST1 in the cranial mesoderm regulate cell-matrix interactions and mesenchyme maintenance. Dev Biol. 2016;418(1):189-203.

CHAPTER 7

General Discussion

General Discussion

The purpose of this thesis was to improve our understanding of structural changes to the developing brain due to pathologic and treatment-related factors in syndromic craniosynostosis. Evaluation of intracranial structures in the craniosynostosis population has traditionally been carried out via gross examination of MRI or CT studies[1]. For example, initial observations made in Apert syndrome include ventriculomegaly, hydrocephalus, hippocampal abnormalities, callosal agenesis, and absent septum pellucidum[1-4]. With improvement in computer technology and segmentation techniques, volumetric analysis on the voxel grid became a possibility[5]. In the following years, automated processing and surface-based analysis has permitted detailed evaluation of neuromorphometry with resolution unrestricted by voxel size[6-9]. This has been used with great success, particularly in the field of neuropsychology, improving our understanding of longitudinal cerebral cortex development and some potential pathologic variations in neural structure associated with disease states[10-13]. In this thesis, we have applied these techniques to the field of craniofacial surgery to better understand brain development in syndromic craniosynostosis. One aim is to determine which changes in neuromorphometry are due to genetic causes and which result from treatable conditions such as ventriculomegaly, hydrocephalus, and intracranial hypertension (ICH). If treatable conditions result in detectable change to structural biomarkers for cognitive function, it may improve treatment decisions and guide clinical protocols. Furthermore, given the wide variety of neurocognitive outcomes even within identical syndromes, detailed neuromorphometry analysis could improve risk stratification and guide parents' expectations of neurocognitive potential for their child.

Implications of results

The current state of craniofacial care is marked by significant variation in clinical protocol on both a regional and international level. Continued debate exists surrounding both the optimal treatment timeline as well as the best technique to be performed on craniosynostosis patients. At the Dutch Craniofacial Center, prophylactic cranial vault expansion procedures are preferred in the first year of life for all syndromic or complex cases. The rationale for this approach is based on the high rates of ICH, lack of reliable screening tool for its timely detection and associated negative sequelae in this population, which are widely agreed upon[14,15]. Yet, in some centers, patients undergo regular screening at follow-up without a prophylactic vault expansion procedure in an effort to reduce

unnecessary operations in children who will not go on to develop ICH[16]. Therefore, additional data characterizing the effect of ICH on the developing brain are needed to inform clinical decisions.

The aim of **chapter 2** was to address this need by assessing thickness of the cerebral cortex as an *in vivo* biomarker for structural maldevelopment. Histologically, cortical thickness is a composite measure of neuronal density, dendritic arborization, and glial support and has been positively correlated with general intelligence[17-19]. We evaluated 171 MRIs of confirmed syndromic craniosynostosis patients and associated ICH indicators and risk factors. Our analysis revealed that both a previous finding of hydrocephalus and previous detection of papilledema on fundoscopy were independently associated with reduced cortical thickness. With regard to hydrocephalus, this is concordant with earlier findings in non-craniosynostosis patients. Zhang et al showed cortical thinning and impaired white matter integrity in a hydrocephalus cohort of school aged children compared to healthy controls[20]. Clinically, hydrocephalus is a known risk in craniosynostosis and is typically treated via cerebrospinal fluid (CSF) diversion (e.g. shunt or ventriculostomy) but a single incidence of papilledema is often met with watchful waiting. Regular fundoscopy and follow up of abnormal findings are common because papilledema may self-resolve due to a variety of factors causing intracranial pressure to fluctuate. At our center detection of papilledema is followed up with repeated fundoscopy 4 to 6 weeks later for confirmation before recommending surgical intervention. In our study, no distinction was made between patients with repeated/confirmed papilledema and those with detection at a single visit. Our findings then indicate that by the time papilledema is detected, thinning of the cerebral cortex has already occurred at a rate greater than that observed in patients with no historical finding of papilledema. Although the effect of surgical intervention was not directly evaluated, our findings support the rationale for efforts aimed at ICH prevention rather than reactionary approaches.

Crouzon-Pfeiffer patients are a unique subset within syndromic craniosynostosis because they often develop normal levels of intelligence yet experience high rates of ICH during the first years of life (61%) and associated cortical thinning[21,22]. Thus, the aim of **chapter 3** was to study regional influences of type of initial cranial vault expansion procedure and synostosis pattern on cortical thickness in this population. We analyzed MRIs of 34 Crouzon-Pfeiffer patients to collect data on global and lobar cortical thickness and determine regional associations with either fronto-orbital advancement or posterior vault expansion. It was previously shown at our center that posterior vault expansion

generates greater intracranial volume gains and reduced postoperative papilledema compared with FOA[23]. Our hypothesis was that local relief of skull growth restriction might translate to a thicker underlying cerebral cortex, indicative of a protective regional advantage. However, our study failed to uncover any association between cortical thickness (regional or global) and type of primary vault expansion procedure. This was likely due to limited power of the study. In the previous study which demonstrated cortical thinning following papilledema, the effect size was statistically significant but small. With a cohort of 34 patients, the current study is powered only for detection of large changes in thickness. With the addition of more patients, more subtle changes in global cortical thickness similar to those observed following papilledema may emerge.

Analysis of synostosis pattern in Crouzon-Pfeiffer patients did show regional effects. Lambdoid synostosis has previously been associated with worse outcomes in craniosynostosis including higher rates of cerebellar tonsillar herniation and greater vulnerability to reductions in IQ or academic performance[24,25]. In our study, we observed widespread thinning associated with patients who had synostosis of one or both lambdoid sutures. Interestingly, the greatest effects were observed not in the occipital lobe of these patients but in the cingulate and frontal lobes. Higher rates of ICH are more likely to occur in Crouzon patients with lambdoid synostosis due to crowding of the posterior fossa and subsequent venous outflow obstruction[26]. Therefore, our findings may reflect varying degrees of sensitivity to ICH within developing cortical regions of the brain.

With regard to white matter, ICH has been shown to result in reduced structural integrity and functional deficits in non-craniosynostosis children suffering from traumatic brain injury[27]. In a previous study at our center, syndromic children were evaluated by diffusion tensor imaging (DTI) fiber tractography (FT) and demonstrated widespread white matter microstructural abnormalities as well, however, the impact of ICH was not evaluated and the study was limited by partial voluming effects and anisotropic voxel size[28]. In **chapter 4**, we measured global and regional corpus callosum volumes in 152 MRIs of syndromic patients and in 36 controls to determine if ICH was associated with volume loss. Because we had previously shown that papilledema and hydrocephalus were associated with cortical thinning, we used these indicators for ICH in this study as well. We also distinguished between progressive (PV) and stable ventriculomegaly (SV), as SV is known to occur at high rates in the syndromic population (particularly in Apert and Crouzon syndromes) yet consensus is lacking on

whether or not this is of pathologic concern[29,30]. Our results show that only PV leads to a reduction in total corpus callosum volume, with the most severe reductions occurring in the mid-body. Similar observations have been made previously in the non-craniosynostosis population. In early radiographic studies by Jinkins et al and Hofmann et al, a structural explanation for callosal flattening and thinning in hydrocephalus is offered[31,32]. As ventricular dilation progresses, the posterior body of the callosum rises to meet the free edge of the falx cerebri where it may be impinged leading to axonal dysfunction[32]. Our results show similar regional effects on the callosum in SV but no total body volume loss. This suggests a similar mechanical susceptibility of the callosal body, yet it is unlikely that Wallerian degeneration has occurred in cases of SV to any significant degree. Clinically, CSF diversion procedures should be reserved for demonstrable hydrocephalus, however, patients with SV should be carefully monitored for any signs or symptoms of concurrent ICH which would warrant intervention.

Lastly, historical finding of papilledema was not associated with any observed loss of callosal volume. This may reflect different sensitivities of white and grey matter to ICH, greater plasticity of the corpus callosum, as well as prompt detection of ICH and intervention to prevent prolonged states of raised intracranial pressure[33].

In **chapter 5** we evaluated outcomes of a rare subset of Crouzon patients with isolated sagittal synostosis following two different surgical approaches. Prior to 2010, fronto-biparietal remodeling (FBP) was performed on all isolated scaphocephaly patients at our center. After this time, spring assisted expansion (SAE) was used due to its favorable outcomes and improved morbidity profile[34-36]. Three Crouzon patients from each group (SAE and FBP) were evaluated with regard to postoperative complications, cranial index, aesthetic outcome, ICH, and the need for reoperation. Our results show worse outcomes in patients treated by SAE. All 3 patients undergoing primary SAE expansion required reoperation with an FBP technique due to inadequate correction of cranial dysmorphology or development of ICH in the postoperative period. The difference in results between scaphocephaly patients with Crouzon syndrome and those non-syndromic patients previously reported to have good outcomes may be explained by the higher rate of ventricular dilation in Crouzon syndrome, dural attachments, and the younger age at the time of operation in SAE.

Crouzon patients are prone to develop ventriculomegaly at higher rates than non-syndromic children[37-39]. Differences in postoperative cranial vault resistance between FBP and SAE may provide expanding ventricles directional guidance in SAE toward the path of least resistance at the vertex. Conversely, FBP remodeling creates a mosaic neocranium comprised of multiple bone flaps which likely form a relatively even distribution of resistance.

Dural attachments, specifically those associated with the sagittal bone strip in SAE, may also play a role in the development of higher rates of ICH. Abnormal flow through the superior sagittal sinus (SSS) has previously been reported in craniosynostosis and due to the influence of dural attachments on SSS shape it is reasonable to suspect a morphologic etiology[40,41]. Any preoperative hemodynamic abnormalities in the SSS due to dural tethers would not be addressed by SAE but would be released in an FBP procedure where complete dissociation of the calvarium and dura are achieved. SAE-treated patients were also younger at the time of operation (4-5 months) compared to a wider range in the FBP group (9-39 months). Yet age at operation for SAE-treated patients in this study was similar to previous analysis in non-syndromic patients, so it is unlikely this fully explains the worse outcomes observed in our Crouzon cohort[34]. Although advantages for early surgical intervention have been reported, postoperative cranial growth or reossification can be difficult to predict[42]. Irrespective of specific etiology, the high rate of reoperation in Crouzon scaphocephaly patients treated by SAE indicate that an FBP operation may be more appropriate for these patients.

In **chapter 6**, cerebral cortex development is explored further in syndromic children and controls. The aim was to evaluate surface area of the cortex in proportion to intracranial volume. In addition to cortical thickness, surface area is the other component of cortical volume. Previous work has shown that these metrics ontogenetically and phylogenetically distinct and offer distinct indices of neurodevelopment and disease[43,44]. Intracranial volume is used because it reflects head size and is often the aim of vault expansion procedures. We evaluated 203 MRIs in total grouped by genetic status (148 *FGFR*, 19 *TWIST1*, and 36 controls) via FreeSurfer pipeline to determine intracranial volume (ICV) and cerebral cortex surface area (CSA) and used log-transformation to calculate a scaling exponent describing this relationship. Our results show that despite larger intracranial volumes in the *FGFR* group compared to controls, there is reduced CSA relative to head size as indicated by a smaller

scaling exponent. This may be the result of primary cortical dysplasia due to genetic influences, mechanical sequalae of cranial growth restriction, or ICH.

FGFR genes are a family of tyrosine kinase receptors which are critical to cerebral cortex developmental processes including neuronal migration and stabilization of dendritic patterning and are implicated in Apert, Muenke, and Crouzon-Pfeiffer syndromes[45,46]. Impairment of these processes may manifest as reduced CSA due to improper cortical folding in the perinatal period. *TWIST1* was not associated with reduced CSA scaling in our study. *TWIST1* is a basic helix-loop-helix (bHLH) domain-containing transcription factor which is involved in mesodermal differentiation and development and is implicated in Saethre-Chotzen syndrome[47,48]. Impaired mesodermal development would be unlikely to result in primary dysplasia of the cerebral cortex which was not observed in *TWIST1* patients. *TWIST1* normally maintains tissue boundaries and prevents neural crest cell migration across the coronal sutures maintaining cellular identity within the developing suture and preventing abnormal mixing[49]. In Saethre-Chotzen syndrome this is impaired ultimately resulting in craniosynostosis. Experimentally it has been shown that this may be overcome by reduced osteogenic drive through crossing of a conditional transgenic allele which encodes an inhibitor of downstream *FGFR* signaling (*Spry1*)[50]. In the *Spry1* experiment, the craniosynostosis phenotype was not observed, indicating contributions from both loss of boundary integrity and increased osteogenic differentiation. This may explain why milder phenotypes are typically observed in Saethre-Chotzen syndrome compared to Apert syndrome which is due to activating mutations in FGFR2 driving abnormal osteogenic differentiation.

Regionally, our results show that reduced CSA scaling in *FGFR* patients occurs most drastically in the parietal and occipital lobes. Maldevelopment of the parietal lobe has been associated with impaired working memory, processing speed, and perceptual organization and underdevelopment of occipital lobe CSA has been linked to reading disability[51,52]. More broadly, CSA growth impairment occurs in various neurobehavioral disorders which are often reported in *FGFR*-mediated syndromes as well[12,53]. In another study by Skranes et al, reduced CSA was associated with lower IQ in preterm infants[51]. Although we did not directly measure IQ in our study, we did gather educational outcomes data which showed higher rates of the need for a modified educational environment or special assistance in *FGFR* patients. Underdevelopment of CSA, particularly within the parieto-occipital region, combined with

worse educational outcomes support the idea that cortical dysplasia may be a neural substrate for some of the neuropsychological issues commonly observed in *FGFR*-mediated forms of craniosynostosis.

Strengths

A unique strength of this thesis is the large cohort of syndromic patients evaluated. Syndromic craniosynostosis is a rare disease ranging in prevalence from 1 in 10,000 to 1 in 100,000 depending on the diagnosis and most studies feature cohorts in the 10-30 participant range[54-57]. The cohorts featured in studies from this thesis contain over 100 patients and many have multiple imaging studies available for analysis. This is possible due to nationally centralized craniosynostosis care throughout the Netherlands at the Dutch Craniofacial Center of Erasmus MC. This broad catchment area includes the total population of the Netherlands (approximately 17 million people) and minimizes selection bias. Another strength is the large amount of diagnostic and clinical data gathered by longitudinal follow-up of our patients and protocolized care.

In addition to the large number of MRI studies available for analysis, we were able to leverage computing power resources allowing for timely processing of scans and robust data collection. Employing surface-based analysis techniques via the FreeSurfer pipeline have enabled sub-voxel resolution of neuromorphometry in syndromic craniosynostosis patients, a population in which structural imaging analysis has previously been limited to voxel-based morphometry techniques.

Limitations

There are several limitations of our data which should be considered when interpreting our findings. First, ICH detection was made by proxy and was therefore not a direct quantitative measure in our studies. Other indicators such as papilledema, optical coherence tomography (OCT), hydrocephalus, occipito-frontal growth curve deflection, and obstructive sleep apnea are assessed regularly at follow-up and used to guide treatment. Direct intracranial pressure monitoring yields quantitative data but is considered too invasive for widespread use as a screening tool and carries risk of infection. Additionally, intracranial pressure is known to fluctuate and normal or acceptable values may vary substantially with age, disease states, and intact cerebral autoregulation[58]. Therefore, in our center direct intracranial pressure monitoring is reserved for patients with inconclusive assessment for ICH.

A second limitation is the high degree of variability among syndromic forms of craniosynostosis as well as intra-syndromic heterogeneity which may limit the generalizability of our findings. For example, in work by Lu et al, Apert syndrome patients were grouped by synostosis pattern and shown to have significant variation in cranial fossa volume as well as airway changes[59,60]. Similar heterogeneity has been reported in Crouzon syndrome[61]. Syndromic-specific analysis was performed in this thesis when possible, notwithstanding statistical power limitations. Variability within specific syndromes, was generally unaccounted for except in **chapter 3** where synostosis pattern effect size was evaluated within Crouzon-Pfeiffer patients.

A major drawback of our analysis is the lack of preoperative neuromorphometric data. This limits our ability to understand the native neuromorphometry in patients prior to intervention as well as assess the effect of surgical expansion on its development. Syndromic patients regularly undergo preoperative MRI but are also scheduled for cranial vault expansion within the first year of life, therefore all preoperative scans occur in infancy. Successful FreeSurfer analysis requires adequate differentiation between white and grey matter for accurate reconstruction of the cortical ribbon from which cortical thickness and surface area estimates are made. In patients younger than 2 years of age, white matter maturation has not typically progressed enough for successful analysis, however current efforts are being made to remedy this[62,63].
Additionally, longitudinal inferences from our data are limited due to inconsistent serial imaging suitable for processing. When available, repeated scans of patients were included and indexed by patient via mixed regression modeling to maximize use of our data, but this was not the case for every patient studied. Regular serial imaging at consistent time points would allow more robust analysis of longitudinal cortex development.

The study of neuromorphometry is complex and unidentified confounders may also exist. We have controlled for those which are easily identifiable such as age and sex, but as study continues additional influential factors may become apparent. Lastly, consistent and quantitative neuropsychological data was unavailable for the majority of participants. Ideally consistent IQ testing across syndromic cohorts would provide us with the ability to directly assess the link between cortical morphometry and functional outcome. For reference to IQ specifically, we rely on previous study establishing this

association in non-craniosynostosis patients. To evaluate functional outcome in our syndromic cohort, we used educational placement data which is likely more informative at lower ends of the performance spectrum but less specific than quantitative IQ.

Conclusion

The purpose of this thesis was to explore neuromorphometry in syndromic craniosynostosis and its relationship with various pathologic and treatment variables. Studies evaluating neuromorphometry as an indicator for ICH exposure revealed several findings. First, by the time ICH is detected by papilledema in syndromic craniosynostosis, global thinning of the cerebral cortex has already occurred, supporting the rationale for preventative treatment strategies. Second, hydrocephalus is associated with both thinning of the cerebral cortex and lower corpus callosum volumes, highlighting the importance of early detection and intervention. Third, cortical surface area development demonstrated inadequate scaling with postoperative intracranial volume in *FGFR*-mediated craniosynostosis. This is indicative of cortical maldevelopment and may represent a neural substrate for neuropsychological impairment since these patients also experienced lower scholastic achievement levels.

With regard to treatment variables, we evaluated type of primary cranial vault expansion procedure in Crouzon-Pfeiffer syndrome and failed to detect any global or regional effects on cortical thickness. Lambdoid suture synostosis was observed to have a large effect on cingulate cortex thinning. Failure to detect significant regional changes in thickness due to local growth restriction or expansion indicate that ICH exposure and global cranial morphology may be more important than local factors on structural cortex development. Finally, we evaluated outcomes from FBP and SAE procedures in Crouzon patients with sagittal synostosis. We observed that SAE-treated patients had worse outcomes leading to reoperation with an FBP procedure. Therefore, we recommend against the use of SAE in sagittal synostosis cases diagnosed with Crouzon syndrome.

Future directions

Future work should focus on several areas. First, more robust data collection with regard to quantitative neurocognitive outcome in craniosynostosis patients should be gathered and correlated to the neuromorphometric biomarkers studied here. This should include both general cognitive

functioning metrics such as IQ as well as behavioral testing for common disorders such as autism spectrum disorder (ASD) and attention deficit hyperactivity disorder (ADHD) which are typically diagnosed later in childhood.

Much work remains to be done regarding native structural neurodevelopment in the untreated infant with craniosynostosis as well. Preoperative MRIs obtained in the first year of life were not included for analysis here due to inadequate distinction between grey and white matter in infancy. As techniques for analyzing infant brain structure become available, this should be an area of focus. Earlier identification of biomarkers at the time of initial imaging may improve risk stratification and expectation management of parents with syndromic children. Preoperative analysis is also essential for direct assessment of surgical intervention on brain development and its relationship to neurocognitive outcome. Ultimately, collaboration with other centers using different surgical techniques and treatment protocols is needed for further study and optimization of care.

As data collection continues, improved power to analyze neuromorphometry within each syndrome independently as well as subgroups within those syndromes is expected. Serial imaging at regular intervals combined with neurocognitive data would improve our ability to make longitudinal inferences at each stage in development.

Lastly, in addition to syndromic children and controls, non-syndromic analysis would help distinguish between neuromorphometric changes due to mechanical influences and those specific to syndromic patients. Parsing genetic, mechanical, and ICH-related effects on brain development will aid in the identification of treatment-sensitive biomarkers for future use in craniosynostosis treatment protocols.

References

1. Cohen Jr MM, Kreiborg S. The central nervous system in the Apert syndrome. *American journal of medical genetics.* 1990;35(1):36-45.
2. de León GA, de León G, Grover WD, Zaeri N, Alburger PD. Agenesis of the corpus callosum and limbic malformation in Apert syndrome (type I acrocephalosyndactyly). *Archives of neurology.* 1987;44(9):979-982.
3. Fishman MA, Hogan GR, Dodge PR. The concurrence of hydrocephalus and craniosynostosis. *Journal of neurosurgery.* 1971;34(5):621-629.
4. Crome L. A critique of current views on acrocephaly and related conditions. *J Ment Sci.* 1961;107:459-474.
5. Dufresne CR, McCarthy JG, Cutting CB, Epstein FJ, Hoffman WY. Volumetric quantification of intracranial and ventricular volume following cranial vault remodeling: a preliminary report. *Plastic and reconstructive surgery.* 1987;79(1):24-32.
6. Dale AM, Fischl B, Sereno MI. Cortical surface-based analysis. I. Segmentation and surface reconstruction. *NeuroImage.* 1999;9(2):179-194.
7. Fischl B, Salat DH, Busa E, et al. Whole Brain Segmentation: Automated Labeling of Neuroanatomical Structures in the Human Brain. *Neuron.* 2002;33(3):341-355.
8. Fischl B, Dale AM. Measuring the thickness of the human cerebral cortex from magnetic resonance images. *Proceedings of the National Academy of Sciences.* 2000;97(20):11050.
9. Rosas HD, Liu AK, Hersch S, et al. Regional and progressive thinning of the cortical ribbon in Huntington's disease. *Neurology.* 2002;58(5):695-701.
10. Salat DH, Buckner RL, Snyder AZ, et al. Thinning of the cerebral cortex in aging. *Cerebral cortex (New York, NY : 1991).* 2004;14(7):721-730.
11. Kuperberg GR, Broome MR, McGuire PK, et al. Regionally localized thinning of the cerebral cortex in schizophrenia. *Arch Gen Psychiatry.* 2003;60(9):878-888.
12. Batty MJ, Palaniyappan L, Scerif G, et al. Morphological abnormalities in prefrontal surface area and thalamic volume in attention deficit/hyperactivity disorder. *Psychiatry Res.* 2015;233(2):225-232.
13. Luders E, Narr KL, Hamilton LS, et al. Decreased callosal thickness in attention-deficit/hyperactivity disorder. *Biol Psychiatry.* 2009;65(1):84-88.
14. Christian EA, Imahiyerobo TA, Nallapa S, Urata M, McComb JG, Krieger MD. Intracranial hypertension after surgical correction for craniosynostosis: a systematic review. *Neurosurgical focus.* 2015;38(5):E6.
15. Gault DT, Renier D, Marchac D, Jones BM. Intracranial pressure and intracranial volume in children with craniosynostosis. *Plastic and reconstructive surgery.* 1992;90(3):377-381.
16. O'Hara J, Ruggiero F, Wilson L, et al. Syndromic Craniosynostosis: Complexities of Clinical Care. *Mol Syndromol.* 2019;10(1-2):83-97.
17. Duncan NW, Gravel P, Wiebking C, Reader AJ, Northoff G. Grey matter density and GABAA binding potential show a positive linear relationship across cortical regions. *Neuroscience.* 2013;235:226-231.
18. S K, Y AD, Rj H, et al. Positive association between cognitive ability and cortical thickness in a representative US sample of healthy 6 to 18 year-olds. *Intelligence.* 2009;37(2):145-155.

19. Karama S, Colom R, Johnson W, et al. Cortical thickness correlates of specific cognitive performance accounted for by the general factor of intelligence in healthy children aged 6 to 18. *NeuroImage.* 2011;55(4):1443-1453.
20. Zhang S, Ye X, Bai G, et al. Alterations in Cortical Thickness and White Matter Integrity in Mild-to-Moderate Communicating Hydrocephalic School-Aged Children Measured by Whole-Brain Cortical Thickness Mapping and DTI. *Neural Plast.* 2017;2017:5167973.
21. Abu-Sittah GS, Jeelani O, Dunaway D, Hayward R. Raised intracranial pressure in Crouzon syndrome: incidence, causes, and management. *Journal of neurosurgery Pediatrics.* 2016;17(4):469-475.
22. Maliepaard M, Mathijssen IM, Oosterlaan J, Okkerse JM. Intellectual, behavioral, and emotional functioning in children with syndromic craniosynostosis. *Pediatrics.* 2014;133(6):e1608-1615.
23. Spruijt B, Rijken BF, den Ottelander BK, et al. First Vault Expansion in Apert and Crouzon-Pfeiffer Syndromes: Front or Back? *Plastic and reconstructive surgery.* 2016;137(1):112e-121e.
24. Fearon JA, Dimas V, Ditthakasem K. Lambdoid Craniosynostosis: The Relationship with Chiari Deformations and an Analysis of Surgical Outcomes. *Plastic and reconstructive surgery.* 2016;137(3):946-951.
25. Speltz ML, Collett BR, Wallace ER, et al. Intellectual and academic functioning of school-age children with single-suture craniosynostosis. *Pediatrics.* 2015;135(3):e615-623.
26. Hayward R. Venous hypertension and craniosynostosis. *Child's nervous system : ChNS : official journal of the International Society for Pediatric Neurosurgery.* 2005;21(10):880-888.
27. Tasker RC, Westland AG, White DK, Williams GB. Corpus callosum and inferior forebrain white matter microstructure are related to functional outcome from raised intracranial pressure in child traumatic brain injury. *Dev Neurosci.* 2010;32(5-6):374-384.
28. Rijken BF, Leemans A, Lucas Y, van Montfort K, Mathijssen IM, Lequin MH. Diffusion Tensor Imaging and Fiber Tractography in Children with Craniosynostosis Syndromes. *AJNR American journal of neuroradiology.* 2015;36(8):1558-1564.
29. Collmann H, Sorensen N, Krauss J. Hydrocephalus in craniosynostosis: a review. *Child's nervous system : ChNS : official journal of the International Society for Pediatric Neurosurgery.* 2005;21(10):902-912.
30. Aldridge K, Collett BR, Wallace ER, et al. Structural brain differences in school-age children with and without single-suture craniosynostosis. *Journal of neurosurgery Pediatrics.* 2017;19(4):479-489.
31. Hofmann E, Becker T, Jackel M, et al. The corpus callosum in communicating and noncommunicating hydrocephalus. *Neuroradiology.* 1995;37(3):212-218.
32. Jinkins JR. Clinical manifestations of hydrocephalus caused by impingement of the corpus callosum on the falx: an MR study in 40 patients. *AJNR American journal of neuroradiology.* 1991;12(2):331-340.
33. Lafrenaye AD, McGinn MJ, Povlishock JT. Increased intracranial pressure after diffuse traumatic brain injury exacerbates neuronal somatic membrane poration but not axonal injury: evidence for primary intracranial pressure-induced neuronal perturbation. *J Cereb Blood Flow Metab.* 2012;32(10):1919-1932.
34. van Veelen MC, Kamst N, Touw C, et al. Minimally Invasive, Spring-Assisted Correction of Sagittal Suture Synostosis: Technique, Outcome, and Complications in 83 Cases. *Plastic and reconstructive surgery.* 2018;141(2):423-433.

35. van Veelen ML, Eelkman Rooda OH, de Jong T, Dammers R, van Adrichem LN, Mathijssen IM. Results of early surgery for sagittal suture synostosis: long-term follow-up and the occurrence of raised intracranial pressure. *Child's nervous system : ChNS : official journal of the International Society for Pediatric Neurosurgery.* 2013;29(6):997-1005.
36. van Veelen ML, Mathijssen IM. Spring-assisted correction of sagittal suture synostosis. *Child's nervous system : ChNS : official journal of the International Society for Pediatric Neurosurgery.* 2012;28(9):1347-1351.
37. Cinalli G, Sainte-Rose C, Kollar EM, et al. Hydrocephalus and craniosynostosis. *Journal of neurosurgery.* 1998;88(2):209-214.
38. Noetzel MJ, Marsh JL, Palkes H, Gado M. Hydrocephalus and mental retardation in craniosynostosis. *J Pediatr.* 1985;107(6):885-892.
39. Proudman TW, Clark BE, Moore MH, Abbott AH, David DJ. Central nervous system imaging in Crouzon's syndrome. *The Journal of craniofacial surgery.* 1995;6(5):401-405.
40. Cornelissen MJ, de Goederen R, Doerga P, et al. Pilot study of intracranial venous physiology in craniosynostosis. *J Neurosurg Pediatr.* 2018;21(6):626-631.
41. Mursch K, Enk T, Christen HJ, Markakis E, Behnke-Mursch J. Venous intracranial haemodynamics in children undergoing operative treatment for the repair of craniosynostosis. A prospective study using transcranial colour-coded duplex sonography. *Childs Nerv Syst.* 1999;15(2-3):110-116; discussion 117-118.
42. Patel A, Yang JF, Hashim PW, et al. The impact of age at surgery on long-term neuropsychological outcomes in sagittal craniosynostosis. *Plastic and reconstructive surgery.* 2014;134(4):608e-617e.
43. Geschwind DH, Rakic P. Cortical evolution: judge the brain by its cover. *Neuron.* 2013;80(3):633-647.
44. Winkler AM, Greve DN, Bjuland KJ, et al. Joint Analysis of Cortical Area and Thickness as a Replacement for the Analysis of the Volume of the Cerebral Cortex. *Cerebral cortex (New York, NY : 1991).* 2018;28(2):738-749.
45. Huang JY, Krebs BB, Miskus ML, et al. Enhanced FGFR3 activity in postmitotic principal neurons during brain development results in cortical dysplasia and axonal tract abnormality. *Sci Rep.* 2020;10(1):18508.
46. Huang JY, Lynn Miskus M, Lu HC. FGF-FGFR Mediates the Activity-Dependent Dendritogenesis of Layer IV Neurons during Barrel Formation. *The Journal of neuroscience : the official journal of the Society for Neuroscience.* 2017;37(50):12094-12105.
47. Zhao Z, Rahman MA, Chen ZG, Shin DM. Multiple biological functions of Twist1 in various cancers. *Oncotarget.* 2017;8(12):20380-20393.
48. Bildsoe H, Fan X, Wilkie EE, et al. Transcriptional targets of TWIST1 in the cranial mesoderm regulate cell-matrix interactions and mesenchyme maintenance. *Dev Biol.* 2016;418(1):189-203.
49. Twigg SRF, Wilkie AOM. A Genetic-Pathophysiological Framework for Craniosynostosis. *Am J Hum Genet.* 2015;97(3):359-377.
50. Connerney J, Andreeva V, Leshem Y, et al. Twist1 homodimers enhance FGF responsiveness of the cranial sutures and promote suture closure. *Dev Biol.* 2008;318(2):323-334.
51. Skranes J, Løhaugen GC, Martinussen M, Håberg A, Brubakk AM, Dale AM. Cortical surface area and IQ in very-low-birth-weight (VLBW) young adults. *Cortex.* 2013;49(8):2264-2271.

52. Raschle NM, Zuk J, Gaab N. Functional characteristics of developmental dyslexia in left-hemispheric posterior brain regions predate reading onset. *Proceedings of the National Academy of Sciences of the United States of America.* 2012;109(6):2156-2161.
53. Sarkar S, Daly E, Feng Y, et al. Reduced cortical surface area in adolescents with conduct disorder. *Eur Child Adolesc Psychiatry.* 2015;24(8):909-917.
54. Janis JE. *Essentials of Plastic Surgery.* 2nd ed2017.
55. Kruszka P, Addissie YA, Yarnell CM, et al. Muenke syndrome: An international multicenter natural history study. *American journal of medical genetics Part A.* 2016;170a(4):918-929.
56. Goh LC, Azman A, Siti HBK, et al. An audiological evaluation of syndromic and non-syndromic craniosynostosis in pre-school going children. *Int J Pediatr Otorhinolaryngol.* 2018;109:50-53.
57. Maximino LP, Ducati LG, Abramides DVM, Corrêa CC, Garcia PF, Fernandes AY. Syndromic craniosynostosis: neuropsycholinguistic abilities and imaging analysis of the central nervous system. *Arq Neuropsiquiatr.* 2017;75(12):862-868.
58. Pedersen SH, Lilja-Cyron A, Astrand R, Juhler M. Monitoring and Measurement of Intracranial Pressure in Pediatric Head Trauma. *Frontiers in neurology.* 2019;10:1376.
59. Lu X, Sawh-Martinez R, Jorge Forte A, et al. Classification of Subtypes of Apert Syndrome, Based on the Type of Vault Suture Synostosis. *Plastic and reconstructive surgery Global open.* 2019;7(3):e2158.
60. Lu X, Forte AJ, Wilson A, et al. Cranial Fossa Volume in Differing Subtypes of Apert Syndrome. *The Journal of craniofacial surgery.* 2019;30(8):2345-2349.
61. Lu X, Sawh-Martinez R, Forte AJ, et al. Classification of Subtypes of Crouzon Syndrome Based on the Type of Vault Suture Synostosis. *The Journal of craniofacial surgery.* 2020;31(3):678-684.
62. Wang F, Lian C, Wu Z, et al. Developmental topography of cortical thickness during infancy. *Proceedings of the National Academy of Sciences of the United States of America.* 2019;116(32):15855-15860.
63. Zöllei L, Iglesias JE, Ou Y, Grant PE, Fischl B. Infant FreeSurfer: An automated segmentation and surface extraction pipeline for T1-weighted neuroimaging data of infants 0-2 years. *NeuroImage.* 2020;218:116946.

CHAPTER 8

Summary

The purpose of this thesis is to improve our understanding of neuromorphometry in syndromic craniosynostosis, which factors influence its development, and which of those may be affected by various treatment considerations.

In **chapter 1**, an introduction is presented, providing background relevant to craniosynostosis, its clinical features, and methodological explanation of automated image analysis techniques used to analyze neuromorphometry. In general, craniosynostosis is characterized by the premature fusion of calvarial sutures in the perinatal period leading to skull growth restriction in the context of rapid brain development and expansion. This occurs during a critical period of neurodevelopment when cerebral cortical folding and patterning is first established and followed by refinement of neural pathways throughout childhood and adolescence. Treatment normally consists of surgical intervention, the timing and details of which vary depending upon suture pattern involvement, clinical risk factors, and craniofacial center-specific protocol.

Syndromic forms of craniosynostosis are rarer (ranging from 1 in 10,000 to 1 in 100,000 compared to approximately 1 in 2,000 for non-syndromic cases) but often complicated by multiple suture involvement, venous anomalies, midface deformity, neurobehavioral disorders, and intellectual impairment. Of particular concern in syndromic patients is the increased prevalence of intracranial hypertension (ICH). Left untreated, ICH can lead to cognitive impairment and even blindness therefore, prevention or timely diagnosis and treatment are paramount. There are multiple factors which contribute to the development of ICH which can be evaluated by various metrics in treatment protocol. Contributing factors include craniocerebral disproportion from suture stenosis, anomalous venous drainage pathways, hydrocephalus, and obstructive sleep apnea (OSA) as a result of midface hypoplasia. In our center, occipitofrontal circumference (OFC) is trended at regular follow up intervals to assess for cranial growth restriction which would be reflected by downward deflections in progression curves. Anomalous venous anatomy as well as hydrocephalus may be detected by magnetic resonance imaging (MRI) and OSA is evaluated by polysomnography revealing an elevated apnea-hypopnea index when present.

The ability to accurately characterize neuromorphometry from MRI scans has greatly improved in recent years. Automated image processing with surface-based analysis has enabled the creation of

detailed topographical maps of the cerebral cortex and the acquisition of thickness, surface area, and curvature measurements from these models. Such analysis is computationally intensive which requires the use of a computing cluster for feasible processing of large cohorts for research purposes. In this thesis, these techniques are used to assess global and regional cortical thickness, cerebral surface area, intracranial volume, and corpus callosum morphology.

In **chapter 2**, global cerebral cortical thickness is evaluated in relation to intracranial hypertension indicators and risk factors. Thickness of the cortex is a composite measure of neuronal density, dendritic arborization, and glial support. It is subject to both temporal and regional variation but as a global measure has been correlated with intelligence and is therefore a useful *in vivo* biomarker. All MRIs which were able to be analyzed properly by FreeSurfer from Apert, Crouzon-Pfeiffer, Muenke, and Saethre-Chotzen patients were included in the study. Data collected with regard to ICH development included historical finding of papilledema, hydrocephalus, tonsillar position, OSA diagnosis, and OFC curve deflections. These and other demographic data were analyzed via mixed regression modeling to determine a potential relationship with cortical thickness. Our results demonstrated independent associations between both historical finding of papilledema and hydrocephalus and reduced global cortical thickness after controlling for age, sex, and repeated measurements. Other ICH risk factors failed to show any associated thickness differences. These findings indicate that ICH negatively influences structural brain development in syndromic craniosynostosis. Although ICH is a universal cause for concern among craniofacial centers and frequently necessitates intervention, this study highlights the importance of its prevention given the cortical thinning observed in patients with previous detection of hydrocephalus or papilledema.

Chapter 3 describes a study investigating the effect of type of surgical cranial vault expansion and synostosis pattern on lobar cortical thickness in Crouzon-Pfeiffer patients. Crouzon-Pfeiffer patients were studied due to their high prevalence of ICH yet typically normal neurocognitive development. Previous work from our center demonstrated greater intracranial volume gain and reduced postoperative papilledema in patients undergoing occipital-first expansion so we compared this technique with fronto-orbital advancement and analyzed lobar cortical thickness to assess for regional associations. Our analysis failed to detect any difference in lobar thickness relative to type of primary surgical expansion, which was likely due to inadequate statistical power. A secondary aim was to

evaluate synostosis pattern effect on lobar thickness. We hypothesized that regions of cortex proximate to skull growth restriction sites would exhibit focal thinning, but this was not observed. Our results show that lambdoid suture involvement is strongly associated with reduced thickness of the cingulate cortex rather than the occipital lobe. From this we conclude that overall cranial shape influences cortical thickness development more than local growth restriction. This may be due to increased rates of ICH from crowding of the posterior fossa leading to thinning in areas with greater pressure-sensitivity or other unidentified vascular causes.

In **chapter 4**, corpus callosum structure is studied in relation to papilledema, stable ventriculomegaly and progressive ventriculomegaly in both syndromic patients and controls. Having demonstrated cortical thinning as a result of ICH we were then interested to determine if a similar association was present with regard to white matter, specifically the corpus callosum. We failed to detect any total volume reduction associated with papilledema or stable ventriculomegaly but did find progressive ventriculomegaly to result in smaller callosal size. Regionally, our results show that volume loss occurs in the mid-body of the callosum in syndromic patients with both stable and progressive ventriculomegaly. These findings indicate that ventriculomegaly in general likely induces mechanical strain on the mid-posterior segment of the callosal body via impingement by the falx cerebri. Clinically, interventions for ventriculomegaly should be reserved for confirmed hydrocephalus cases but this study highlights the importance of careful monitoring of patients with stable ventriculomegaly for signs of ICH who would require intervention.

In **chapter 5,** spring-assisted expansion (SAE) and fronto-biparietal remodeling (FBP) surgical techniques are reviewed in Crouzon patients presenting with sagittal synostosis. SAE is known to be effective in non-syndromic cases of scaphocephaly with some advantages over FBP including reduced operative time and blood loss. Patients with a diagnosis of Crouzon syndrome present with added complexity, therefore our goal was to determine if SAE achieved similar levels of efficacy in these unique cases. Our results revealed that all patients undergoing a primary SAE procedure required a secondary cranial vault operation (FBP) and that none of the index FBP cases required revision. Indications for reoperation were persistent skull deformity and ICH. Persistent or worsening skull deformity following SAE may have been related to ventriculomegaly since it is more likely to develop in Crouzon patients compared to those with non-syndromic scaphocephaly. We suggest different

resistances in the neocranium between the two procedures as well as dural attachments may play a role in facilitating asymmetric expansion in SAE cases. Further study with larger cohorts is needed to draw more meaningful conclusions.

In **chapter 6**, a study of allometric scaling of the cerebral cortex in both syndromic patients and controls is presented. As the brain grows and develops, cortical surface area increases by both geometric proportion due to increased volume as well as increased gyrification from refinement of neural pathways. By plotting cortical surface area and intracranial volume in a log-log space we were able to derive a coefficient which describes their relationship in *FGFR*-mediated and *TWIST1*-mediated craniosynostosis patients as well as controls. Our results show that patients from the *FGFR* group have a reduced scaling coefficient compared to both the *TWIST1* and control groups. Lobar coefficients were calculated as well demonstrating lesser values in the parietal and occipital lobes. Lastly, educational placement data were gathered which demonstrated a greater need for modified learning environments in the *FGFR* group. Inadequate scaling of cortical surface area to volume in *FGFR* patients combined with worse educational outcomes suggest maldevelopment of the cerebral cortex.

In **chapter 7**, the results of this thesis are discussed. ICH remains a major concern in children with craniosynostosis, particularly those with syndromic variants. Appropriate risk stratification and efforts to prevent ICH from occurring are advisable due to the neuromorphometric findings described in this thesis. The cortex appears to be sensitive any etiology resulting in detectable papilledema and the corpus callosum is smaller in patients with progressive ventriculomegaly. In Crouzon-Pfeiffer syndrome, lambdoid suture stenosis is associated with a thinner cingulate cortex which may be due to posterior fossa overcrowding. Although rare, Crouzon-Pfeiffer patients presenting with scaphocephaly from sagittal synostosis may be better treated with a primary FBP procedure rather than SAE, as the latter has been shown in our cohort to result in higher reoperation rates. Lastly, we have identified inadequate cortical surface area development relative to intracranial volume in *FGFR*-mediated forms of craniosynostosis as well as worse scholastic outcomes in these patients. This thesis has employed automated MRI analysis techniques to explore structural brain development in syndromic craniosynostosis and contributed to our knowledge of how various clinical and pathophysiologic factors are influential.

CHAPTER 9

Nederlandse Samenvatting

Het doel van dit proefschrift is om ons begrip van neuromorfometrie bij syndromale craniosynostose te verbeteren, welke factoren de ontwikkeling ervan beïnvloeden en welke van die factoren beïnvloed kunnen worden door verschillende behandelingen.

In **hoofdstuk 1** wordt een inleiding gepresenteerd met achtergrondinformatie die relevant is voor craniosynostose, de klinische kenmerken ervan en methodologische uitleg van geautomatiseerde beeldanalysetechnieken die worden gebruikt om neuromorfometrie te analyseren. In het algemeen wordt craniosynostose gekenmerkt door de voortijdige fusie van calvariale naden in de perinatale periode die leidt tot beperking van de schedelgroei in een periode waar juist veel hersenontwikkeling plaatsvindt. In deze periode van neurologische ontwikkeling wordt de cerebrale corticale vouwing en patroonvorming voor het eerst vastgesteld. Dit wordt gevolgd door verfijning van neurale paden gedurende de kindertijd en adolescentie. De behandeling van craniosynostose bestaat normaal gesproken uit een chirurgische ingreep, waarvan de timing en details variëren afhankelijk van de betrokkenheid van specifieke naden, klinische risicofactoren en het centrumspecifieke protocol.

Syndromale vormen van craniosynostose zijn zeldzamer (variërend van 1 op 10.000 tot 1 op 100.000 vergeleken met ongeveer 1 op 2.000 voor niet-syndromale gevallen) maar vaak gecompliceerd door betrokkenheid van meerdere naden, veneuze afwijkingen, misvorming van het middengezicht, neurologische gedragsstoornissen en verstandelijke beperking. Bijzonder zorgwekkend bij syndromale patiënten is de verhoogde prevalentie van intracraniële hypertensie (ICH). Onbehandeld, kan ICH leiden tot cognitieve stoornissen en zelfs blindheid, daarom zijn preventie of tijdige diagnose en behandeling van het grootste belang. Er zijn meerdere factoren die bijdragen aan de ontwikkeling van ICH die kunnen worden geëvalueerd aan de hand van verschillende meetgegevens in het behandelingsprotocol. Bijdragende factoren zijn onder meer craniocerebrale disproportie door naadstenose, afwijkende veneuze drainagebanen, hydrocephalus en obstructieve slaapapneu (OSA) als gevolg van hypoplasie van het middengezicht. In ons centrum wordt de occipitofrontale omtrek (OFC) regelmatig gevolgd om te beoordelen of er sprake is van craniale groeirestrictie, die zou worden weerspiegeld door neerwaartse deflecties in progressiecurves. Afwijkende veneuze anatomie en hydrocephalus kunnen worden gedetecteerd door middel van magnetische resonantiebeeldvorming (MRI) en OSA wordt geëvalueerd door polysomnografie waarbij een verhoogde apneu-hypopneu-index wordt aangetoond.

Het vermogen om neuromorfometrie nauwkeurig te karakteriseren op basis van MRI-scans is de afgelopen jaren sterk verbeterd. Geautomatiseerde beeldverwerking met analyse op basis van het oppervlak heeft het mogelijk gemaakt om gedetailleerde topografische kaarten van de hersenschors te maken en de dikte, het oppervlak en de kromming van deze modellen te meten. Een dergelijke analyse is rekenkundig intensief en vereist het gebruik van een rekencluster voor haalbare verwerking van grote cohorten voor onderzoeksdoeleinden. In dit proefschrift worden deze technieken gebruikt om de globale en regionale corticale dikte, het cerebrale oppervlak, het intracraniële volume en de morfologie van het corpus callosum te beoordelen.

In **hoofdstuk 2** wordt de globale cerebrale corticale dikte geëvalueerd in relatie tot intracraniële hypertensie indicatoren en risicofactoren. De dikte van de cortex is een samengestelde maat voor neuronale dichtheid, dendritische arborisatie en gliale ondersteuning. Het is onderhevig aan zowel temporele als regionale variatie, maar is als globale maat gecorreleerd met intelligentie en is daarom een nuttige in vivo biomarker. Alle MRI's die goed konden worden geanalyseerd door FreeSurfer van Apert-, Crouzon-Pfeiffer-, Muenke- en Saethre-Chotzen-patiënten werden in het onderzoek opgenomen. Gegevens verzameld met betrekking tot ICH-ontwikkeling omvatten historische bevindingen van papiloedeem, hydrocephalus, tonsillaire positie, OSA-diagnose en OFC-curve-afbuigingen. Deze en andere demografische gegevens werden geanalyseerd via regressiemodellen om een mogelijke relatie met corticale dikte te bepalen. Onze resultaten toonden onafhankelijke associaties aan tussen zowel papiloedeem en hydrocephalus en verminderde globale corticale dikte na correctie voor leeftijd, geslacht. Andere ICH-risicofactoren lieten geen bijbehorende dikteverschillen zien. Deze bevindingen geven aan dat ICH een negatieve invloed heeft op de structurele hersenontwikkeling bij syndromale craniosynostose. Hoewel ICH een universele reden tot bezorgdheid is in alle craniofaciale centra en vaak interventie noodzakelijk maakt, benadrukt deze studie het belang van preventie, gezien een dunnere cortex wordt waargenomen bij patiënten met eerdere detectie van hydrocephalus of papiloedeem.

Hoofdstuk 3 beschrijft een studie die het effect onderzoekt van het type chirurgische schedeluitbreiding en synostosepatroon op de lobaire corticale dikte bij Crouzon-Pfeiffer-patiënten. Patiënten met Crouzon-Pfeiffer werden bestudeerd vanwege hun hoge prevalentie van ICH, maar toch

typisch normale neurocognitieve ontwikkeling. Eerder werk vanuit ons centrum toonde een grotere intracraniële volumetoename en verminderd postoperatief papiloedeem bij patiënten die primaire een occipitale expansie ondergingen, dus we vergeleken deze techniek met fronto-orbitale vooruitgang en analyseerden de lobaire corticale dikte om te beoordelen op regionale associaties. Onze analyse kon geen verschil in lobaire dikte ten opzichte van het type primaire chirurgische expansie detecteren, wat waarschijnlijk te wijten was aan onvoldoende statistische power. Een secundair doel was om het effect van het synostosepatroon op de lobaire dikte te evalueren. Onze hypothese was dat gebieden van de cortex in de buurt van plaatsen met beperkingen voor de groei van de schedel focaal dunner zouden worden, maar dit werd niet waargenomen. Onze resultaten tonen aan dat de betrokkenheid van lambdoïde naden sterk geassocieerd is met een verminderde dikte van de cingulaire cortex in plaats van de achterhoofdskwab. Hieruit concluderen we dat de algehele schedelvorm de ontwikkeling van de corticale dikte meer beïnvloedt dan de lokale groeibeperking. Dit kan te wijten zijn aan verhoogde ICH-percentages door verdringing van de achterste fossa, wat leidt tot dunner worden in gebieden met grotere drukgevoeligheid of andere niet-geïdentificeerde vasculaire oorzaken.

In **hoofdstuk 4** wordt de corpus callosum structuur bestudeerd in relatie tot papiloedeem, stabiele ventriculomegalie en progressieve ventriculomegalie bij zowel syndromale patiënten als gezonde controles. Nadat we corticale uitdunning als resultaat van ICH hadden aangetoond, waren we geïnteresseerd om te bepalen of een vergelijkbare associatie aanwezig was met betrekking tot witte stof, met name het corpus callosum. We hebben geen totale volumevermindering gevonden die verband houdt met papiloedeem of stabiele ventriculomegalie, maar vonden wel dat progressieve ventriculomegalie resulteerde in een kleiner corpus callosum. Onze resultaten laten zien dat volumeverlies optreedt in het midden van het lichaam van het callosum bij syndromale patiënten met zowel stabiele als progressieve ventriculomegalie. Deze bevindingen geven aan dat ventriculomegalie in het algemeen waarschijnlijk mechanische spanning induceert op het midden-posterieure segment van het callosale lichaam via botsing door de falx cerebri. Klinisch gezien moeten interventies voor ventriculomegalie worden gereserveerd voor bevestigde gevallen van hydrocephalus, maar deze studie benadrukt het belang van zorgvuldige monitoring van patiënten met stabiele ventriculomegalie op tekenen van ICH die interventie nodig hebben.

In **hoofdstuk 5** worden chirurgische technieken met veerondersteunde expansie (SAE) en fronto-biparietale remodellering (FBR) besproken bij Crouzon-patiënten met sagittale synostose. Van SAE is bekend dat het effectief is in niet-syndromale gevallen van scaphocefalie met enkele voordelen ten opzichte van FBR, waaronder een kortere operatieduur en minder bloedverlies. Patiënten met de diagnose Crouzon-syndroom vertonen extra complexiteit, daarom was ons doel om te bepalen of SAE even effectief was in deze unieke gevallen. Onze resultaten toonden aan dat alle patiënten die een primaire SAE-procedure ondergingen, een secundaire craniale kluisoperatie (FBR) nodig hadden en dat geen van de index-FBR-gevallen herziening behoefde. Indicaties voor heroperatie waren aanhoudende schedelvervorming en ICH. Aanhoudende of verslechterende schedelafwijking na SAE kan verband houden met ventriculomegalie, aangezien de kans zich groter is bij Crouzon-patiënten dan bij patiënten met niet-syndromale scaphocefalie. We suggereren dat verschillende resistenties in het neocranium tussen de twee procedures en durale hechtingen een rol kunnen spelen bij het vergemakkelijken van asymmetrische expansie in SAE-gevallen. Verdere studie met grotere cohorten is nodig om meer zinvolle conclusies te trekken.

In **hoofdstuk 6** wordt een studie gepresenteerd van allometrische schaalvergroting van de cerebrale cortex bij zowel syndromale patiënten als gezonde controles. Naarmate de hersenen groeien en zich ontwikkelen, neemt het corticale oppervlak toe met zowel geometrische proporties als gevolg van een groter volume als een verhoogde gyrificatie door verfijning van neurale paden. Door het corticale oppervlak en het intracraniële volume in een log-log-ruimte uit te zetten, konden we een coëfficiënt afleiden die hun relatie beschrijft bij FGFR-gemedieerde en TWIST1-gemedieerde craniosynostosepatiënten en bij controles. Onze resultaten laten zien dat patiënten uit de FGFR-groep een lagere schaalcoëfficiënt hebben in vergelijking met zowel de TWIST1- als de controlegroep. Lobaire coëfficiënten werden ook berekend en lieten ook mindere waarden zien in de pariëtale en occipitale lobben. Ten slotte werden gegevens over aanpassingen in onderwijsvormen verzameld die een grotere behoefte aan aangepaste leeromgevingen in de FGFR-groep aantoonden. Onvoldoende schaalvergroting van het corticale oppervlak naar volume bij FGFR-patiënten in combinatie met slechtere educatieve resultaten duiden op een slechte ontwikkeling van de hersenschors.

In **hoofdstuk 7** worden de resultaten van dit proefschrift besproken. ICH blijft een groot probleem bij kinderen met craniosynostose, vooral bij kinderen met syndromale varianten. Passende risicostratificatie en inspanningen om ICH te voorkomen zijn aan te raden vanwege de

neuromorfometrische bevindingen die in dit proefschrift worden beschreven. De cortex lijkt gevoelig te zijn voor elke etiologie, wat resulteert in detecteerbaar papiloedeem en een kleiner corpus callosum bij patiënten met progressieve ventriculomegalie. Bij het Crouzon-Pfeiffer-syndroom wordt lambdoïde naadstenose geassocieerd met een dunnere cingulaire cortex die mogelijk het gevolg is van overbevolking van de posterieure fossa. Hoewel zeldzaam, kunnen Crouzon-Pfeiffer-patiënten met scafocefalie van sagittale synostose beter worden behandeld met een primaire FBR-procedure in plaats van SAE, aangezien dit laatste in ons cohort is aangetoond dat het leidt tot hogere reoperaties. Ten slotte hebben we een inadequate ontwikkeling van het corticale oppervlak geïdentificeerd in verhouding tot het intracraniële volume in FGFR-gemedieerde vormen van craniosynostose, evenals slechtere scholastische resultaten bij deze patiënten. Dit proefschrift heeft geautomatiseerde MRI-analysetechnieken gebruikt om de structurele hersenontwikkeling bij syndromische craniosynostose te onderzoeken en heeft bijgedragen aan onze kennis van de invloed van verschillende klinische en pathofysiologische factoren.

APPENDICES

Publications in this thesis

Intracranial Hypertension and Cortical Thickness in Syndromic Craniosynostosis.

Wilson AT, den Ottelander BK, de Goederen R, et al.

Developmental Medicine and Child Neurology 2020 Jul;62(7):799-805.

Cortical thickness in Crouzon-Pfeiffer syndrome: findings in relation to primary cranial vault expansion.

Wilson AT, de Planque CA, Yang SS, et al.

Plastic and Reconstructive Surgery Global Open. 2020 Apr 11;8(10): e3204

Intracranial hypertension and corpus callosum volume in syndromic craniosynostosis: a retrospective cohort study.

Wilson AT, Ottelander BK, Tasker RC, et al.

European Journal of Paediatric Neurology, *(submitted)*

Disappointing results of spring-assisted cranial vault expansion in Crouzon patients presenting with sagittal synostosis

Wilson AT, Gaillard L, Versnel SL, et al.

Neurosurgical Focus 2020 Apr;50(4): E12

Cerebral cortex maldevelopment in syndromic craniosynostosis: An allometric study.

Wilson AT, Ottelander BK, van Veelen MLC, et al.

Developmental Medicine and Child Neurology, *(Accepted)*

Other publications

Trends in Revision Elbow Ulnar Collateral Ligament Reconstruction in Professional Baseball Pitchers.

Wilson, AT, Pidgeon TS, Morrell NT, DaSilva MF

Journal of Hand Surgery 2015 Volume 40, Issue 11, 2249 – 2254

In Reply: Letter regarding "Trends in Revision Elbow Ulnar Ligament Reconstruction in Professional Baseball Pitchers"

Pidgeon TS, Morrell NT, Wilson AT, DaSilva MF.

Journal of Hand Surgery 2016 Apr;41(4):574-6

Does Type of Cleft Palate Repair Influence Postoperative Eustachian Tube Dysfunction?

Wilson AT, Grabowski GM, Mackey WS, Steinbacher DM.

Journal of Craniofacial Surgery 2016. Nov. 9

Fibrin Tissue Sealant as an Adjunct to Cleft Palate Repair.

Wu RT, Wilson AT, Travieso R, Steinbacher DM.

Journal of Craniofacial Surgery, 2017 July; 28(5): 1164-1166.

Helping young physicians advance their leadership and advocacy skills – The Young Physicians' Leadership Curriculum (YPLC) of the Connecticut State Medical Society (CSMS).

Stretz C, Wagner C, Katz M, Tannenbaum S, Wilson AT, Hass D.

Connecticut Medicine 2017 Dec. Vol. 81 (581-586).

Total disc arthroplasty and anterior interbody fusion in the lumbar spine have relatively few differences in short-term adverse events.

Shultz BN, Wilson AT, Ondeck NT, et al.

Spine 2018 Jan. 1;43(1): E52-E59

Osteogenesis of Crouzon Mutated Cells in a Murine Model.

Alcon A, Metzler P, Eswarakumar J, Wilson AT, Steinbacher DS.

Journal of Craniofacial Surgery 2018 Jan. 29(1): 237-242

Classification of Subtypes of Apert Syndrome, Based on Type of Vault Suture Synostosis.

Lu X, Sawh-Martinez R, Jorge Forte A, Wu R, Cabrejo R, Wilson AT, et al.

Plastic and Reconstructive Surgery Global Open 2019 Mar 20;7(3); e2158

Mandibular Spatial Reorientation and Morphological Alteration of Crouzon and Apert Syndrome.

Lu X, Sawh-Martinez, Forte AJ, Wu R, Cabrejo R, Wilson AT, et al.

Annals of Plastic Surgery. 2019 Apr 3, e-pub

Segmental Maxillary Osteotomy to Close Wide Alveolar Clefts.

Wilson AT, Wu RT, Sawh-Martinez R, Steinbacher DM.

Journal of Oral and Maxillofacial Surgery 2019 Apr; 77(4):850. e1-850.e5

Complete Reoperation in Orthognathic Surgery.

Wu RT, Wilson AT, Gary C, Steinbacher DM.

Plastic and Reconstructive Surgery**.** 2019 May;143(5):1053e-1059e.

Spatial and Temporal Changes of Midface in Apert's Syndrome.

Lu X, Forte AJ, Sawh-Martinez R, Wu R, Cabrejo R, Wilson AT, et al.

Journal of Plastic and Hand Surgery 2019 Jun;53(3); 130-137

Conformity of the Actual to Planned Result in Orthognathic Surgery.

Wilson AT, Gabrick K, Wu RT, Madari S, Sawh-Martinez R, Steinbacher DM.

Plastic and Reconstructive Surgery 2019 Jul;144(1):89e-97e.

A Machine Learning Framework for Automated Diagnosis and Computer Assisted Planning in Plastic and Reconstructive Surgery.

Knoops PGM, Pappaioannou A, Borghi A, Breakey RWF, Wilson AT, et al.

Scientific Reports. 2019 Sep. 19; 9(1) 13597.

Cranial Fossa Volume in Differing Subtypes of Apert Syndrome.

Lu X, Forte AJ, Wilson AT, Alperovich M, Steinbacher DM, Alonso N, Persing JA.

Journal of Craniofacial Surgery 2019 Nov-Dec;30(8):2345-2349.

Classification of Subtypes of Crouzon Syndrome Based on the Type of Vault Suture Synostosis.

Lu X, Sawh-Martinez R, Forte AJ, Wu R, Cabrejo R, Wilson AT, et al.

Journal of Craniofacial Surgery. 2020 May/Jun;31(3):678-684.

Staged Abbe-Rhinoplasty Technique to Correct Bilateral Cleft Deformity.

Veeramani A, Wilson AT, Saw-Martinez R, Steinbacher DM.

Plastic and Reconstructive Surgery 2020 Feb;145(2):518-521

Cranial Fossa Volume and Morphology Development in Apert Syndrome.

Lu X, Forte AJ, Wilson AT, Steinbacher DM, Alperovich M, Alonso N, Persing JA.

Plastic and Reconstructive Surgery 2020 Apr;145(4):790e-802e

What is the difference in Cranial Base Morphology in Isolated and Syndromic Bicoronal Synostosis?

Lu X, Forte AJ, Wilson AT, Park EK, Allam O, et al.

Plastic and Reconstructive Surgery 2020 Sep;146(3):599-610

Respective Roles of Craniosynostosis and Syndromic Influences on Cranial Fossa Development.

Lu X, Forte AJ, Wilson AT, Park EK, Allam O, Alperovich M, Steinbacher DM, Alonso N, Persing JA.

Plastic and Reconstructive Surgery (*accepted*)

Growth patterns of the airway in Crouzon syndrome patients with different types of cranial vault suture synostosis.

Lu X, Forte AJ, Wilson AT, Park EK, Allam O, et al.

International Journal of Oral and Maxillofacial Surgery. 2020 Dec 28;S0901-5027(20)30439-2.

Respective roles of craniosynostosis and syndromic influences on cranial fossa development.

Lu X, Forte AJ, Wilson AT, Park EK, Allam O, Alperovich MA, Steinbacher DM, Alonso N, Persing JA.

Plastic and Reconstructive Surgery (*accepted*)

Comprehensive Analysis of Temporomandibular Joint and Condylar Changes in Robin Sequence Patients Undergoing Mandibular Distraction.

Pourtaheri N, Chandler L, Singh A, Maniskas S, Wilson AT, Sun AH, Steinbacher DM.

Journal of Craniofacial Surgery (*accepted*)

Orbital and Periorbital Dysmorphology In Untreated Pfeiffer Syndrome.

Lu X, Forte AJ, Allam O, Park EK, Wilson AT, et al.

Plastic and Reconstructive Surgery (*accepted*)

PhD Portfolio

Name of PhD Student:	Alexander Tate Wilson
Erasmus MC Department:	Plastic and Reconstructive and Hand Surgery
PhD Period:	2018-2021
Promotor:	Prof. dr. I.M.J. Mathijssen
Copromotor:	Dr. ir. H.A. Vrooman

PhD Training	**Year**	**ECTS**
General Academic Skills		
Basiscursus Regelgeving en Organisatie (BROK)	2019	1
Erasmus University Medical Center		
Scientific Integrity Course	2019	0.3
Erasmus University Medical Center		
Basic Course on 'R'	2019	2
Erasmus University Medical Center		
In-depth courses		
R-statistical programming	2018	1
Datacamp		
Shell programming for data science	2018	1
Datacamp		
Introduction to Python	2018	1
Datacamp		
Freesurfer training	2018	10
Martinos Center for Biomedical Imaging		

Skills training

Microsurgery skills lab	2019	6
Erasmus University Medical Center		
Provider ACLS certification	2020	1
American Heart Association		
Provider BLS certification	2020	0.3
American Heart Association		

Podium Presentations

'Synostosis Pattern, Type of Vault Expansion, and Intracranial Volume Do Not Correlate with Cortical Thickness in Crouzon-Pfeiffer Patients'	2020	1
American Society for Plastic Surgery Meeting		
(virtual)		
'Is cortical complexity affected by syndromic craniosynostosis?'	2020	1
American Society for Plastic Surgery Meeting		
(virtual)		
'Temporomandibular Joint Space and Condyle Morphology in Robin Sequence Before and After Mandibular Distraction Osteogenesis'	2019	1
European Cleft Palate and Craniofacial Association		
Utrecht, NL		
'Intracranial hypertension and cortical thickness in syndromic craniosynostosis'	2019	1.5
American Society for Plastic Surgery Meeting		
San Diego, CA, USA		
'Intracranial hypertension and cortical thickness in syndromic craniosynostosis'	2019	1.5
International Society for Craniofacial Surgery Meeting		
Paris, FR		

Conference Attendance

American College of Surgeons Clinical Congress	2020	1.5
(virtual)		
Northeast Society of Plastic Surgeons Annual Meeting	2020	0.6
(virtual)		
New York University Total Cleft Care: From Birth to Adulthood	2018	0.6
New York, NY, USA		

Research Funding

Michael K. Gershon Research Fellowship ($25,000)	2019
Yale University	
James G. Hirsch Research Fellowship ($25,000)	2020
Yale University	

Curriculum Vitae

Alexander Tate Wilson was born and raised in South Carolina, USA (April 3, 1991). He graduated from Landrum High School in 2009 and enrolled in Wofford College where he completed his premedical coursework and graduated *magna cum laude* in 2013 with a Bachelor of Science (B.S.) in chemistry. While at Wofford he was a member of the men's baseball team and was selected by the Atlanta Braves in the 15th round of the 2012 Major League Baseball draft after his junior year. He competed professionally for 3 years before beginning his medical training at Yale University. During his tenure at Yale, he began working on various research projects in craniofacial surgery related to 3-dimensional planning in orthognathic surgery, craniosynostosis, and cleft lip and palate care with Dr. Derek Steinbacher and Dr. John Persing. Following completion of his clerkships he was awarded an endowed research fellowship to travel to the Erasmus MC in Rotterdam and study structural brain development in children with syndromic craniosynostosis under the supervision of Dr. Irene Mathijssen. He graduated with a Doctor of Medicine (M.D.) from Yale in May of 2021 and is currently a resident in training in plastic and reconstructive surgery at the Hospital of the University of Pennsylvania and the Children's Hospital of Philadelphia.

Acknowledgements

Professor Mathijssen, thank you so much for the opportunity to join your team and pursue this research. I've learned so much under your supervision and consider it a privilege to have trained in your lab. Your commitment to patients and their families both clinically and through research efforts is inspiring.

Henri, your expertise in all things technical has been tremendously helpful throughout my time at the Erasmus MC. This work simply would not be possible without your help. I'm forever grateful for your patience and willingness to help me with image processing.

Dr. Persing, thank you for your constant support in my pursuit of a career as a plastic surgeon. Your enthusiasm for training the next generation of surgeons is always evident. Thank you for your critical review of these projects and thought-provoking questions raised.

Dr. Tasker, your critical analysis of this work and stimulating discussions regarding its implications have greatly improved its quality. Thank you for your commitment to rigorous and thoughtful analysis.

Dr. Steinbacher, thank you for introducing me to craniofacial research and creating opportunities for me to be involved with your work. Your support and mentorship is appreciated more than you know.

Bianca, I would not have completed this were it not for your encouragement to pursue it in the first place. Thank you for that and for your constant help with data collection, R, and navigating Rotterdam and Erasmus MC.

Robbin, thank you for welcoming me to the cranio group, helping me brainstorm project ideas, and introducing me to Dutch soccer.

To all my co-authors, thank you for your constant willingness to critically review manuscripts, improve study designs, and help with the interpretation of our results. This work would not be possible without you and is greatly enhanced by your efforts.

Mark, I appreciate your seemingly endless knowledge of R and statistics and your willingness to share that expertise with me regularly. I also want to thank you for your help in translating my summary and introducing me to the best restaurants in Rotterdam as well as the only American-style diner with free coffee refills.

Cranio researchers, this work is truly the result of a team effort spanning years of careful data collection and documentation. I'm indebted to all of you for your selflessness in helping me navigate Dutch patient records, sharing your work, and sharpening ideas daily.

15th floor, you made Rotterdam a second home for me. I'm incredibly lucky to have had the chance to work alongside you all and learn from you on a daily basis. This experience has been better than I ever could have hoped for and that is in large part due to you.

Mom and Dad, thank you raising me. I know it must have been hard at times. Although I'm constantly learning, life's most enduring lessons seem to be learned in childhood. I'm thankful for parents like you who thought it worthwhile to teach me the importance of truth and virtue, always pointing to Jesus as the perfect example.

Kayla and Mark, your love and support are energizing every time we see each other. I'm so grateful for siblings like you who are not only fun but also sharpen me intellectually and spiritually with every conversation.

Jack, Darian, and Martijn, thank you for making the Netherlands a home. You are some of the best roommates I could have asked for and I will always fondly remember our taco Tuesdays and docuseries nights.

To the rest of my family, thank you for your love and support. Your encouragement has motivated me and your prayers sustained me throughout the ups and downs of this process. Thank you from the bottom of my heart.